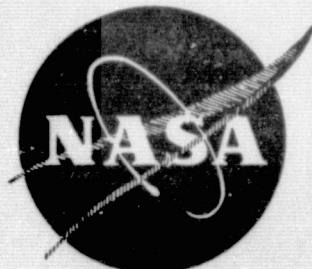# ADVANCED LOW NO$_x$ COMBUSTORS FOR SUPERSONIC HIGH-ALTITUDE AIRCRAFT GAS TURBINES

by P.B. Roberts, D.J. White and J.R. Shekleton

SOLAR DIVISION OF INTERNATIONAL HARVESTER

prepared for

NATIONAL AERONAUTICS AND SPACE ADMINISTRATION

LEWIS RESEARCH CENTER

Contract NAS3 -18028

1. Report No. NASA CR 134889	2. Government Accession No.	3. Recipient's Catalog No.
4. Title and Subtitle ADVANCED LOW NO$_x$ COMBUSTORS FOR HIGH-ALTITUDE SUPERSONIC AIRCRAFT GAS TURBINES		5. Report Date **November 1975**
		6. Performing Organization Code
7. Author(s) P. B. Roberts, D. J. White and J. R. Shekleton		8. Performing Organization Report No. RDR 1814
		10. Work Unit No.
9. Performing Organization Name and Address Solar Division of International Harvester 2200 Pacific Highway San Diego, California 92138		
		11. Contract or Grant No. NAS3-18028
		13. Type of Report and Period Covered Contractor Report
12. Sponsoring Agency Name and Address National Aeronautics and Space Administration Washington, D.C. 20546		
		14. Sponsoring Agency Code

15. Supplementary Notes

Project Manager: H. F. Butze, Air Breathing Engines Division
NASA-Lewis Research Center, Cleveland, OH 44135

16. Abstract

A test rig program was conducted with the objective of evaluating and minimizing the exhaust emissions, in particular NO$_x$, of three advanced aircraft combustor concepts at a simulated, high-altitude cruise condition.

The three combustor designs, all members of the lean-reaction, pre-mixed family, are the Jet Induced Circulation (JIC) combustor, the Vortex Air Blast (VAB) combustor, and a catalytic combustor. They were rig tested in the form of reverse flow can combustors in the 0.127 m. (5.0 in.) size range.

Various configuration modifications were applied to each of the initial JIC and VAB combustor model designs in an effort to reduce the emissions levels. The VAB combustor demonstrated a NO$_x$ level of 1.1 gm NO$_2$/kg fuel with essentially 100% combustion efficiency at the simulated cruise combustor condition of 50.7 N/cm^2 (5 atm), 833°K (1500°R), 833°K (1500°R) inlet pressure and temperature respectively and 1778°K (3200°R) outlet temperature on Jet-A1 fuel. Early tests on the catalytic combustor were unsuccessful due to a catalyst deposition problem and were discontinued in favor of the JIC and VAB tests.

In addition emissions data were obtained on the JIC and VAB combustors at low combustor inlet pressure and temperatures that indicate the potential performance at engine off-design conditions.

17. Key Words (Suggested by Author(s)) Combustor, Exhaust Emissions, Fuel Vaporization, Air/Fuel Mixing, Oxides of Nitrogen	18. Distribution Statement Unclassified – Unlimited		
19. Security Classif. (of this report) Unclassified	20. Security Classif. (of this page) Unclassified	21. No. of Pages 80	22. Price* $3.00

FOREWORD

The research program described within this report was conducted by the Solar Division of International Harvester under Contract NAS3-18028 with Mr. Helmut F. Butze of the Air Breathing Engines Division, NASA-Lewis Research Center as Project Manager.

The period of performance for the contract was March 1974 through June 1975.

Page intentionally left blank

CONTENTS

CONTENTS (Contd)

ILLUSTRATIONS

ILLUSTRATIONS (Contd)

ILLUSTRATIONS (Contd)

TABLES

1

SUMMARY

A test rig program was conducted with the objective of evaluating the low emissions potential of three advanced aircraft gas turbine combustor concepts.

Previous research and analytical considerations have indicated that an idealized, pre-mixed type of well-stirred combustor might be capable of achieving nitrogen oxide (NO_x) levels as low as 1.0 gm NO_2/kg fuel at a typical high-altitude, supersonic cruise condition. The subject program goal, therefore, was to demonstrate a NO_x level of 1.0 gm NO_2/kg fuel at a cruise condition with combustor hardware that while not designed specifically for any given aircraft engine or cycle, could conceivably be suitable for eventual incorporation in an aircraft gas turbine.

The emphasis of the program was strongly upon minimizing NO_x while maintaining high efficiency levels with carbon monoxide (CO) and unburned hydrocarbon (UHC) levels of 1.0 gm/kg fuel and 0.5 gm/kg fuel respectively. The scope of the program did not include detailed evaluation of other combustor performance parameters such as exhaust temperature pattern factor, liner temperatures or altitude relight capability.

The three combustor designs, all members of the lean-reactor, pre-mixed group are the Jet Induced Circulation (JIC) combustor, the Vortex Air Blast (VAB) combustor and a catalytic combustor. They differ basically in the manner whereby the reaction occurs and is stabilized and the type of fuel/air preparation system.

The JIC combustor utilizes a system of multiple air/fuel mixing tubes external to the combustor reaction zone proper to produce a well-mixed system. The mixing tubes are inclined towards the dome of the combustor and the impingement of the individual, mixed jets is the driving force for the establishment of the recirculation zone. In contrast, in the VAB combustor the reaction air and fuel are mixed within the vortex field produced by an inward, radial flow swirler. The resultant static pressure gradients in the reaction chamber serve to produce the recirculation zone necessary for flame stabilization.

The catalytic combustor differs from other combustors inasmuch as the oxidation of the fuel occurs along the length of a fixed platinum-catalyst bed rather

than within the more usual confined reaction zone of the JIC and VAB systems. The catalytic bed is supplied with a homogeneous fuel/air charge by using a fuel preparation system adopted from the VAB combustor that incorporates air-blast atomization and an inward radial flow swirler for fuel/air mixing.

All combustors were rig tested in the form of reverse flow can combustors to facilitate modifications and were configured as essentially reaction zones only with a minimal amount of convective cooling for the liner surfaces. No dilution flow was incorporated so as to minimize the reaction zone equivalence ratio for the required outlet temperature.

The initial designs of the combustors were based on a total pressure drop of 6 percent and a reference velocity of 30.48 m/sec (100 ft/sec). All three reaction zone diameters were initially 0.133 m (5.25 in.).

The program approach was to assess the emissions signatures of the initial designs and to make various configuration modifications intended to minimize the emissions, in particular NO_x, at the simulated cruise condition test point.

The supersonic cruise condition adopted as the test point was characterized by a combustor inlet pressure and temperature of 50.7 N/cm^2 (5 atm) and 833°K (1500°R) at a combustor outlet temperature of 1778°K (3200°R) which corresponds to an equivalence ratio of 0.43. The test fuel was Jet-A1. Due to facility problems during the course of the test program, however, much of the screening test data were obtained at lower pressures than the 50.7 N/cm^2 (5 atm) design point.

By decreasing the design reference velocity of the VAB combustor to approximately 13.72 m/sec (45 ft/sec), increasing the reaction zone volume, and improving the fuel injection distribution, a NO_x level of 1.1 gm NO_2/kg fuel with both CO and UHC levels less than 0.3 gm/kg fuel was obtained at the design point cruise condition. The JIC combustor, operating at 15.24 m/sec (50 ft/sec) produced somewhat higher NO_x levels, extrapolated to be in the 3.0-4.0 gm NO_2/kg range. This was attributed to the lack of an adequate degree of pre-mixing being attained in the mixing tubes prior to combustion.

Testing on the catalytic combustor was delayed until a late point in the program pending a finalization of the VAB combustor fuel atomization/pre-mixing system configuration that was conceptually similar to that of the catalytic combustor. The preliminary tests of the catalytic combustor, using natural gas fuel rather than Jet-A1, were unsuccessful, with the catalyst bed failing to demonstrate a self-starting ability at the 833°K (1500°R) test point combustor inlet temperature. Testing on the catalytic combustor was subsequently curtailed in order to divert the total remaining program resources towards the JIC and VAB combustors.

At the completion of the screening tests, data were recorded for both the JIC and VAB combustors at reduced inlet temperatures in an effort to assess the potential emissions level at off-design conditions such as engine idle.

The low inlet temperature characteristics of the JIC and VAB combustors proved to be similar. At a constant reaction temperature, decreasing inlet temperatures produced increasing NO_x and CO levels due to the reduced degree of vaporization and premixing in the respective fuel preparation devices.

At inlet temperatures below approximately 478°K (400°F) this increasing NO_x trend was reversed at high reaction zone equivalence ratios by the decrease in the post-hydrocarbon reaction oxygen availability.

It was concluded that NO_x levels in the order of 1.0 gm NO_2/kg fuel with combustion efficiencies in excess of 99 percent could be attained at the simulated cruise condition with a combustor design that would conceivably be amenable to incorporation within future aircraft engines. The available low emissions operating range between the NO_x limit and the lean stability point of such a well-mixed combustor is severely limited, however, and would be insufficient for operation across the complete engine envelope without further development of such concepts as pilot combustors or variable geometry.

2

INTRODUCTION

In recent years the role of oxides of nitrogen (NO_x) within the overall production mechanism of photochemical smog has been recognized, if not completely understood and in consequence these oxides are currently considered as serious, immediate, environmental pollutants.

Concern has also been expressed, however, as to the possible harmful effects of NO_x and other pollutants emitted from future generations of high-altitude, supersonic, commercial and military aircraft on the delicate chemical balance of the stratosphere possibly resulting in, for example, ozone depletion and concomitant increases in sea-level radiation levels.

A program currently being conducted under contract from the NASA-Lewis Research Center is designated as the "Experimental Clean Combustor Program" and has as its main objective the development and demonstration of practical combustor technology to reduce exhaust pollutants from advanced jet aircraft engines to be developed during the 1980-1985 time period. One goal of the "Experimental Clean Combustor Program" is to reduce the emission index for oxides of nitrogen to a level of 5 gm NO_2/kg fuel or less for an Advanced Supersonic Transport at cruise conditions. As a comparison, current commercial supersonic aircraft operate at cruise levels of approximately 18-20 gm NO_2/kg fuel.

Although beyond the reach of any current combustor technology, theoretical considerations suggest that NO_x levels as low as 1.0 gm NO_2/kg fuel should be attainable. It was the purpose of this experimental study, therefore, to explore new combustor concepts designed to minimize the formation of NO_x in aircraft gas turbines. Although the combustors were to have eventual application to aircraft gas turbines, the scope of the subject program did not include the demonstration of performance criteria such as exhaust pattern factor, altitude relight capability or emissions during off-design conditions such as the engine idle mode.

It was the goal of this program to demonstrate that a NO_x emission index of 1 gm NO_2/kg fuel could be achieved with maximum carbon monoxide (CO) and unburned hydrocarbon (UHC) emission indices of 1 gm/kg fuel and 0.5 gm/kg fuel, respectively

at the simulated supersonic cruise condition represented by a combustor inlet temperature and pressure of 833°K (1500°R) and 50.7 N/cm^2 (5 atm) with a combustor outlet temperature of 1778°K (3200°R) on Jet-A1 fuel.

Three combustors incorporating the pre-mixed, lean reaction zone concept for NO_x limitation were rig tested. The results demonstrated that the program NO_x level goals could be achieved with a "quasi-conventional" combustor where the required physical envelope could conceptually be accommodated within future aircraft engines without drastic redesign of the complete engine layout.

3

COMBUSTOR CONCEPTS

The design of the three combustion systems was based on both the program operational constraints and Solar's past background investigations on these systems. No integrated design codes were available, however, although the basic nature of the combustors is such that the design can be treated in a modular fashion with the fuel preparation section uncoupled from the reaction zone proper. For the initial baseline designs some emphasis was placed on simplicity in terms of fuel injection system.

All three combustors are of the lean reaction, pre-mixed family of well-stirred systems differing in both the type of fuel/air preparation device utilized and the manner in which the reaction occurs and is stabilized. NO_x control is effected by minimizing the mean reaction zone equivalence ratio and the local equivalence ratio deviations that can cause high NO_x levels.

The three model combustors were tested as reverse-flow can configurations. Although realizing that the current practice in aircraft gas turbines of utilizing annular combustion systems will likely continue, it was initially decided that the efficacy of the concepts could best be demonstrated in can combustor form.

Similarly, while cognizant of the important role that inlet air maldistribution can play in the emissions signature displayed by a combustor this was not made an area of interest in the program and reverse flow configurations were adopted for ease of combustor changeover.

In order to minimize the reaction zone equivalence ratio, no dilution scheme was incorporated for any system other than a minimal amount of convective cooling applied to the combustor liners that is re-injected and mixed into the reaction zone products prior to the emissions sampling plane.

The following sections describe the construction and operation of the three combustion systems.

3.1 JET INDUCED CIRCULATION (JIC) COMBUSTOR

3.1.1 Combustor Description

Sections through the JIC combustor are shown in Figures 1 and 2 which show the salient points of the combustor design and the major dimensions. A photograph of the assembled combustor is given in Figure 3.

In order to produce a reaction zone with a maximum degree of homogeneity the reaction airflow and fuel flow are pre-mixed in a system of four mixing tubes that are external to the reaction zone of the combustor and inclined at 30 degrees to the combustor axis.

The fuel is air-blast atomized at the entrance to each mixing tube, initially through a simple, single-point, fuel injector tube 0.0016 m (0.060 in.) diameter located at the center of the port section. This system was subsequently modified (see Section 5.2.1). The fuel flow supply from the fuel system is separated into the four individual injector flows by means of an external flow divider block. This consists of a set of four, fixed orifices in a manifold. Pre-test calibration of this unit showed a maximum ±3 percent deviation from the mean flow over the test fuel flow range. This level becomes the "baseline" maldistribution in the system and can be reduced to a lower level of ±1.0 percent, for example, only with an inordinate amount of effort applied to the careful hand matching of the orifices and frequent cleaning.

The fuel is vaporized and mixed with the reaction air in the mixing tubes and emerges as a near-homogeneous jet into the reaction zone of the combustor. The four separate jets impinge towards the axis of the combustor forming two derived jets. The major derived jet flows upstream into the reaction zone towards the combustor dome, impinges on the dome and then flows rearwards towards the entering mixing tube jets. The resultant recirculation pattern is anchored by the mixing tube jets with a fraction of the reaction products being entrained into the mixing tube jets to act as a continuous ignition source, the remainder of the products flowing out of the reaction zone between the mixing tube jets. The small, minor derived jet flows rearwards from the impingement point of the separate mixing tube jets and is reacted partially in the secondary zone and partially by recirculation and entrainment into the mixing tube jets.

The secondary zone downstream of the mixing tubes can be considered as a continuation of the reaction zone where some CO oxidation continues.

The baseline combustor was initially cooled by a combination of convective and splash cooling. The reaction zone is convectively cooled by approximately 10 percent of the total airflow flowing rearwards and into the dome where it is discharged into the reaction zone. The secondary zone is similarly convectively cooled by approximately
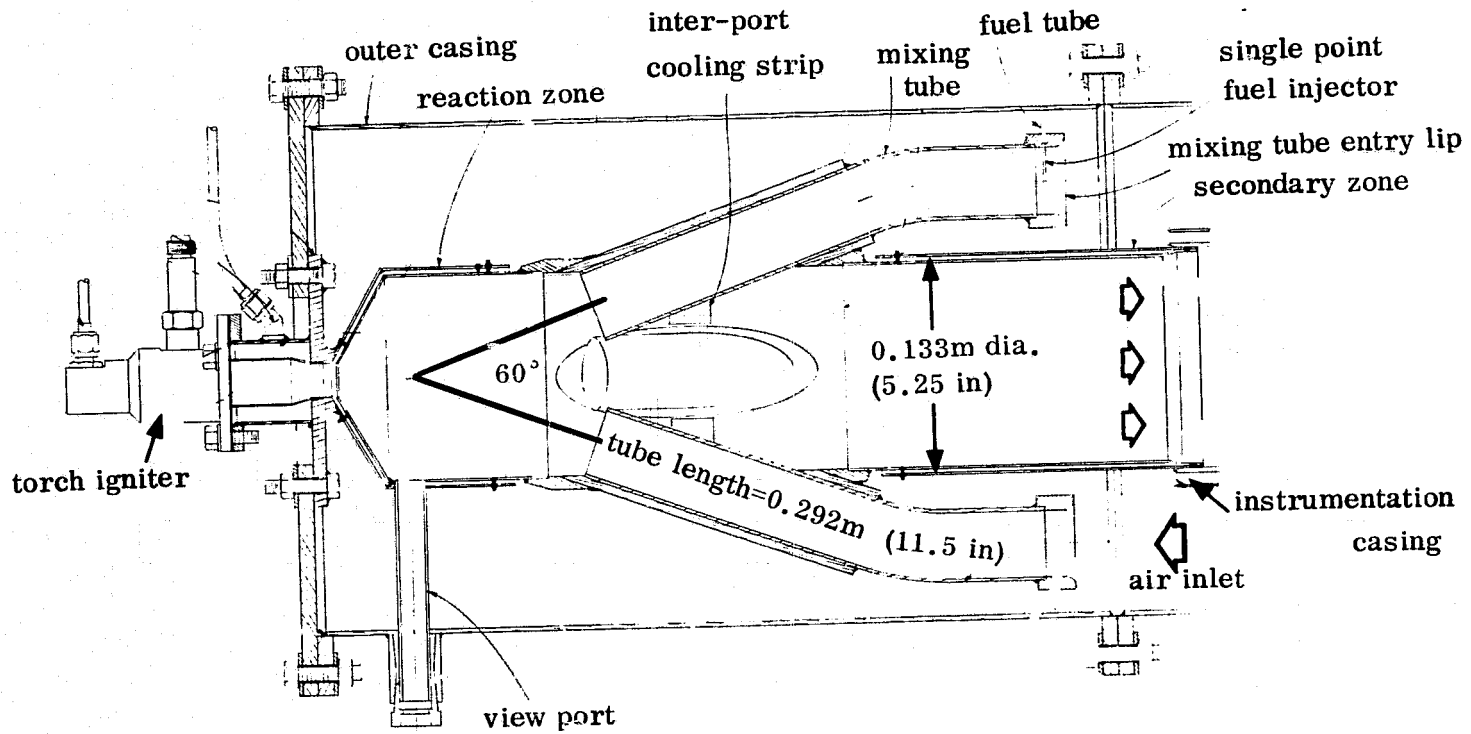
FIGURE 1. JIC COMBUSTOR DETAILS

mixing tube

inter-port cooling strip

single point fuel injector

view port
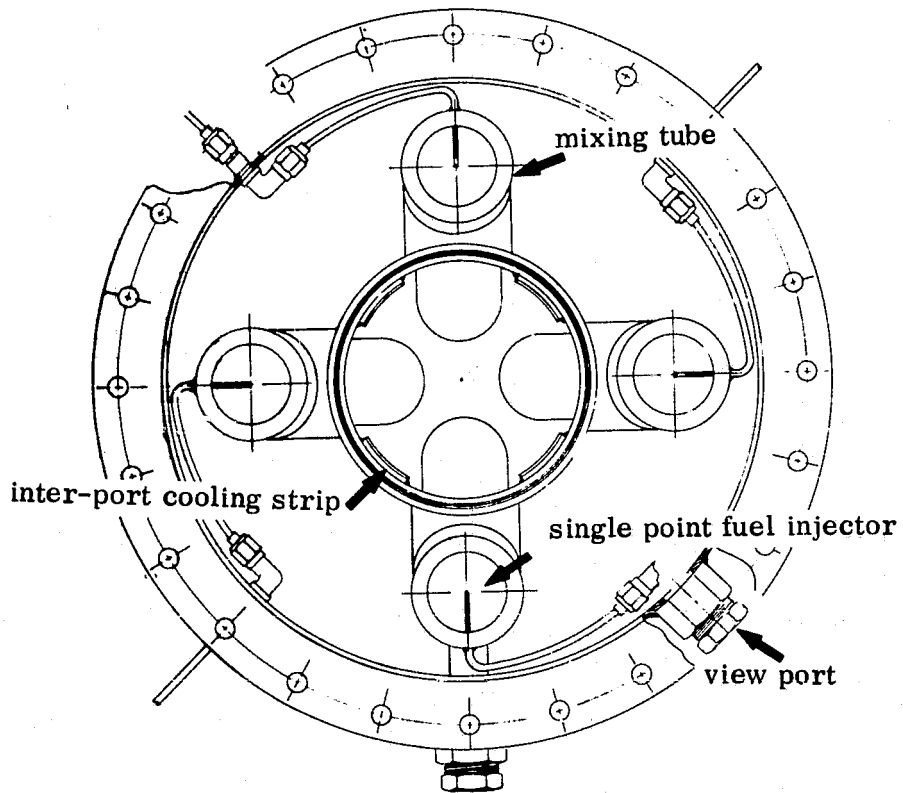
REAR VIEW ON COMBUSTOR OUTLET
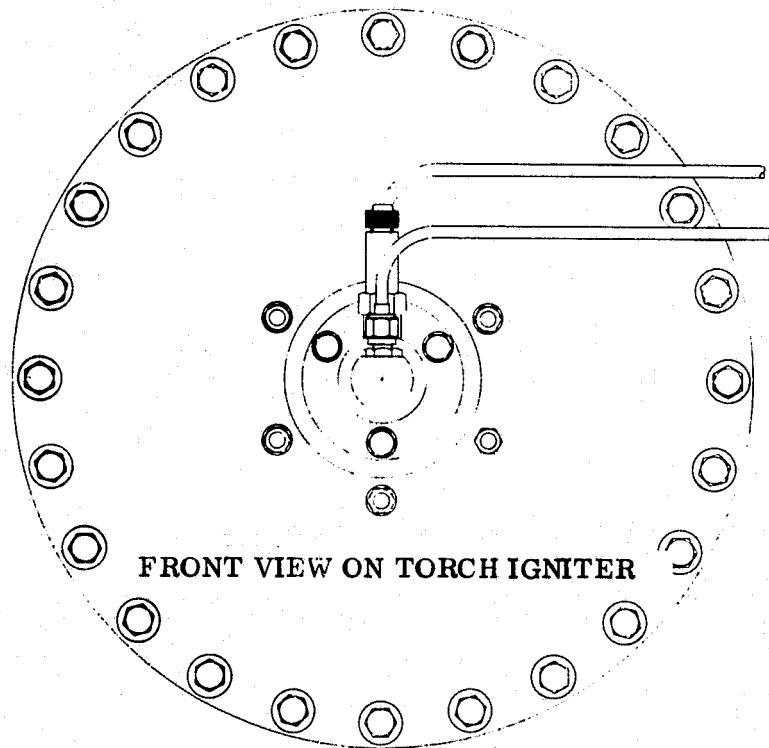
FRONT VIEW ON TORCH IGNITER

FIGURE 2. JIC COMBUSTOR DETAILS
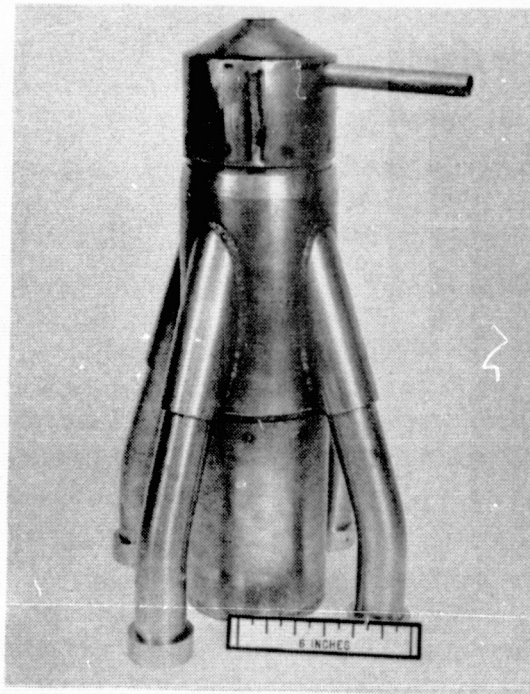
FIGURE 3. JIC COMBUSTOR

3 percent of the total airflow flowing rearwards and being discharged into the exhaust products at the end of the combustor through a set of metering orifices. The central section of the combustor was initially locally cooled by four inter-mixing tube splash cooling strips. These were subsequently removed (see Section 5.2.1).

Ignition of the combustor is by a torch igniter positioned on the combustor axis and firing through the combustor dome. This is only utilized for light-off and is isolated during normal running.

The construction of the combustor is generally of 0.0012 m (0.045 in.) thick Hastelloy X sheet with the combustor center section and mixing tubes of 321 stainless steel.

3.1.2 Design Considerations

The airblast atomization quality can be estimated from the work of Nukiyama and Tanasawa (Ref. 1) where the following empirical expression was proposed:

$$do = \frac{586\sqrt{\sigma}}{U\sqrt{\rho}} + 597\left(\frac{\mu}{\sqrt{\sigma\rho}}\right)^{0.45} \left(\frac{1000 V_f}{V_{air}}\right)^{1.5} \tag{1}$$

where,

$$do = \text{S.M.D. of spray, micron}$$

$$U = \text{relative air velocity, m/sec}$$

$$V_f, V_{air} = \text{volume rates of flow of fuel and air respectively}$$

$$\sigma = \text{surface tension, dynes/cm}$$

$$\rho = \text{fuel density, g/cm}^3$$

$$\mu = \text{fuel viscosity, poises}$$

It was also shown that for high volumetric air/fuel ratios (in excess of 5,000) the drop size was a function of the air blast velocity and the fuel properties only, thus:

$$do = \frac{586\sqrt{\sigma}}{U\sqrt{\rho}} \qquad (2)$$

The design point combustor pressure drop was set at 6.0 percent. Using Jet A-1 fuel and the cruise test point combustor inlet conditions of 50.68 N/cm^2 (5 atm) and 833°K (1500°R) a mean drop size of approximately 20 micron is calculated. This is considerably smaller than the drop size to be expected from a conventional pressure atomizer where mean droplet sizes of 100 to 200 micron are typical.

The design of the mixing tube length is a compromise between providing sufficient residence time for the fuel vaporization and fuel/air mixing processes and yet avoiding the twin problems of autoignition and flashback within a practical physical envelope. For the program purposes the reference velocity was defined using the reaction zone diameter only and did not include the physical envelope occupied by the mixing tube.

With a mixing tube length of 0.292 m (11.5 in.) the residence time at design point conditions is 1.7 millisec. This is considerably less than the required ignition delay time for auto-ignition to occur at the same conditions which for Jet-A1 fuel is in excess of 10 millisec. Such a simplistic approach however, does not guarantee that auto-ignition will not occur as it ignores boundary layer effects and the possibility of high-temperature, surface pre-ignition.

Fuel vaporization at high air temperatures is controlled by the rate of heat transfer from the air to the fuel droplet and for a single spherical droplet evaporating in air, the droplet diameter can be expressed as a function of time by using the "d^2 law" (Ref. 2):

$$d^2 = do^2 - \lambda t \qquad (3)$$

where,

λ = evaporation coefficient (cm^2/sec)

do = initial droplet diameter, cm

d = droplet diameter, cm at time t, sec

The evaporation coefficient is temperature dependent and can be calculated from the following expression:

$$\lambda = \frac{8k}{\rho f \, Cp} \quad \ell n \quad \left(1 + \frac{Cp}{L} \quad (T - T_f)\right) \tag{4}$$

where,

λ = evaporation coefficient in still air, cm^2/sec

k = thermal conductivity of air, cal/cm sec°K

ρf = fuel density, g/cm^3

Cp = fuel specific heat, cal/gm °K

T = air temperature, °K

T_f = temperature of fuel droplet, °K

L = latent heat of vaporization, cal/gm

Inserting the properties of Jet-A1 fuel we obtain a value of approximately 0.006 for λ, the evaporation coefficient at 833°K (1500°R) air temperature.

Thus for an initial droplet size of 20 micron it can be shown that a time of 0.7 millisec is required for complete evaporation. It should be noted however, that the evaporation rate is considerably enhanced when there is relative motion between the air and fuel droplets; a conservative value of evaporation time is thereby obtained when the "still air" evaporation constant is utilized.

A preliminary estimate of the degree of mixing obtained at the mixing tube exit can be made using a standard point-source diffusion equation, as below:

$$f = \frac{wf \, U}{4\pi \, Wa \, Ex} \quad \exp \left(\frac{-r^2 \, U}{4 \, Ex}\right) \tag{5}$$

where,

f = local fuel air ratio

wf = total fuel flow rate, Kg/sec

wa = total air flow rate per unit duct area, Kg/sec m^2

E = eddy diffusivity, m^2/sec

U = mixing tube velocity, m/sec

x = mixing tube length, m

r = mixing tube radius, m

This assumes that diffusion in the axial direction can be neglected and that E and U are constant. No wall effects are considered and the fuel is assumed to be vaporized although droplet effects can be accommodated. The effect of the presence of droplets is to lower the eddy diffusivity; the larger the drop size, the lower the diffusivity will be compared to a vaporized fuel.

Using a value of $E/U = 0.00024$ m for the single phase case, it can be shown for the mixing tube length used that for the single point fuel injection the minimum local fuel/air ratio occurring at the mixing tube outer diameter and the maximum local fuel/air ratio occurring at the mixing tube axis are 34.7 and 138.1 percent respectively of the overall average fuel/air ratio.

The problem of flashback is less amenable to analysis and occurs when the turbulent flame speed is greater than the local air/fuel mixture velocity. Turbulent flame speeds of the order of 60 m/s (197 ft/sec) are typical at the inlet temperature of 833°K (1500°R) and although this is considerably lower than the nominal mixing tube velocity of 171.3 m/s (562 ft/sec) at the design point conditions, flashback can occur through low velocity boundary layers or separated regions.

The design of the mixing tubes in regard to the number and orientation was based on previous parametric tests conducted by Solar on this type of system although some preliminary indications of the mixing tube jet impingement splits can be obtained from the analysis of Baron and Bollinger (Ref. 3). Although the entrainment level increases as the number of jets or the jet exposed surface is increased, there is an optimum value for the number of jets. With an excessive number of jets the diameter of the major derived jet is excessive and the flow area available for the products to exit the reaction zone is insufficient. This results in the periodic deflection of the incoming mixing tube jets and combustion instability.

3.2 VORTEX AIR BLAST (VAB) COMBUSTOR

3.2.1 Combustor Design

A section through the VAB combustor is shown in Figure 4 with the major details and sizes noted.

In the case of the VAB combustor, pre-mixing is accomplished within a radial, inflow swirler rather than a system of mixing tubes as is the case of the JIC combustor. The swirler radial inlet has a set of twenty-four flat vanes set at a fixed angle of forty-five degrees with the axial, annular discharge section communicating with the reaction zone. The swirler inlet section is shown in Figure 5.

The fuel is air-blast atomized at twenty-four separate points slightly downstream of each vane-channel throat section. The 0.0016 m (0.06 in.) diameter fuel tubes protrude to the mid-point of each channel width. This system was subsequently modified (see Section 5.2.1). The swirler centerbody with fuel injectors is shown in Figure 6. The fuel flow supply from the fuel system is separated into the twenty-four injector flows by means of an external flow divider block as in the case of the JIC combustor. Pre-test calibration of the unit showed a maximum "baseline" fuel maldistribution of ±3 percent from the average.

The fuel is vaporized and mixed with the reaction air in the swirler passage and enters the reaction zone of the combustor as a near homogeneous stream with a nominal outlet swirl cone angle of ninety degrees. The radial static pressure gradients produced in the vortex serve to drive the reaction zone recirculation necessary for flame stabilization.

The combustor reaction zone is convectively cooled by approximately seven percent of the total airflow flowing downstream and discharging into the exhaust products at the end of the combustor through a set of metering orifices.

Ignition of the combustor is by a torch igniter firing radially into the reaction zone. As in the case of the JIC combustor, this is utilized only for light-off purposes and is isolated during normal running.

The construction of the combustor is generally of 0.0012 m (0.045 in.) thick Hastelloy X sheet with swirler vanes and bodies of 321 stainless steel.

3.2.2 Design Considerations

It was noted in Section 3.1.2 that evaporation rates of fuel droplets are considerably enhanced when there is a relative velocity existing between the droplet

outer casing

swirl vane

torch igniter

fuel tubes

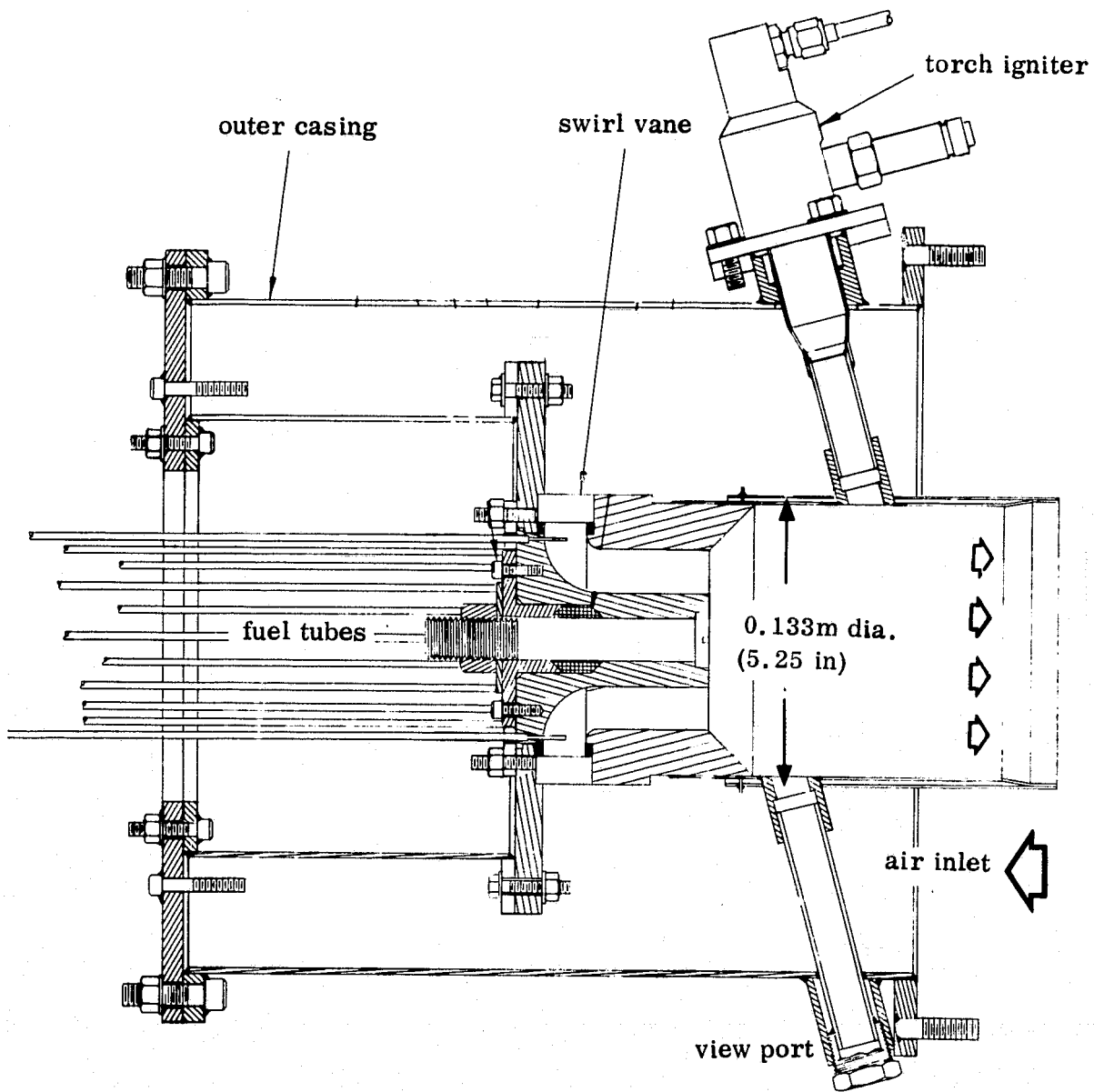0.133m dia.
(5.25 in)

air inlet
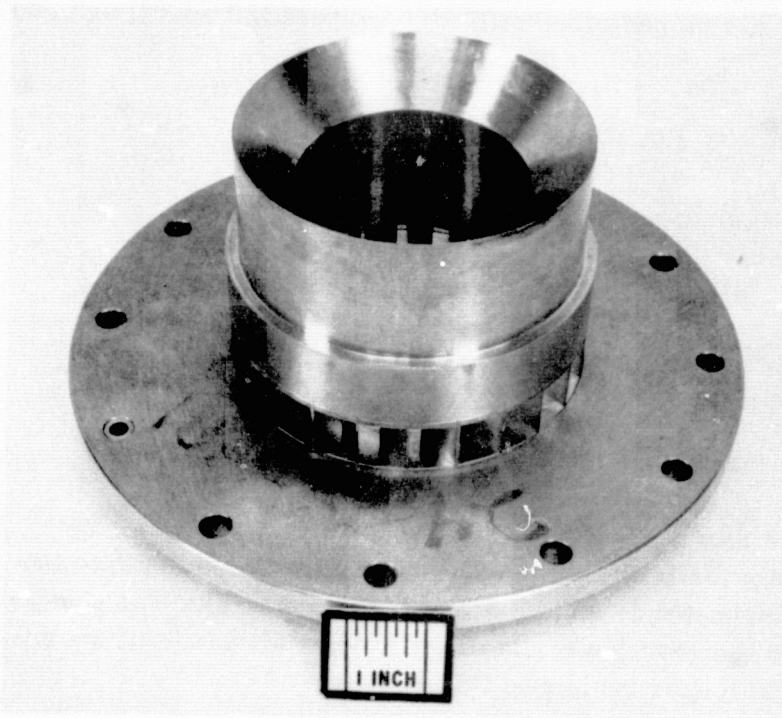
view port

FIGURE 4. VAB COMBUSTOR DETAILS

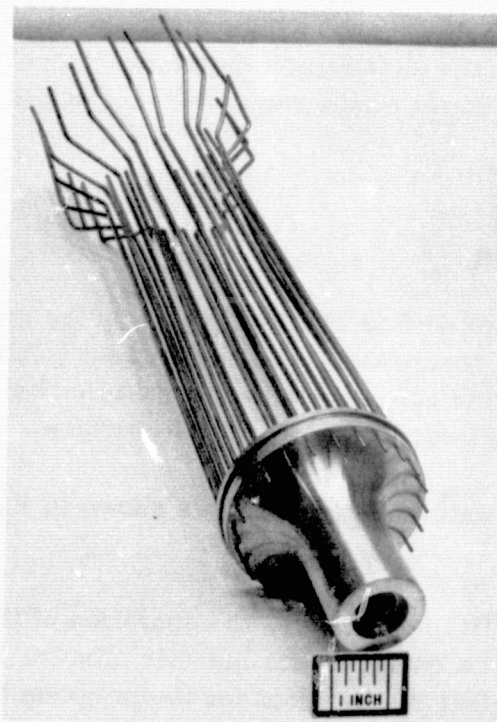FIGURE 5.   VAB COMBUSTOR SWIRLER INLET

FIGURE 6.   VAB COMBUSTOR SWIRLER CENTERBODY
AND FUEL TUBE ASSEMBLY

and the flowing air. In this case the "still air" evaporation coefficient can be modified as follows:

$$\lambda = \lambda_0 \ (1 + 0.276 \ Re^{1/2} \ Sc^{1/3}) \tag{6}$$

where,

λ_0 = "still air" evaporation coefficient, cm^2/sec

λ = modified evaporation coefficient, cm^2/sec

Re = Reynolds number

Sc = Schmidt number

When fuel is injected into a flowing air stream the droplets accelerate to the air stream velocity, consequently the initially high evaporation rates diminish to the "still air" levels. The VAB combustor is an attempt to obtain controlled relative motion between the fuel droplets and the reaction air in order to take advantage of the resulting higher evaporation rates and longer residence times.

Within the radial vortex field a fuel droplet will tend to rotate at a constant radius at which the drag force is balanced by the imposed centrifugal force. As the droplet evaporates, this equilibrium radius decreases and the droplet spirals inwards. In this way, any large droplets at the end of the distribution spectrum have proportionally larger residence times in the swirler and the dependency of the degree of homogeneity of the air/fuel mixture on the vaporization process is minimized.

3.3 CATALYTIC COMBUSTOR

3.3.1 Combustor Description

The catalytic combustor differs significantly from the more conventional combustion system where the fuel oxidation occurs without a third body interaction inasmuch as the overall reaction rate is generally controlled by diffusion of the reactants to, and the products away from, a catalytic surface.

A section through the catalytic combustor is shown in Figure 7 with the major details and sizes noted.

As with the VAB and JIC combustors, the operation of the catalytic combustor relies upon the preparation of a homogeneous fuel/air mixture for delivery to the catalytic bed. It was an original requirement for the program that the design and testing effort allotted to the catalytic combustor be less than that of the JIC or VAB combustors. The fuel preparation section of the catalytic combustor was therefore
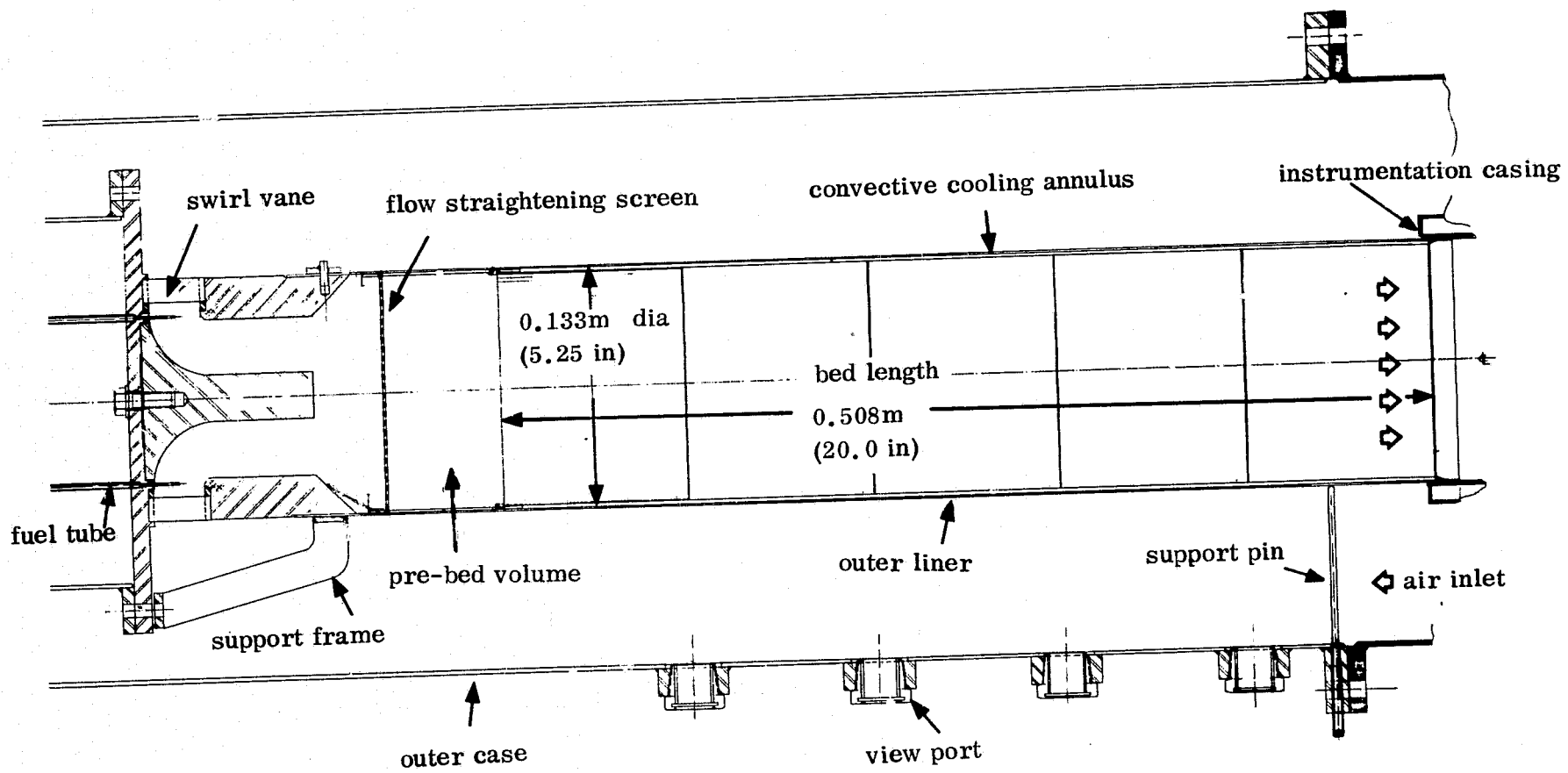
18

FIGURE 7. CATALYTIC COMBUSTOR DETAILS

adapted from the VAB combustor with the intention that the optimized system design resulting from the VAB combustor investigations would be adapted for the catalytic combustor.

As in the case of the VAB combustor, pre-mixing is accomplished within a radial, inflow swirler. The swirler radial inlet has a set of twenty-four flat vanes set at a fixed angle of forty-five degrees with the axial, annular discharge section communicating with a pre-bed volume.

The liquid fuel is air-blast atomized at twenty-four separate points slightly downstream of each vane-channel throat section. The 0.0016 m (0.06 in.) diameter fuel tubes protrude to the mid-point of each channel width. The fuel flow supply from the fuel system is separated into the twenty-four injector flows by means of an external flow divider block as in the case of the JIC and VAB combustors.

The homogeneous fuel/air mixture enters the pre-bed volume where the flow is de-swirled by a perforated sheet across the flow path before entering the catalytic bed.

The catalytic bed consists of five separate monolithic substrate modules sensitized with platinum, stacked in series and enclosed in an outer liner with spacers forming a convective cooling system. Approximately five percent of the total airflow is used to convectively cool the outer liner before being discharged into the exhaust products at the end of the combustor through a set of metering orifices.

The initial four of the five bed modules are fabricated from kanthal A1 strip 0.00024 m (0.009 in.) thick. A photograph of one of the completed cores is shown in Figure 8. The fully annealed flat strip is formed to a triangular corrugation and wrapped to the required final diameter.

The final high-temperature bed module was originally intended to be constructed of silicon carbide, however, last minute availability problems forced a change to cordierite which has the ternary oxide composition $2MgO \cdot 2Al_2O_3 \cdot 5SiO_2$ and represents at best only a compromise due to its marginal ability to withstand the combustor design outlet temperature of 1778°K (2740°F). A photograph of the cordierite stacked cell structure is shown in Figure 9.

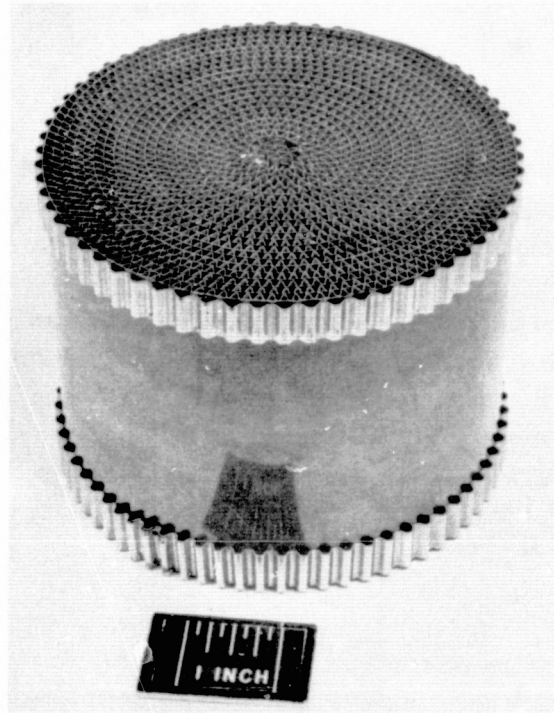The general construction of the combustor is of 321 stainless steel.
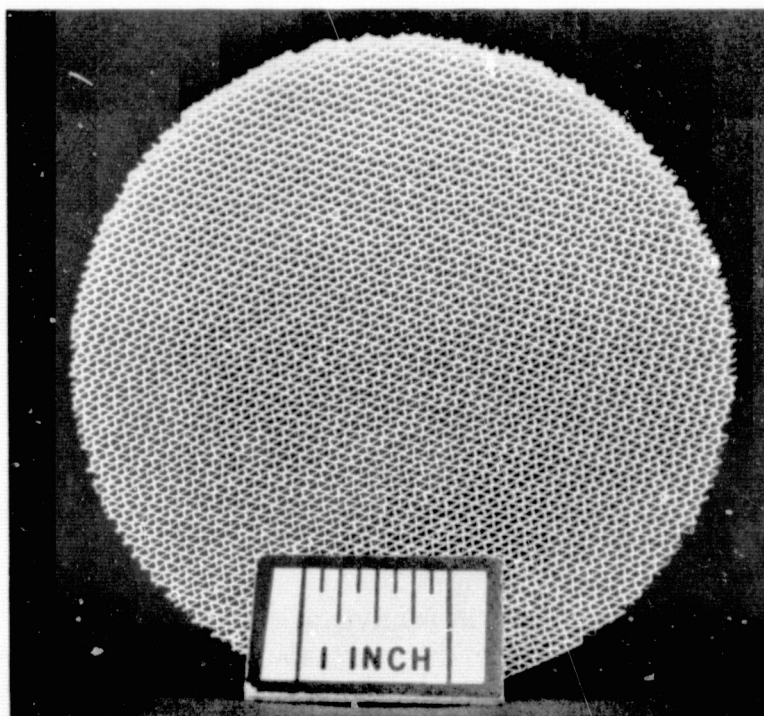
FIGURE 8.   KANTHAL CORE MODULE

FIGURE 9.   CORDIERITE CORE MODULE

3.3.2 Design Considerations

Space Velocity

The space velocity of the catalytic bed is a measure of the reference residence time available for reaction and is based on the void volume velocity throughout the bed at the combustor inlet conditions.

From the geometry of the core modules a void fraction of 0.79 is calculated hence with the design point reference velocity of 100 ft/sec, the void volume velocity becomes 38.58 m/s (126.6 fps). With a total bed length of 0.508 m (20 in.) the bed residence time is calculated as 13.16 msec giving a space velocity of approximately 278,000 hr^{-1}. Previous Solar sponsored work on oxidation catalysts had shown this to be a relatively moderate space velocity level for effective combustor operation.

Catalyst Concentration

The design concentration of catalyst on the substrate was based partially on current commercial practice where typical platinized alumina pellets in the 0.0032 m (0.125 in.) diameter by 0.0038 m (0.150 in.) long size range are utilized at concentration levels of 0.5 percent by weight of platinum. This corresponds to a specific surface concentration of 4.58×10^{-3} KgPt/m^2 (6.51×10^{-6} lb Pt/$in.^2$) based on the geometric area only. The effective concentration is considerably lower than this level due to the high level of microporosity of gamma alumina.

As a starting point a more moderate design concentration level of 2.14×10^{-3} KgPt/m^2 (3.0×10^{-6} lb Pt/$in.^2$) was evaluated on both the kanthal and cordierite modules in view of the high reaction temperatures that would necessarily exist throughout the later bed stages and the moderate design point space velocity.

Catalyst Application

The various stages of the process are described below and are essentially identical for both the kanthal and cordierite substrates. The basic intent is to coat the substrate with a thin, uniform layer of gamma alumina within which is distributed the metallic catalytic agent. The gamma alumina possesses a high degree of microporosity and thus offers an effective reaction area orders of magnitude greater than the geometric area.

Stage 1 - Solution Preparation. A solution of aluminum nitrate, $Al(NO_3)_3$ and chloroplatinic acid, $H_2PtCl_6 \cdot 6H_2O$, is prepared, the relative concentrations depending upon the required final level of platinum required. The modules are dipped in the solution.
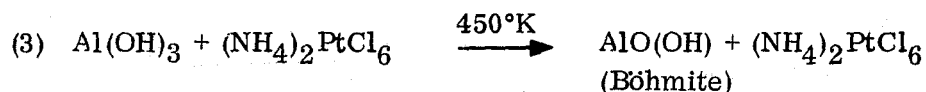
Stage 2 - Module Pre-oxidation. This step does not apply to the cordierite modules and is used to prepare the surface of the kanthal modules by building a uniform oxide layer of alumina, Al_2O_3. The modules are pre-oxidized by heating in air at 1422°K (2100°F) for a period of one hour.

Stage 3 - Hydrolyzing. After the modules are dipped in the solution, they are hydrolyzed in ammonia gas, NH_3. This is done by supporting the modules over gently heated ammonium hydroxide, NH_4OH, for a few minutes. Hydrolysis forms a gelatinous mixture of aluminum hydroxide, $Al(OH)_3$, ammonium chloroplatinate, $(NH_4)_2PtCl_6$, and ammonium nitrate, NH_4NO_3, over the surfaces of the modules. The chemical equations are shown below.

(1) $Al(NO_3)_3 + 3NH_3 + 3H_2O \longrightarrow Al(OH)_3 + 3NH_4NO_3$

(2) $H_2PtCl_6 + 2NH_3 \longrightarrow (NH_4)_2PtCl_6$
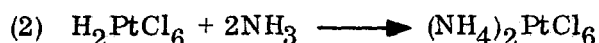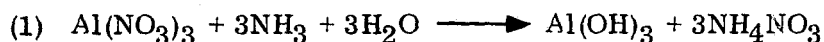
This stage was repeated for the kanthal modules in an effort to ensure adequate deposition layer thickness. This was unnecessary for the cordierite module due to the high level of natural porosity.

Stage 4 - Drying. The hydrolized modules are air dried for two hours followed by oven drying at 450°K (350°F) for 8 hours. During the oven drying, the ammonium nitrate, NH_4NO_3, volatilizes and is driven off and the aluminum hydroxide is converted to Böhmite as water is lost.

(3) $Al(OH)_3 + (NH_4)_2PtCl_6 \xrightarrow{450°K} AlO(OH) + (NH_4)_2PtCl_6$
$\phantom{(3) \quad Al(OH)_3 + (NH_4)_2PtCl_6 \xrightarrow{450°K} \quad} \text{(Böhmite)}$

Stage 5 - Hydrogen Reduction. The modules are next exposed to a hydrogen atmosphere at 561°K (550°F) for three hours. This reduces the ammonium chloroplatinate to platinum.

(4) $(NH_4)_2PtCl_6 + 2H_2 \xrightarrow{561°K} Pt + 2(NH_4)Cl + 4HCl$
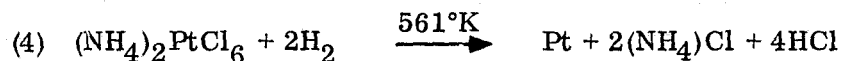
Stage 6 - Firing. The final stage of the process is a high-temperature firing in air at 1228°K (1750°F) for two hours, during which time the Böhmite is converted to gamma alumina, γ-Al_2O_3. The final result is a layer of highly porous gamma alumina with a uniform dispersion of metallic platinum within it.

4

TEST FACILITY

4.1 FLOW PATH

A schematic of the test rig facility is shown in Figure 10. A description of the flow path is as follows:

The main air mass flow is controlled before entering a gas-fired, indirect, air preheater that raises the temperature from essentially ambient to the required temperature at the combustor inlet. The flow then passes through a pipe section that contains a standard, ASME, sharp-edged orifice run for air-flow metering purposes before entering the instrumentation casing that reverses the flow through two straightening screens, in series (see Fig. 11) from where it passes into the combustor test section. The combustors are therefore operating as reverse-flow configurations. This facilitates the changeover from one combustor type to the other as each uses a separate outer casing.

The exhaust flow from the combustor passes through the water-cooled inner duct of the instrumentation casing where, after emissions and temperature monitoring, the outlet exhaust gas is quenched by direct water injection. The operational combustor-outlet pressure level is provided by a variable butterfly back-pressure valve mounted downstream of the instrumentation casing. The flow finally exhausts to atmosphere through a silencer.

4.2 INSTRUMENTATION

The various instrumentation stations are shown for reference in the rig flow path schematic of Figure 10.

The air mass flow is metered with a standard, ASME, sharp-edged orifice run equipped with D and D/2 pressure taps. The orifice run upstream static pressure is taken at instrumentation station 1 and displayed on a Bourdon type gage. Orifice static depression is displayed on three water manometers and measured between stations 1 and 2 at points equally spaced circumferentially. Orifice flow total temperature is monitored with three C/A thermocouples equally spaced circumferentially at station 3.
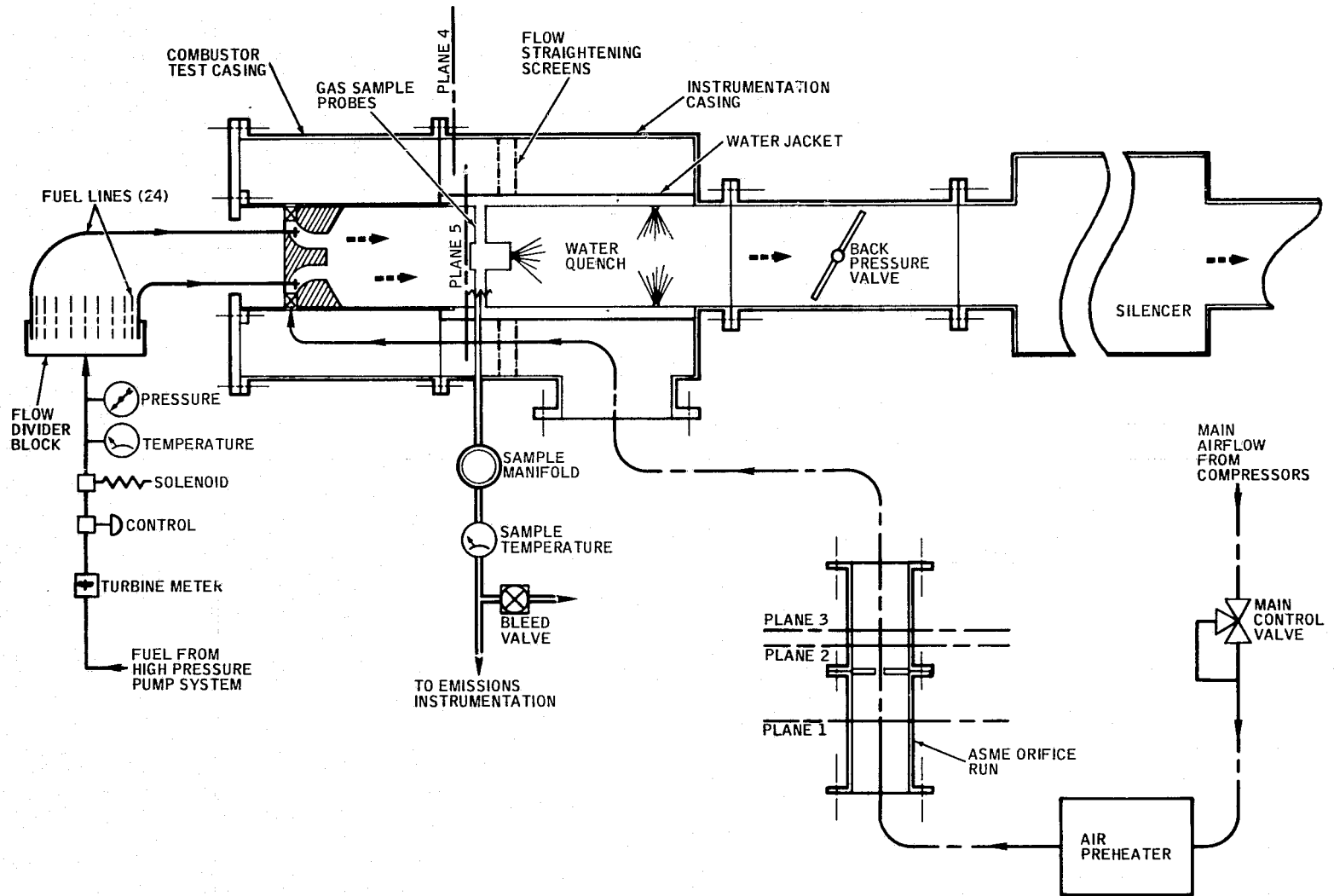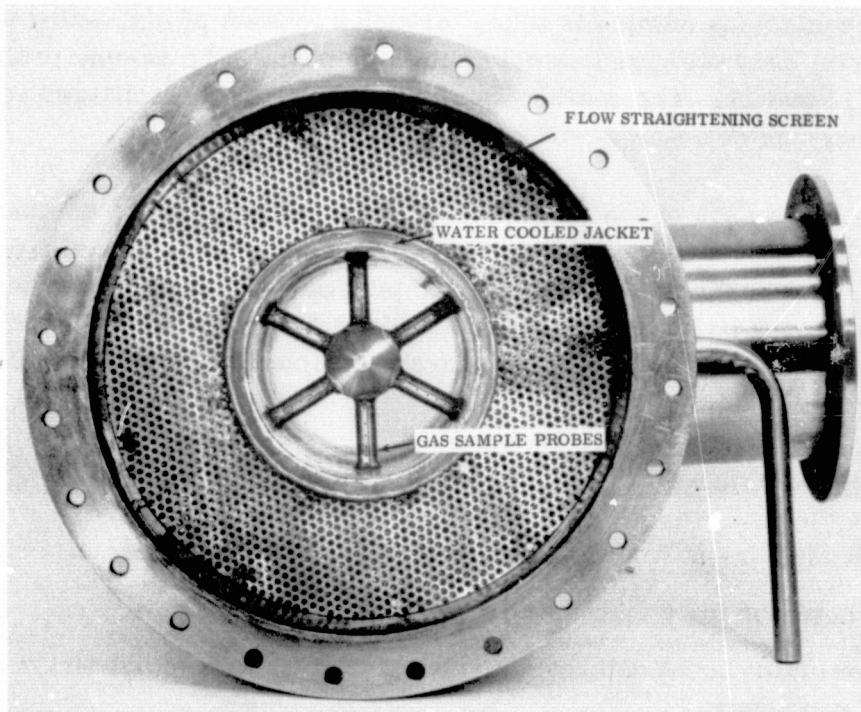
FIGURE 10. TEST RIG SCHEMATIC

FIGURE 11. INSTRUMENTATION CASING SECTION

The fuel temperature is measured with a single C/A thermocouple just upstream of the flow divider block that splits the main fuel flow into the separate and equal flows to each of the combustor injectors (see Sections 3.2.1; 3.1.1). The flow divider block upstream fuel pressure is indicated on a Bourdon type gage. Fuel flow rate is determined by a turbine meter installed in the delivery line. This is used as the primary fuel flow measurement. A secondary reading is obtained utilizing the pressure drop across the previously calibrated flow divider block.

The combustor inlet pressure and temperature are measured at station 4, downstream of the flow straightening screens. Due to the low inlet velocities involved, only static combustor inlet pressures and combustor pressure drops are taken. The combustor inlet pressure is displayed on a precision Bourdon-type gage and the combustor static-to-static pressure drop on three separate mercury manometers between stations 4 and 5 at points equally spaced circumferentially. The combustor inlet total temperature at station 4 is taken with three C/A thermocouples equally spaced circumferentially.

The combustor outlet temperature is measured (for reference and light-off indication purposes only) at station 5 by a single closed-end Type B thermocouple indicating through a digital millivoltmeter. All other thermocouple readout is through a digital temperature indicator and tape output.

The exhaust emissions sample is taken through a system of six, water-cooled, radial probes with six, area-weighted sample points on each. The sample probe can be seen in Figures 11 and 12. The cooling water for the probe is discharged into the combustor exhaust stream downstream of the probes.

The samples from each of the radial rakes are discharged into a common manifold (see Fig. 12) before passing to the sample line. The sample pressure is reduced to essentially atmospheric by bleeding the bulk of the flow to atmosphere before the sample enters a heated teflon line maintained at a constant 450°K (350°F) along its length. Sample temperature at entry to the sample line is monitored with a single C/A thermocouple.

The emissions instrumentation includes the following:

- NDIR instrument for carbon monoxide and carbon dioxide

- FID detector for unburned hydrocarbons

- Chemiluminescent detector for nitrogen oxide with molybdenum coil NO_2 converter
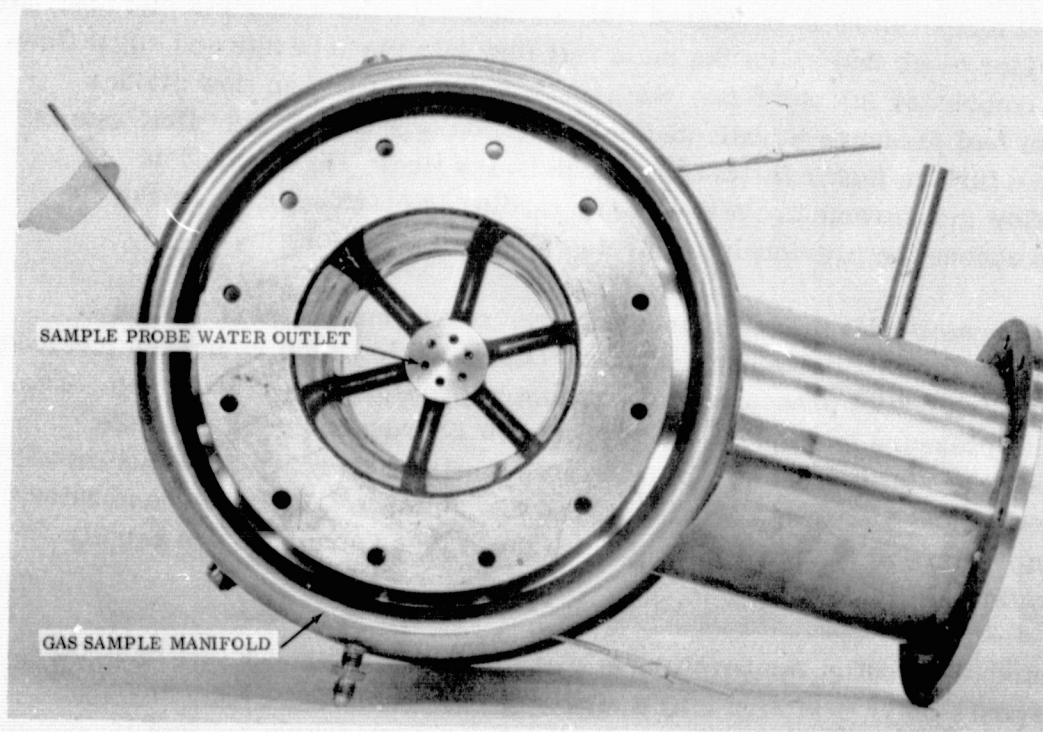
- Van Brand smokemeter

FIGURE 12. INSTRUMENTATION CASING SECTION

Utilization of the emissions equipment and emissions data reduction is performed to the requirements of SAE ARP 1256 (Ref. 4).

A dew point meter is utilized to monitor the rig inlet air humidity. This reading is utilized to correct the observed NO_x levels to a zero humidity figure using the correlation expression developed by Marchionna (Ref. 5).

4.3 TEST PROCEDURE

The test procedure adopted during the program was to establish the required levels of combustor inlet temperature, pressure and massflow. The fuel flow to the combustor was then modulated to give combustor outlet temperatures ranging from the design point down to a value just in excess of the lean stability limit of the system where the CO and UHC readings increase rapidly. Several data points were generally obtained between these two limits.

The emissions results represented in the body of the report are based on the exhaust gas analysis and the test fuel characteristics. The combustor temperature rise displayed is the ideal figure, including dissociation, computed from the fuel/air ratio obtained in turn from the exhaust analysis carbon balance using the calculation techniques of SAE ARP 1256 (Ref. 4). The direct measurements of air and fuel flow to the combustor were utilized as a check on the sampling accuracy. The fuel/air ratio calculated from the exhaust analysis agreed to within ±7.0 percent of that from the direct measurements.

4.4 TEST POINT

The high-altitude, cruise combustor conditions were specified as follows:

Combustor inlet temperature:	833°K (1500°R)
Combustor inlet pressure:	50.7 N/cm^2 (5 atm)
Combustor outlet temperature:	1778°K (3200°R)

5

RESULTS AND DISCUSSION

Although the screening tests of the various combustor modifications were intended to be carried out at the simulated cruise test point condition, rig facility problems required the use of lower combustor inlet pressures for much of the program. This is not thought to invalidate any of the conclusions reached for a particular configuration however.

The emphasis of the program was on obtaining experimental results from the combustor configurations; no attempt was made to analytically model the combustors or to back correlate the results in any fashion. The modifications made were generally those that attempted to produce a closer approximation to an idealized, well-stirred, pre-mixed reactor.

Preliminary tests were made to check on the various items of instrumentation to ensure representative results. Radial traverses of the orifice and combustor inlet thermocouples were made; no significant variations were found.

The following sections contain the test results of the VAB, JIC and catalytic combustor modifications.

5.1 VAB COMBUSTOR

5.1.1 Combustor Modifications

The initial tests of the VAB combustor were conducted on the configuration described in Section 3.2.1.

The emissions characteristics of this baseline configuration are shown in Figure 13 with the emissions indices of NO_x, CO and UHC plotted as a function of combustor temperature rise. It can be seen that the characteristics do not extend to the design temperature rise of 944°K (1700°F), the broken line at the lower temperature rise representing combustion instability occurring prior to lean extinction.

Past experience at Solar with the VAB type of combustor had indicated a lean stability limit of approximately 1589°K (2400°F) could be obtained for a premixed system, this value varying only slightly with pressure. The problem with the baseline VAB configuration was thought therefore to be one of insufficient reaction stabilization
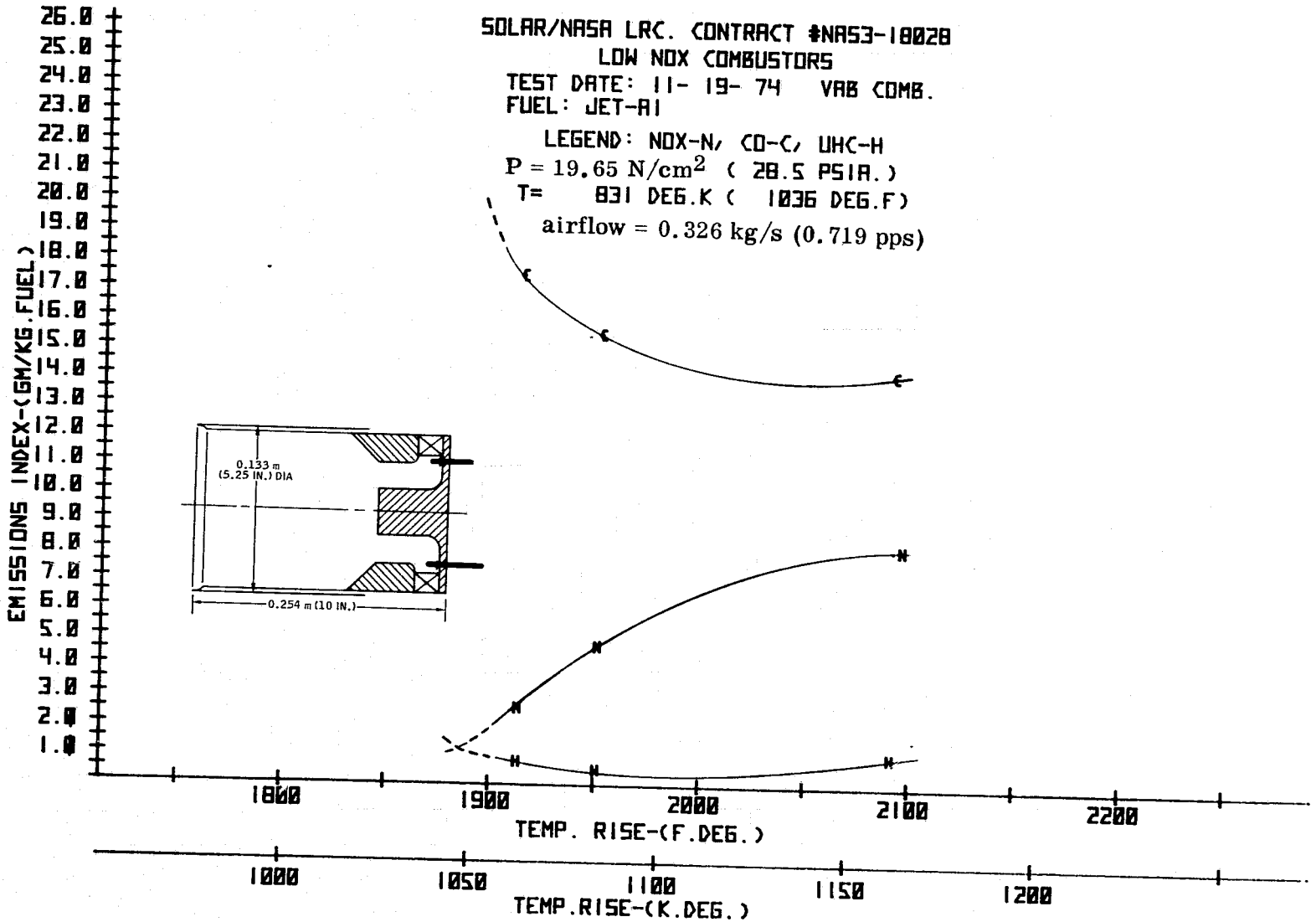
31

FIGURE 13. VAB COMBUSTOR TEST RESULTS - INITIAL CONFIGURATION

due to an inadequate diameter ratio between the swirler outlet channel and the reaction zone diameter. This parameter had been initially constrained by the imposition of the design reference velocity level of 30.48 m/sec (100 ft/sec). Inspection of the combustor at the completion of the initial tests indicated two potential secondary problems, namely:

- Overheating of the swirler centerbody caused by a flow separation at some point in the radial-to-axial flow transition zone with combustion stabilization in the separated region. This condition is shown in Figure 14.

- Fuel streaking on the swirler inner and outer walls caused by excessive fuel stream penetration prior to breakup and fuel "drips" attached to the fuel tubes in the flow wakes migrating to the inner wall.

Any combustion stabilization in the swirler throat due to flashback or auto-ignition would mean that the maximum, potential degree of pre-mixing was not being achieved prior to reaction. A modification of the swirler centerbody was made to increase the diameter from 0.043m (1.69 in.) to 0.051 m (2.0 in.) diameter in an effort to obviate the separation problem rather than instigate a comprehensive series of swirler tests. A yaw probe traverse was performed to characterize the modified
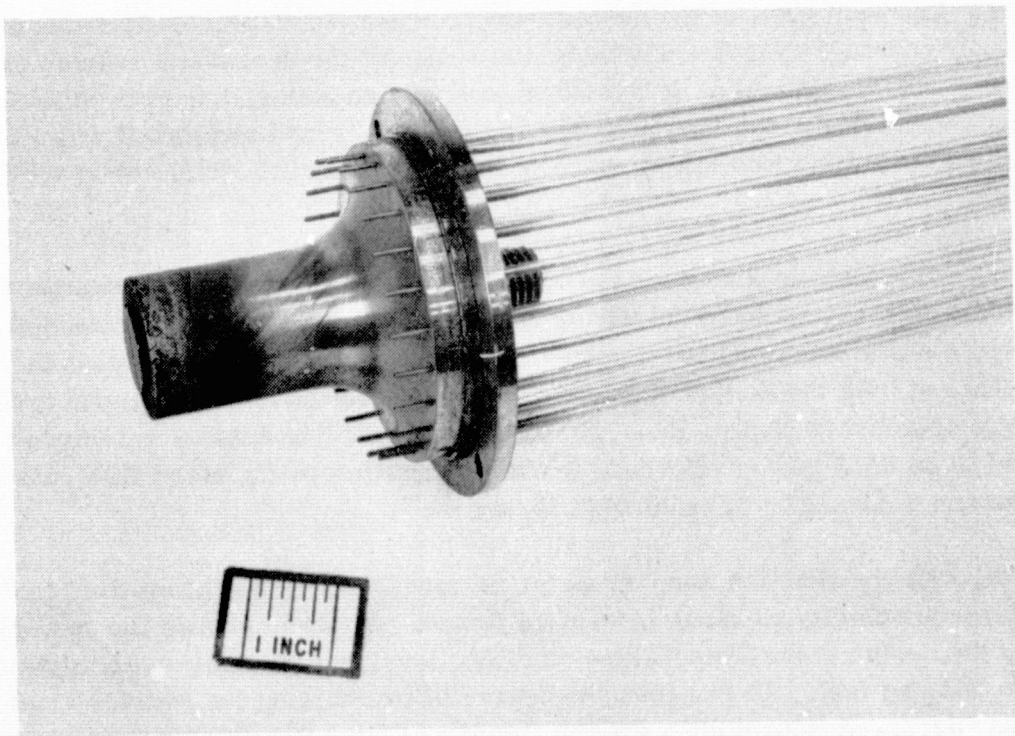

FIGURE 14. VAB COMBUSTOR - OVERHEATED SWIRLER CENTERBODY

swirler outlet flow. These results are shown in Figure 15 and depict the variation of swirl angle and absolute velocity across the swirler channel. Distinct values of both angle and velocity vector were monitored immediately adjacent to the swirler centerbody indicating the absence of any significant separation. The increase in swirler centerbody diameter resulted in a somewhat smaller outlet angle than the design figure of 90 degrees included.

The fuel streaking problem was obviated by a modification to the fuel injectors as shown in Figure 16. The penetration depth of the injector tube across the channel width was reduced and a drip fence added to prevent fuel running to the wall. Although Maybach (Ref. 5) demonstrated that film evaporation rates can be much higher than droplet evaporation rates, the much reduced surface area of such a film produces an overall lower rate of vaporization per unit time.

To improve the stabilization characteristics of the combustor, a major modification to the reaction zone size was made by increasing the outside diameter to 0.2 m (7.88 in.). The change is shown schematically in Figure 17. It can be seen that the overall length of the combustor was maintained constant and the same swirler components utilized. This required the step change in reaction zone diameter at inlet and outlet as shown.

The emissions characteristics of the configuration resulting from the fuel injection, swirler channel and reaction zone diameter modifications are shown in Figure 18. The lean limit of the system was improved to a combustor outlet temperature of approximately 1561°K (2350°F) by the action of the decreased swirler outlet/ reaction zone diameter ratio. It was concluded that an adequate degree of recirculation was being achieved with the reaction zone diameter increase and that it was likely that only solid body rotation was taking place in the initial smaller diameter reaction zone combustor.

As a result of concern over the operational combustor liner temperature levels, a preliminary assessment was obtained by attaching two thermocouples at opposite points midway along the combustor inner liner during the previous test run. The readings of both the thermocouples were closely comparable and the average results are depicted in Figure 19. The design point cooling annulus velocity was calculated to be 31.3 m/sec (103 ft/sec) with a specific cooling mass flow rate of approximately 1.158 kg/m^2 sec (0.0016 lb/sec in.^{2}).

Although the reaction zone diameter increase and the attendant drop in design point reference velocity to 13.48 m/sec (44 ft/sec) greatly improved the system stability, the design point temperature rise NO$_x$ level was at a relatively high level of 5.5 gm NO$_2$/kg fuel. To improve the degree of pre-mixing the swirler axial throat length was increased to provide a greater residence time for vaporization and mixing. This arrangement is shown schematically in Figure 20. In order to simplify the mod-
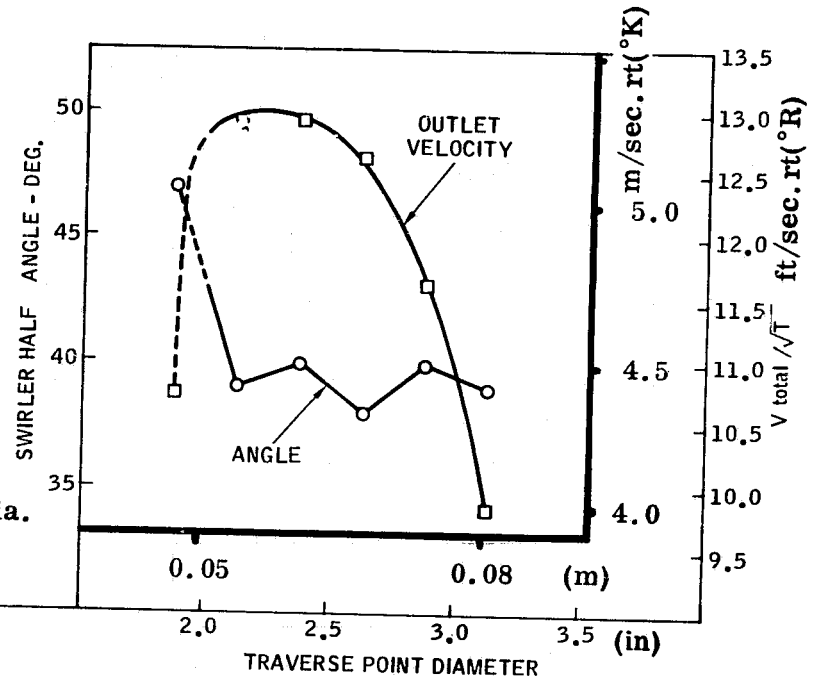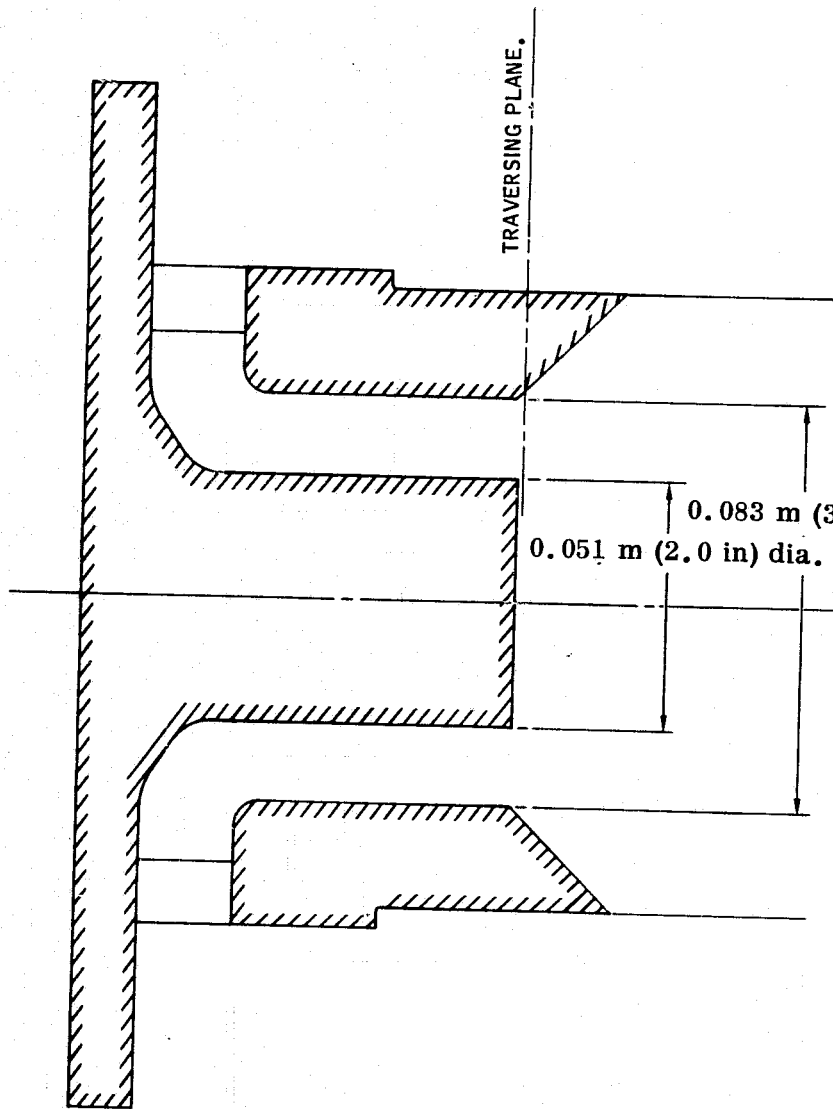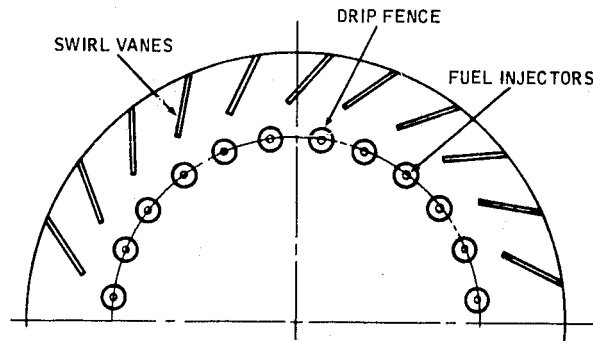
FIGURE 15. VAB COMBUSTOR – SWIRLER OUTLET CHARACTERISTICS

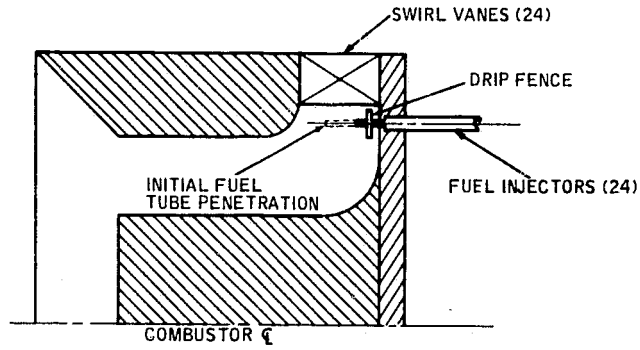FIGURE 16. VAB COMBUSTOR – FUEL INJECTOR MODIFICATION

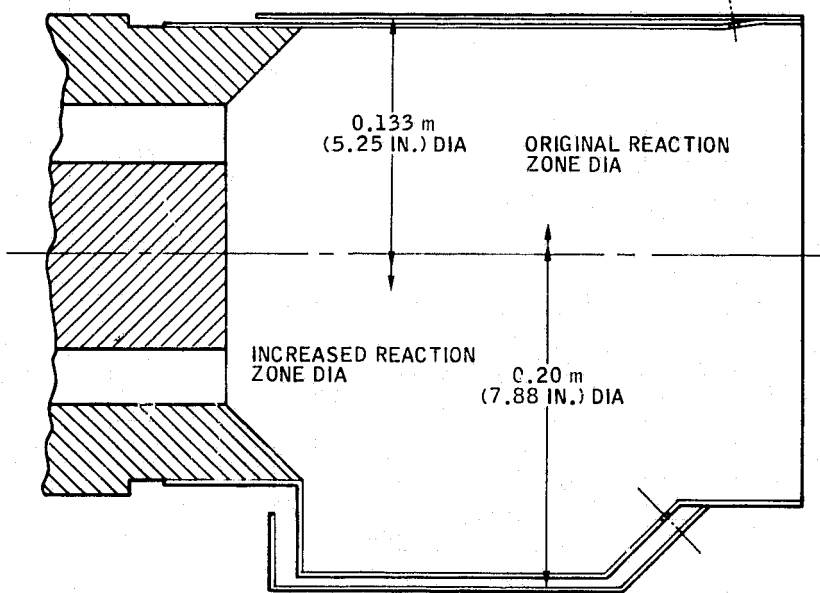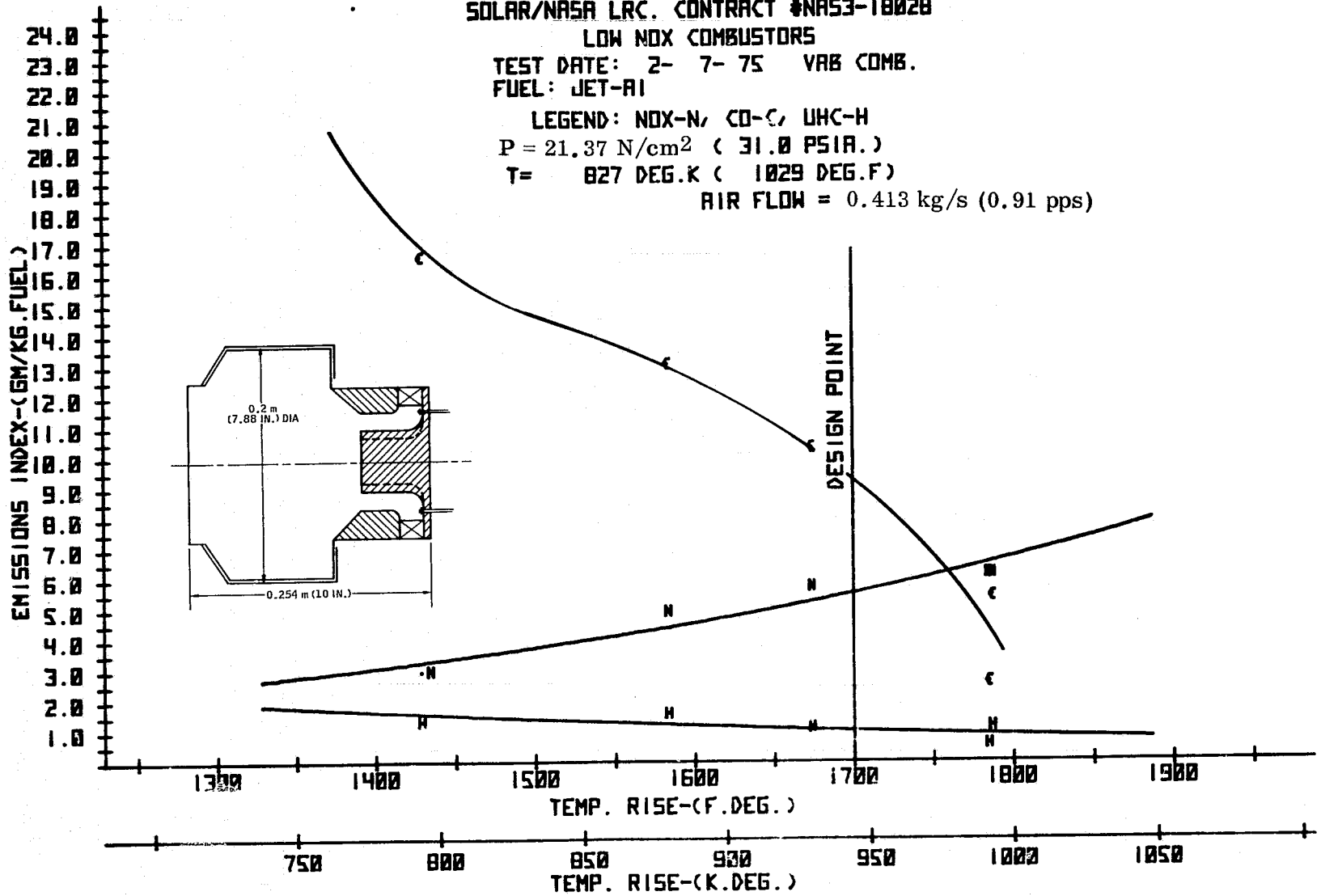FIGURE 17. VAB COMBUSTOR – REACTION ZONE DIAMETER INCREASE

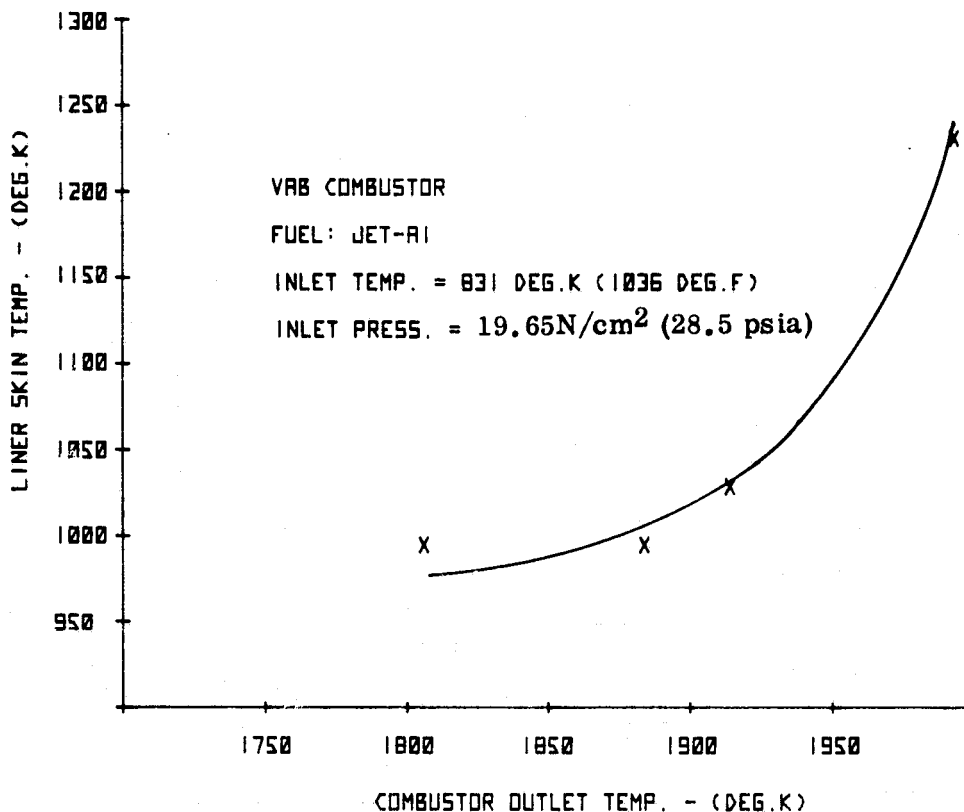FIGURE 18. VAB COMBUSTOR TEST RESULTS – INCREASED DIAMETER REACTION ZONE

FIGURE 19. VAB COMBUSTOR - LINER TEMPERATURES

ification, the swirler throat was extended into the reaction zone; hence a portion of the available reaction zone volume was effectively removed.

The emissions results of this configuration did demonstrate substantially lower NO_x levels but at the expense of considerably increased levels of CO and UHC. The results indicated that the reduction in available reaction volume had been too severe and that reaction was incomplete at the combustor outlet section where sampling was taking place.

To determine the exact required combustor length would have required an extensive sampling procedure at several axial planes. In order to expedite the test series, a gross change to the combustor length, greater than the effective reduction resulting from the increased swirler length, was made for evaluation. This is shown in Figure 21. The previous fuel injector and swirler throat length modifications were retained.

The emissions test results from this configuration are shown in Figure 22. It can be seen that the design temperature rise NO_x level was reduced to 2.4 gm NO_2/kg fuel with corresponding CO and UHC levels of 1.8 gm/kg fuel and 0.9 gm/kg fuel, respectively. The increase of the combustor volume was assumed to be instrumental in the reduction in the level of the unburnt species with the NO_x level reduction being obtained from the extended, axial, swirler throat producing a higher degree of premixing of the air and fuel.
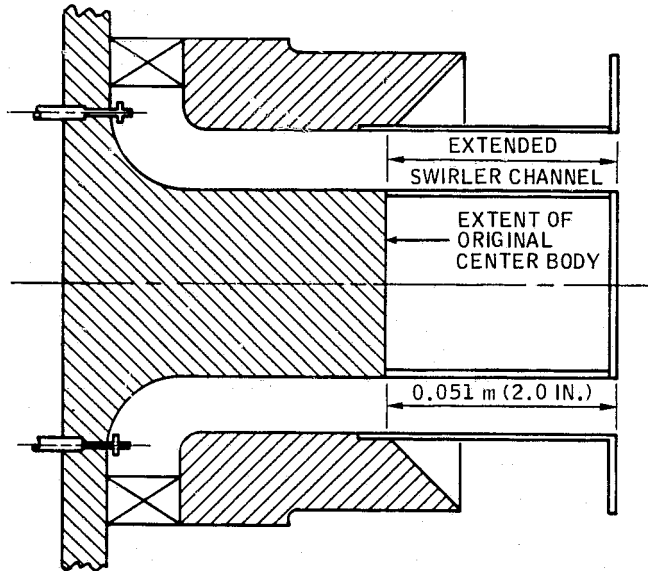
38

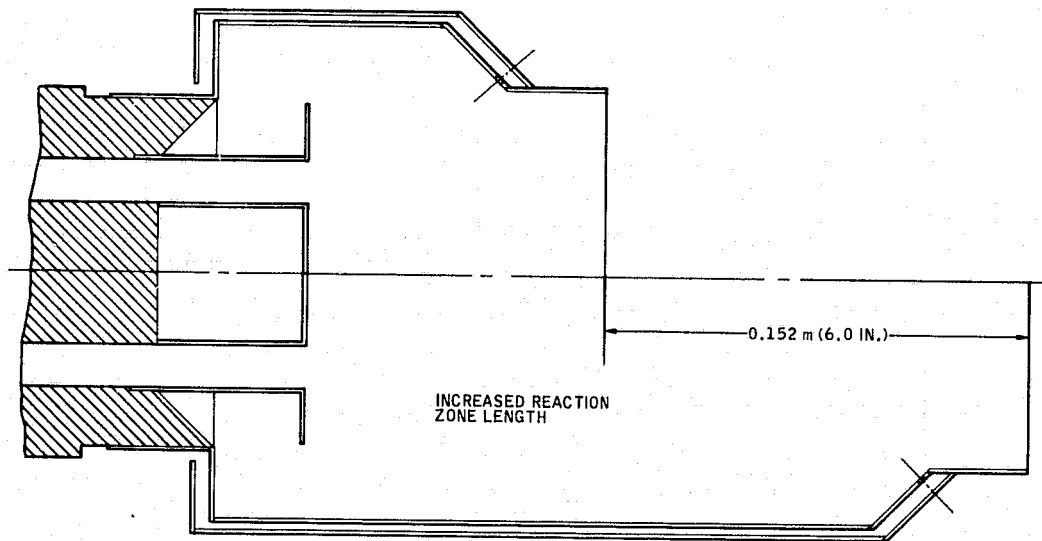FIGURE 20. VAB COMBUSTOR – SWIRLER THROAT LENGTH INCREASE

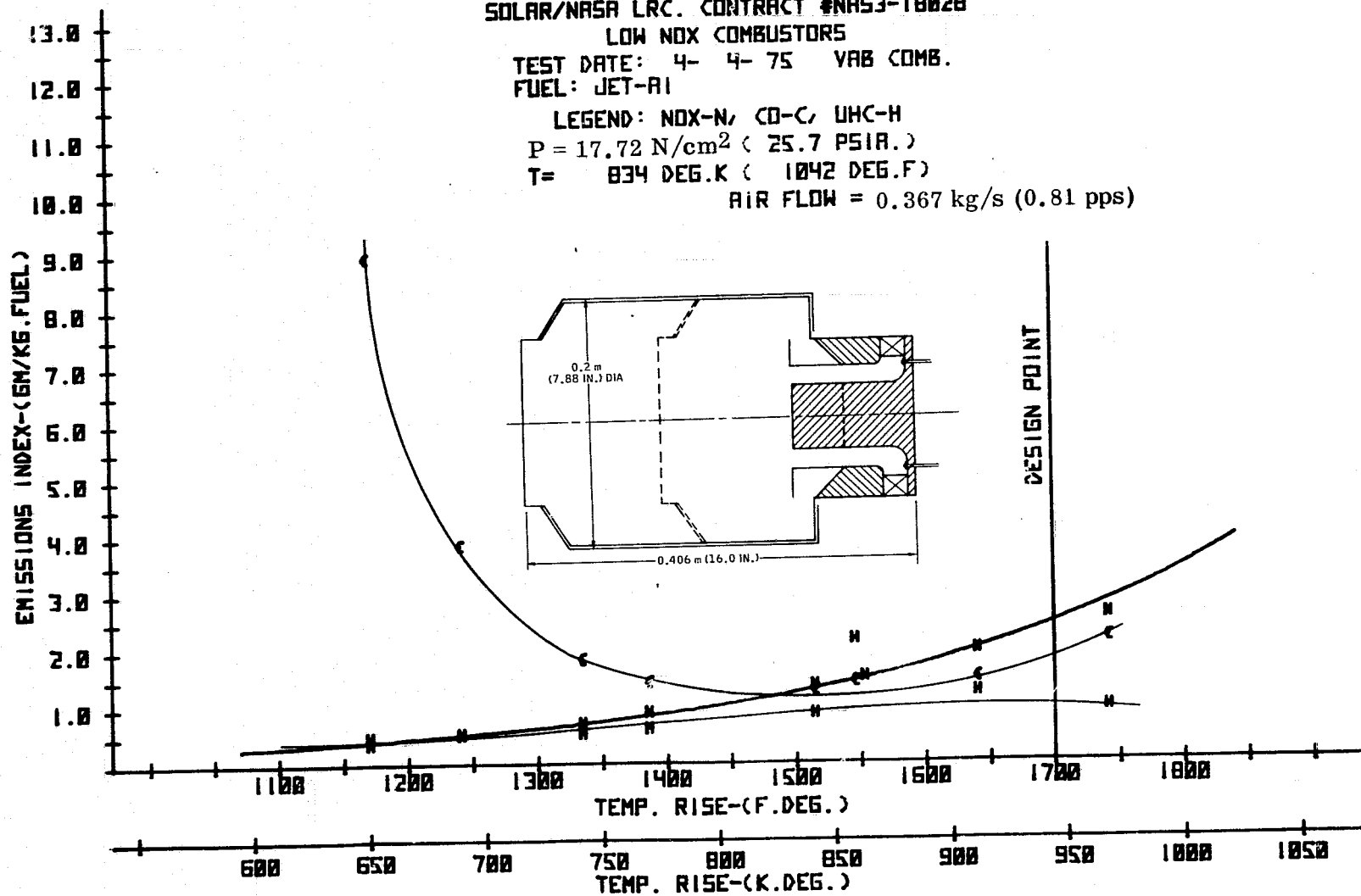FIGURE 21. VAB COMBUSTOR – REACTION ZONE LENGTH INCREASE

FIGURE 22. VAB COMBUSTOR TEST RESULTS – INCREASED LENGTH REACTION ZONE

The final modification to the VAB combustor consisted of a further change to the method of fuel injection. The modified scheme is shown in Figure 23. The existing fenced, single-point, fuel injector tubes situated slightly downstream of the vane trailing edge diameter were replaced by a system of 24 fuel tubes, 0.0032 m (0.125 in.) diameter, at the swirler vane inlet diameter, equally spaced between vanes. Each fuel tube was constructed with five, equally spaced, downstream injector holes each 0.0004 m (0.015 in.) diameter. This modification was intended to increase the degree of pre-mixing at the swirler exit by improving the initial fuel distribution.

By moving the fuel injection points outwards to a greater pitch diameter two effects are produced; a probable deterioration in atomization quality because of the reduced local air-blast velocities and an increase in the available radial mixing length.

The emissions results are depicted in Figure 24 where it can be seen that the design temperature rise NO_x level was reduced to 1.2 gm NO_2/kg fuel with CO and UHC levels of 1.0 gm/kg fuel and 0.1 gm/kg fuel respectively. It was considered likely that the improvement in NO_x emissions resulted largely from the enhanced initial fuel distribution and that the effects attendant upon the fuel injector pitch diameter change were only of secondary importance. A survey was made with a Von Brand smokemeter during this test run. Essentially zero smoke was measured across the complete characteristic.

A review of the effects on the NO_x emissions of the various modifications is given in Figure 25. The initial and final combustor configurations are outlined in Table I for comparison purposes. All subsequent tests were made with the final combustor configuration shown in Table I.

No further modifications to the combustor were made at this point due to program schedule restrictions, although it was recognized that further NO_x improvements were perhaps possible by further investigation or extensions of the ideas that had already been shown to be effective, such as swirler throat length increases or a larger number of fuel injection points.

5.1.2 Effect of Fuel Type

As a demonstration of the importance of adequate control of the vaporization and fuel/air mixing processes, comparative tests were run with the final VAB combustor configuration on a #2 Diesel fuel and an EPA reference gasoline. These emissions characteristics are shown in Figure 26 and Figure 27 respectively. The composite results are shown in Figure 28. It can be seen that the gasoline NO_x characteristic was closely comparable to that of the main test fuel Jet-A1, the differences being in the realm of experimental error levels. This suggests that the performance of the combustor was largely limited by the air/fuel mixing levels attained within the swirl passage as the lighter, more volatile, gasoline fuel with its higher vaporization rates had not produced a significant NO_x improvement.
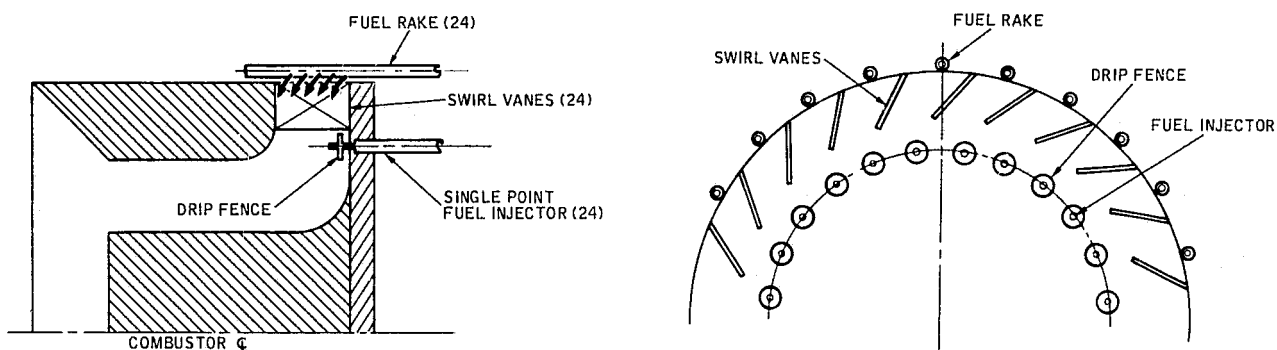
FIGURE 23. VAB COMBUSTOR - FUEL INJECTION MODIFICATION

The heavier #2 Diesel fuel displayed a considerably higher level of NO_x formation; the design temperature rise NO_x of almost 4.0 gm NO_2/kg fuel can be compared to the figure of 1.2 gm NO_2/kg fuel obtained with the Jet-A1 test fuel. It should be noted, however, that an analysis of the #2 Diesel for bound nitrogen content showed a level of 490 ppm N by weight. The same modified Kjeldahl test method showed essentially zero bound nitrogen in the Jet-A1 and gasoline fuels.

Recent work by Heywood and Appleton (Ref. 7) suggests that conversion of fuel bound nitrogen in lean, well-mixed reactors is very rapid and can occur at essentially 100 percent conversion efficiency. The same trend has been noted by others, especially at low values of nitrogen concentration (Ref. 8).

If the total bound nitrogen in the #2 Diesel were to be converted to NO_x with 100 percent conversion efficiency, then a level of approximately 1.6 gm NO_2/kg fuel would have resulted; hence a large portion of the NO_x level deterioration was considered due to a reduced degree of pre-mixing attained in the swirler passage due to the combination of a slight increase in the mean droplet size and the reduced vaporization rates of the less volatile fuel.

The CO levels for the three fuels were closely comparable at the design point temperature rise although the gasoline characteristic was surprisingly higher than
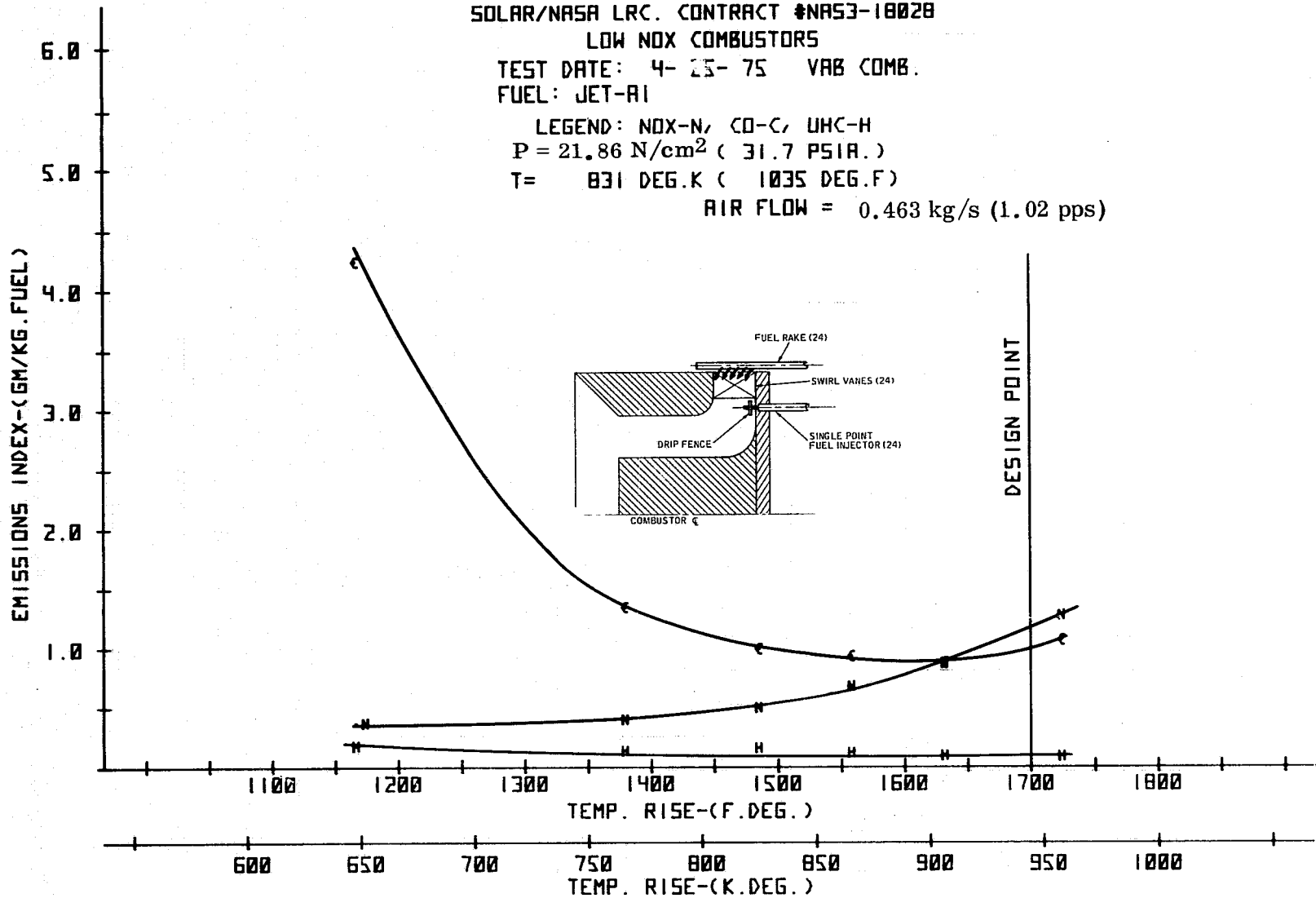
FIGURE 24. VAB COMBUSTOR TEST RESULTS – MODIFIED FUEL INJECTION
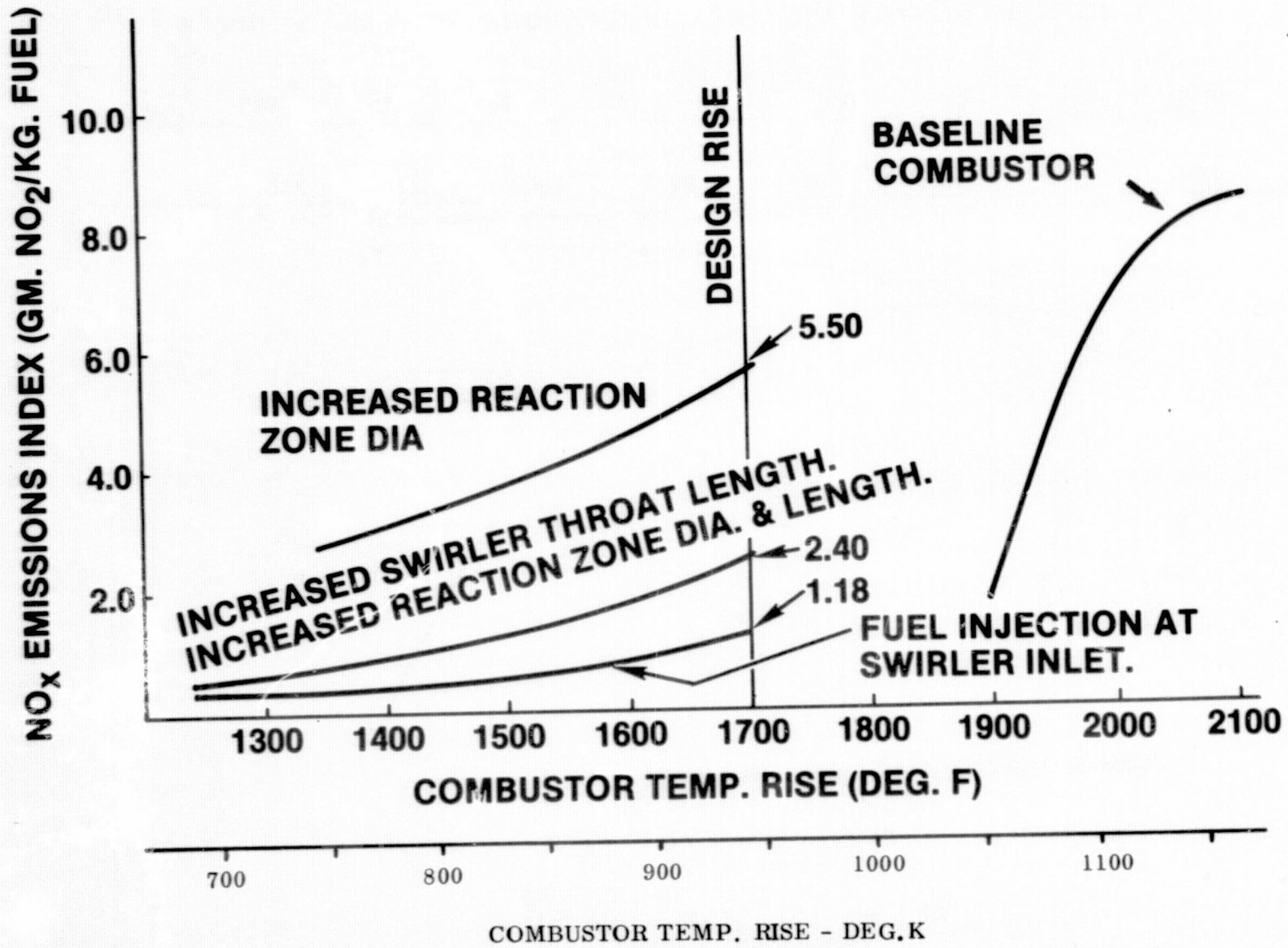
FIGURE 25. VAB COMBUSTOR NO$_x$ TEST RESULTS

TABLE I

VAB COMBUSTOR CONFIGURATIONS

Item	Initial	Final
Fuel Injection	. Air Blast . Single mid-channel point . Downstream of vane trailing edge	. Air Blast . Five points across channel width . Upstream of vane leading edge
Swirler Channel	Outlet section: . Inner diameter = 0.043 m . Outer diameter = 0.083 m	Outlet section: . Inner diameter = 0.051 m . Outer diameter = 0.083 m Outlet channel length increased by 0.054 m
Reaction Zone	Outside diameter = 0.133 m Overall length = 0.140 m	Outside diameter = 0.200 m Overall length = 0.291 m

either the Jet-A1 or #2 Diesel fuels over most of the operating range. There appears to be no satisfactory explanation for this effect and experimental error seems likely.

5.1.3 Effect of Combustor Inlet Pressure

As previously noted, the screening test data were obtained at combustor inlet pressures considerably lower than the design point cruise pressure of 50.68 N/cm^2 (5 atm). The effects of combustor inlet pressure were evaluated, however, on the final VAB combustor configuration.

An emissions signature was obtained at a pressure closely comparable to the design point inlet pressure and this is shown in Figure 29. The CO level was reduced markedly by the decrease in combustor loading as would be expected from well-stirred reactor theory. The high and low pressure NO_x characteristics are compared in Figure 30, and it can be seen that the high pressure NO_x level was slightly lower than the low pressure characteristic. This in itself is not significant as the difference is small and approaching the limits of experimental accuracy. The lack of a significant pressure effect is unusual, however, when the NO_x formation kinetics for a well-stirred reactor predict a square root pressure effect at constant reaction temperature. The lack of a NO_x dependency on pressure, at least within the tested range, could be explained by an improvement in vaporization rates due to the higher heat transfer with increased Reynolds number and improved atomization at the high pressure level.

46

EMISSIONS INDEX-(GM/KG.FUEL)

5.0

4.0

3.0

2.0

1.0

SOLAR/NASA LRC. CONTRACT #NAS3-18028
LOW NOX COMBUSTORS
TEST DATE: 4- 25- 75   VAB COMB
FUEL: #2 D.
    LEGEND: NOX-N, CO-C, UHC-H
 $P = 22.55 \text{ N/cm}^2$ (32.7 PSIA.)
 T=   831 DEG.K (1035 DEG.F)
              AIR FLOW = 0.467 kg/s (1.03 pps)

DESIGN POINT

1100   1200   1300   1400   1500   1600   1700   1800

TEMP. RISE-(F.DEG.)

650   700   750   800   850   900   950   1000

TEMP. RISE-(K.DEG.)

FIGURE 26.   VAB COMBUSTOR TEST RESULTS - #2 DIESEL FUEL
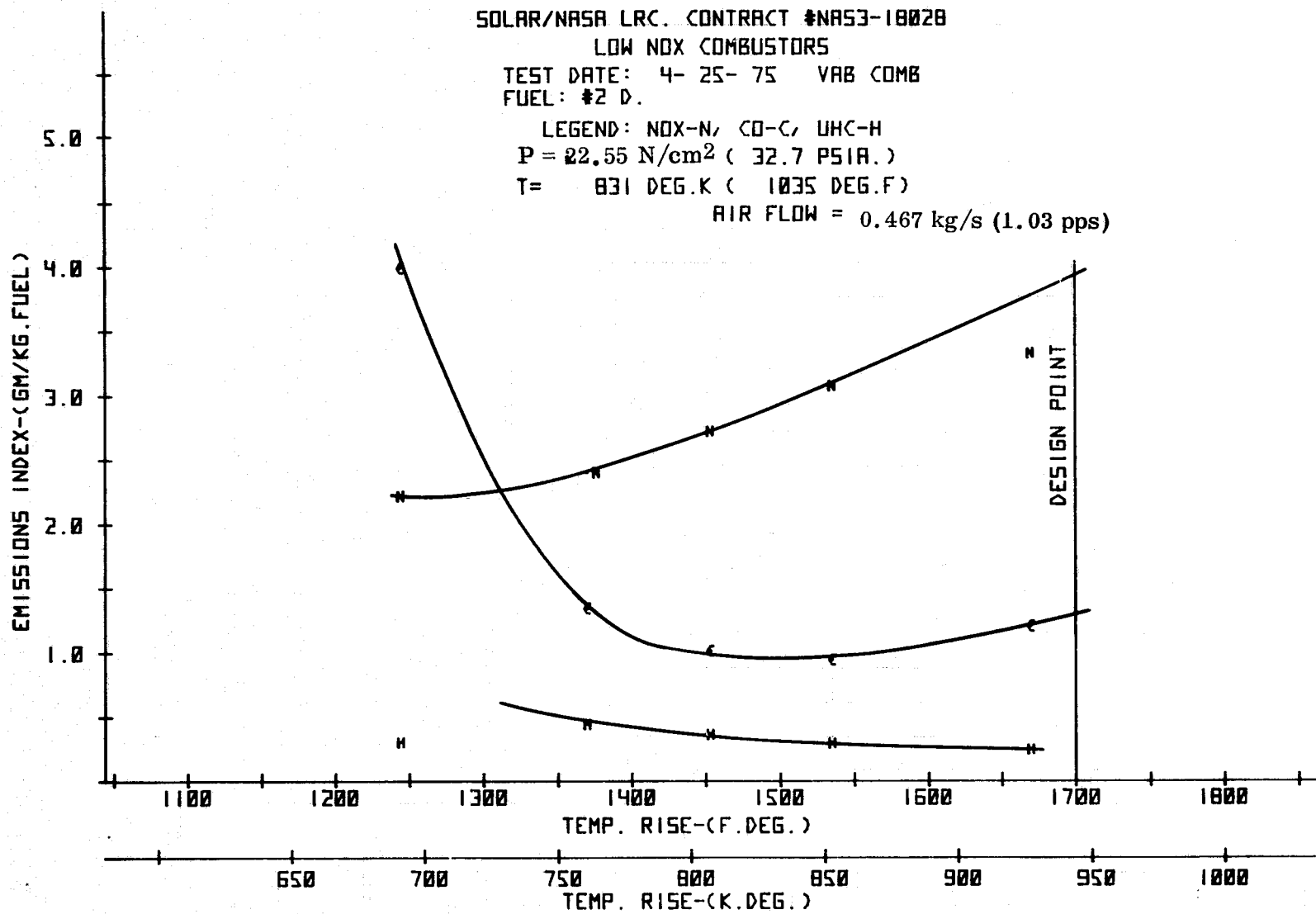
SOLAR/NASA LRC. CONTRACT #NAS3-18028
LOW NOX COMBUSTORS
TEST DATE: 6- 4- 75   VAB COMB.
FUEL: GASOLINE.
LEGEND: NOX-N, CO-C, UHC-H
$P = 20.48 \text{ N/cm}^2$ (29.7 PSIA.)
T=   833 DEG.K (1040 DEG.F)
AIR FLOW = 0.422kg/s (0.93 pps)

EMISSIONS INDEX-(GM/KG.FUEL)

DESIGN POINT

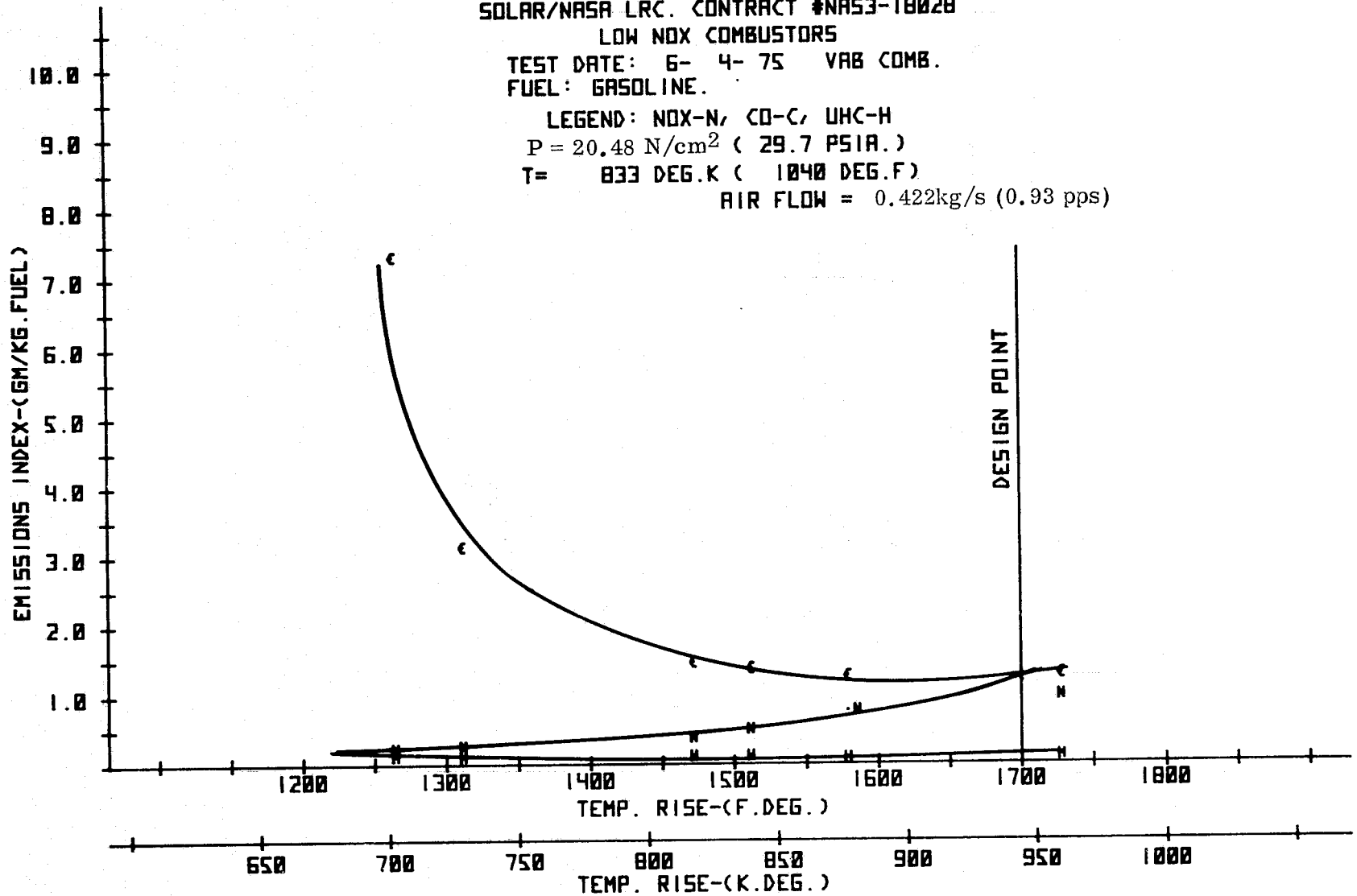TEMP. RISE-(F.DEG.)

TEMP. RISE-(K.DEG.)

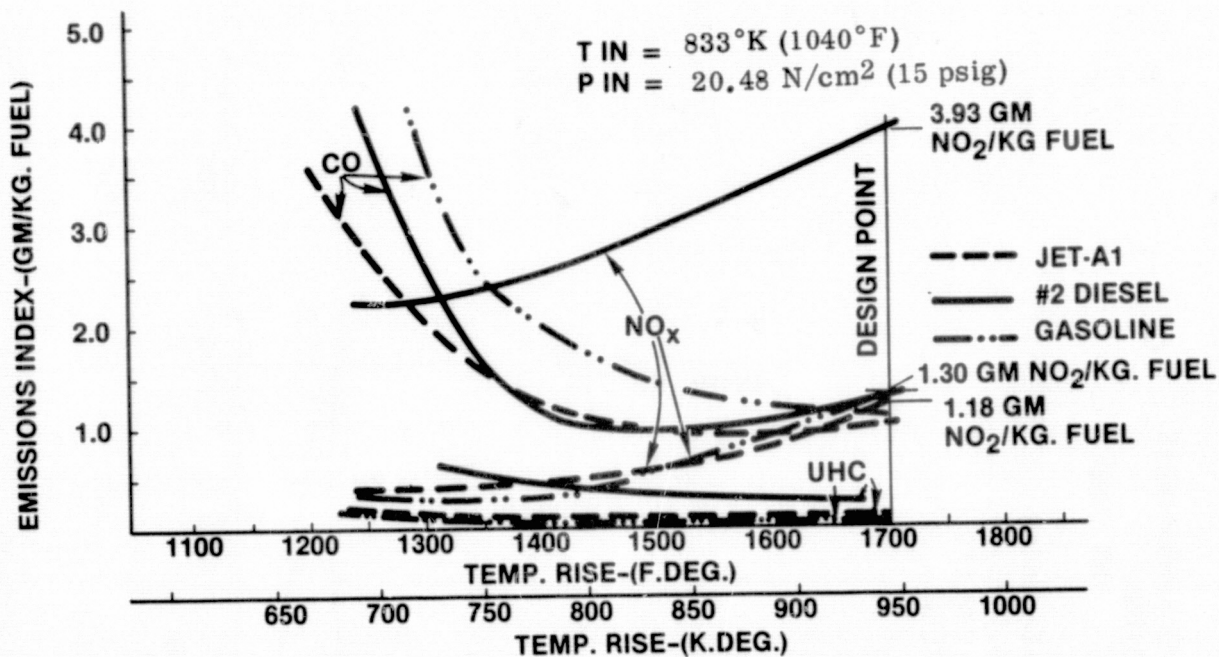FIGURE 27.   VAB COMBUSTOR TEST RESULTS - GASOLINE FUEL

FIGURE 28.   VAB COMBUSTOR TEST RESULTS – EFFECT OF FUEL TYPE

The lack of a pressure dependency was confirmed at a slightly lower combustor inlet temperature.   Comparative NO_x level characteristics for high and low combustor inlet pressures at two combustor inlet temperatures are given in Figure 31.

5.1.4   Effect of Combustor Inlet Temperature

The final VAB combustor configuration was tested over a range of inlet temperatures as a preliminary attempt to assess the potential emissions of such a system at an engine off-design condition, such as idle.

The results, shown in Figures 32 and 33, represent the NO_x and CO emissions signatures, respectively, over a range of combustor inlet temperatures from 831°K (1035°F) to 419°K (295°F).   It can be seen that as the combustor inlet temperature was reduced at constant reaction temperature, the NO_x level increased initially.   This is a result of the decrease in the driving force level for the vaporization process, the net result being a progressively higher degree of "unmixedness" as the inlet temperature decreases.   At an inlet temperature of 756°K (900°F) the NO_x was only slightly higher than that at the 831°K (1035°F) inlet, indicating that the available degree of premixing with the combustor configuration in question had already been closely reached at an inlet of 756°K (900°F).

48

SOLAR/NASA LRC. CONTRACT #NAS3-18028
LOW NOX COMBUSTORS
TEST DATE: 5- 10- 75   VAB COMB.
FUEL: JET-A1
LEGEND: NOX-N, CO-C, UHC-H
$P = 49.44 \text{ N/cm}^2$ (71.7 PSIA.)
T=   819 DEG.K (1015 DEG.F)
AIR FLOW = 0.916 kg/s (2.02 pps)

DESIGN POINT

EMISSIONS INDEX-(GM/KG.FUEL)

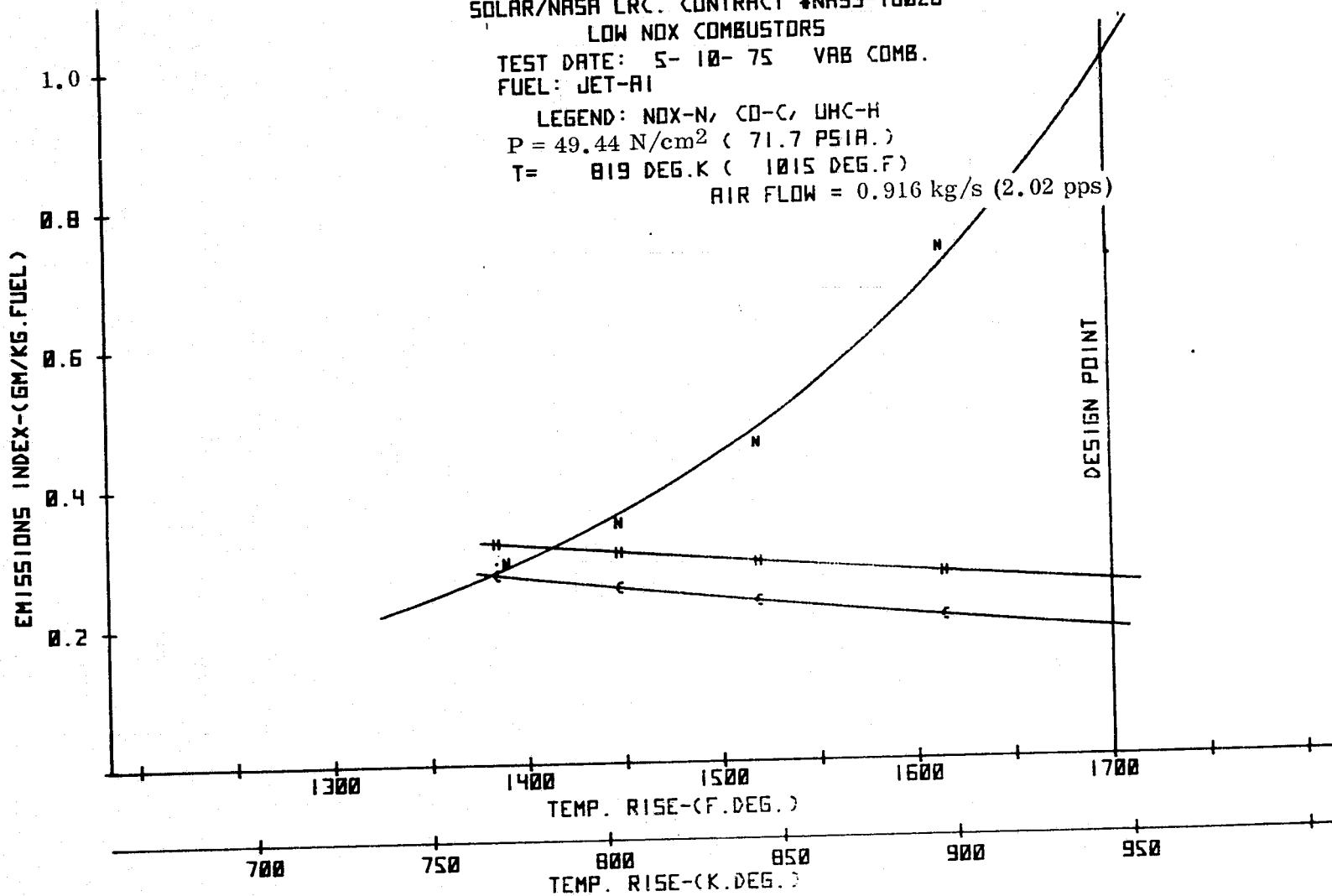TEMP. RISE-(F.DEG.)

TEMP. RISE-(K.DEG.)

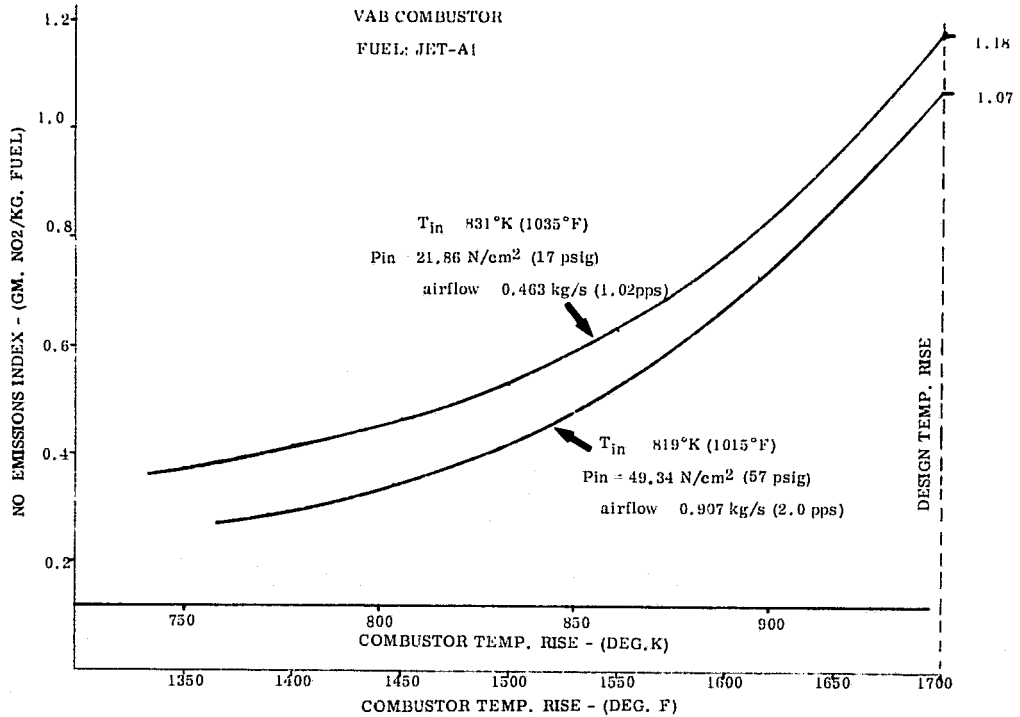FIGURE 29.   VAB COMBUSTOR TEST RESULTS - HIGH PRESSURE

49

FIGURE 30. VAB COMBUSTOR TEST RESULTS

At levels below approximately 478°K (400°F) the trend of increasing NO_X with decreasing inlet temperature reversed at the high equivalence ratios. This can be seen from Figure 34 that represents the NO_X emission index as a function of combustor inlet temperature at a constant reaction temperature. This can be understood by reference to a typical global rate equation for NO production obtained from the forward rate of the controlling reaction in the Zeldovich two step mechanism,

$$\frac{d}{dt}[NO] = 6.62 \times 10^{13} \exp\left[\frac{-67,000}{T}\right] \left\{\frac{[N_2][O_2]^{1/2} P^{1/2}}{T^{1/2}}\right\} \tag{7}$$

where,

$$[O_2], [N_2], [NO] = \text{mole fractions}$$

$$T = \text{temperature, °K}$$

$$P = \text{pressure, atm}$$

$$\frac{d}{dt}[NO] = \text{mole fraction per sec}$$

Examination of the expression reveals that the dominant factor is the exponential dependency of the NO formation rate upon the reaction temperature. At constant

50

VAB COMBUSTOR

FUEL: JET-A1

756°K, 20.48 N/cm²
(900°F, 15 psig)
756°K, 51.51 N/cm²
(900°F, 60 psig)
819°K, 49.44 N/cm²
(1015°F, 57 psig)
831°K, 22.55 N/cm²
(1035°F, 17 psig)

FIGURE 31. VAB COMBUSTOR TEST RESULTS – EFFECT OF COMBUSTOR INLET PRESSURE

FUEL: JET-A1

COMB. PRESS. IN. = $20.48 \ N/cm^2$ (15 psig)

VAB COMBUSTOR

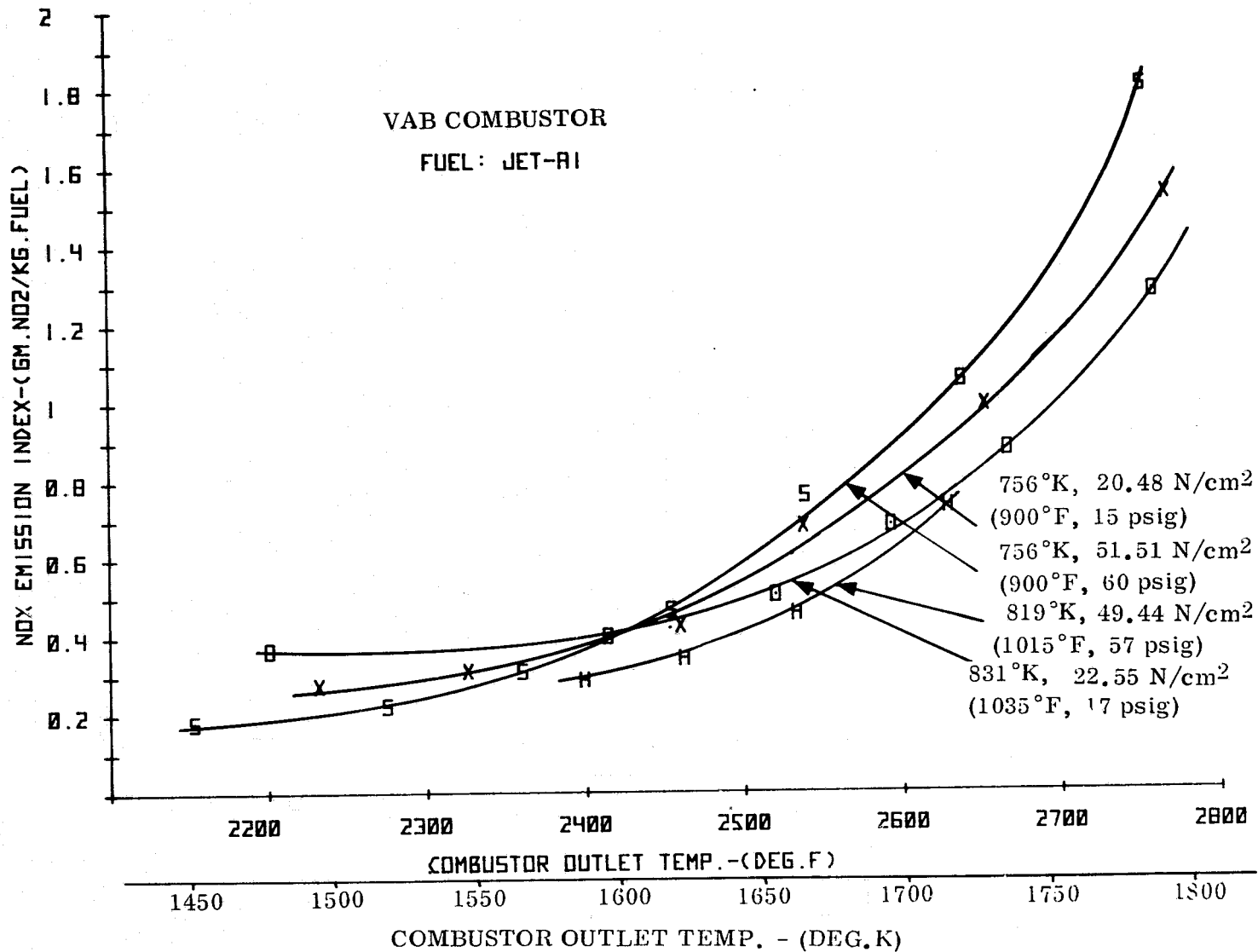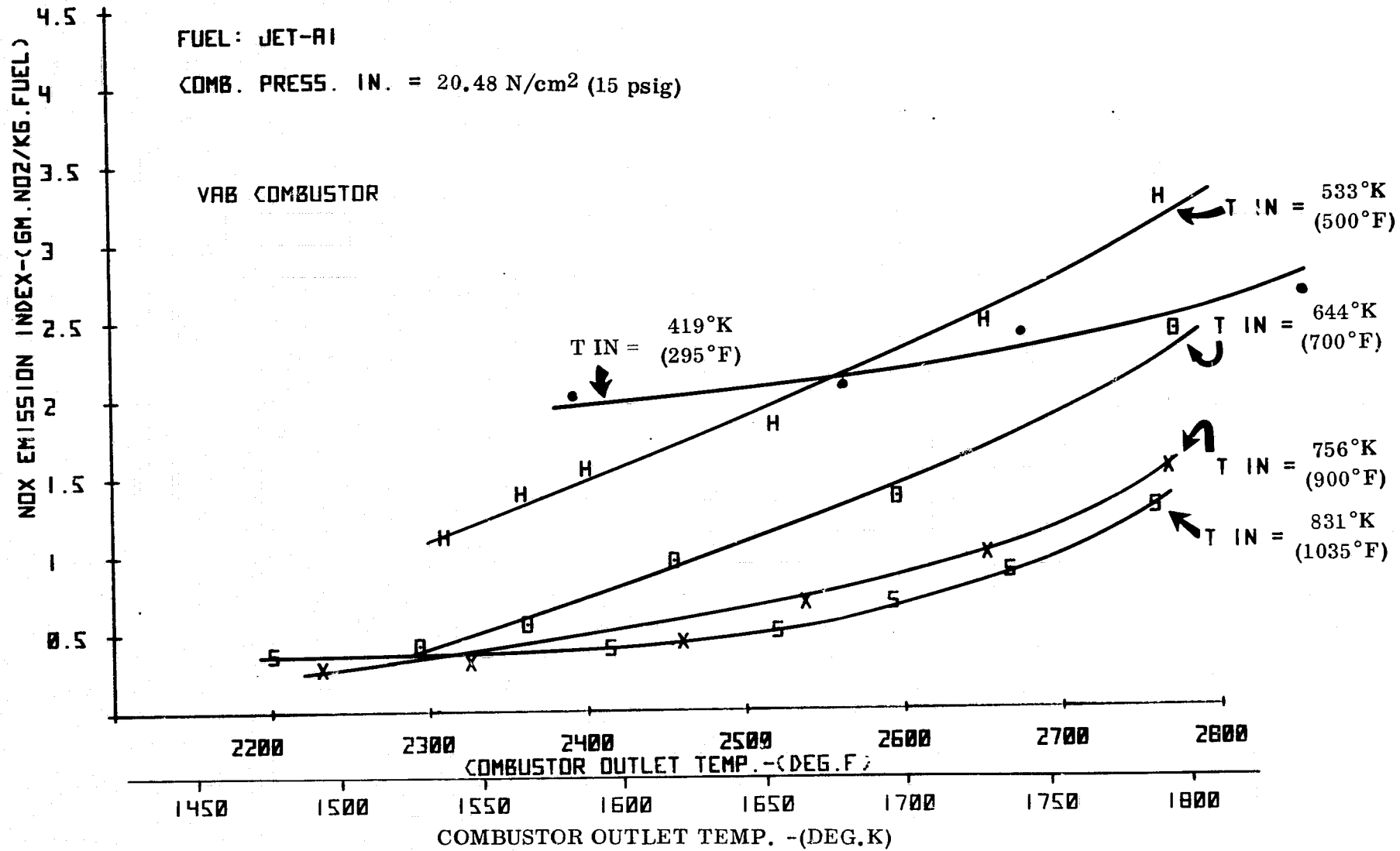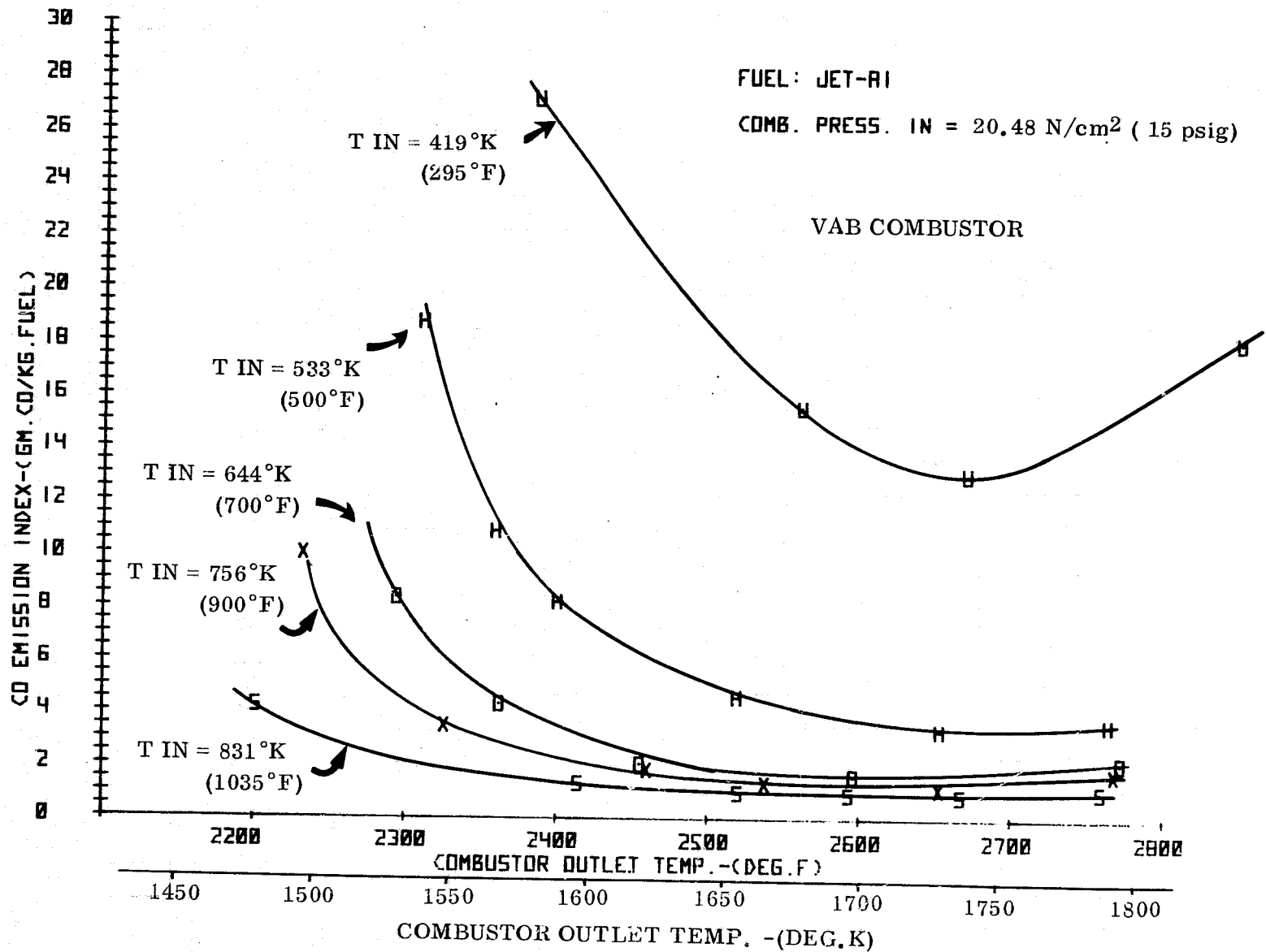FIGURE 32. VAB COMBUSTOR NO_x TEST RESULTS – EFFECT OF COMBUSTOR INLET TEMPERATURE

FIGURE 33. VAB COMBUSTOR CO TEST RESULTS – EFFECT OF COMBUSTOR INLET TEMPERATURE
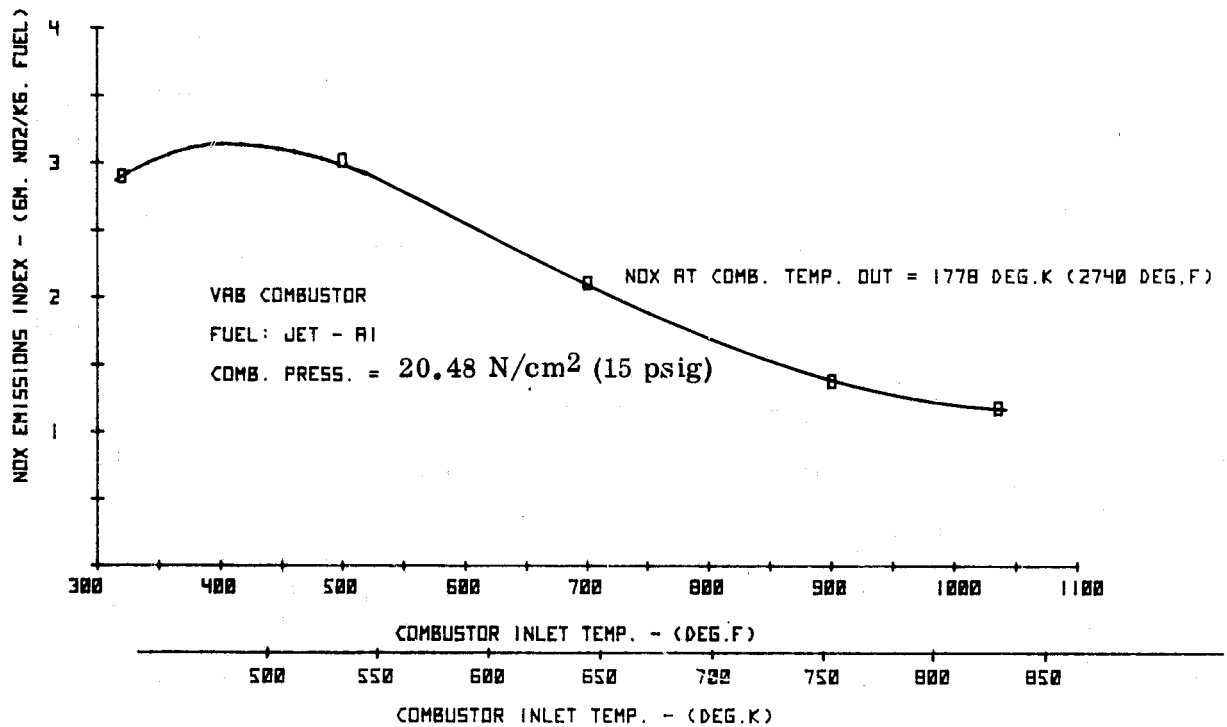
FIGURE 34. VAB COMBUSTOR NO_x TEST RESULTS

reaction temperature, however, as the combustor inlet temperature is reduced, the reaction zone equivalence ratio increases and the post-hydrocarbon reaction oxygen concentration decreases. At low inlet temperatures below approximately 478°K (400°F), and high equivalence ratios, the $[O_2]^{1/2}$ factor in the NO formation equation becomes significant and overall NO levels drop. The reduction in NO_x at very low temperatures and high equivalence ratios would not normally be of interest within the context of the operation of an aircraft gas turbine combustor. At the low combustor inlet temperatures representative of idle, the required combustor exit temperatures would also be quite low and the combustor would likely be operating in the region where the effect is not apparent.

In addition, the shape of the lowest inlet temperature NO_x characteristic differs somewhat from the other characteristics, particularly those at the intermediate inlet temperatures, the former being less sensitive to high levels of reaction zone equivalence ratio. This may be the result of the high level of "unmixedness" in the fuel/air charge at the low inlet temperatures in addition to the post-reaction oxygen effect mentioned previously and tends to confirm the findings of Appleton and Heywood (Ref. 7) and Heywood and Pompei (Ref. 9) in their studies of the role of mixing in nitric oxide generation, where nitric oxide formation rate was found to increase with increasing "unmixedness" at low mean equivalence ratios and to decrease with increasing "unmixedness" at a stoichiometric condition. In addition, the dependency of the nitric oxide production rate on the mean reaction equivalence ratio decreased markedly as

54

"unmixedness" increased, moving from a strong exponential dependency at high levels of mixing to an almost constant rate independent of equivalence ratio at high values of "unmixedness".

The corresponding CO characteristics are depicted in Figure 33. As might be expected the CO levels increased with decreasing combustor inlet temperatures, this again is predicted by "unmixedness" considerations. At the lowest inlet temperatures, the CO levels increased with increasing combustor outlet temperature. This is due to an increasing equilibrium CO level for a given combustor configuration and an over-loading of the reaction zone at the high equivalence ratios possibly resulting in some premature quenching of the reaction by the liner cooling air injection. At an inlet temperature of 419°K (295°F) CO levels were generally between 15 gm/kg fuel and 30 gm/kg fuel depending on the operating point. This is indicative of the level of CO emissions that might be obtained at an engine idle condition.

As the combustor inlet temperature decreased, the lean stability limit, as defined by rapid increases in CO emissions, occurred at increasingly higher combustor outlet temperatures.

Particulate emissions surveys taken during the high inlet pressures and the low inlet temperature test runs indicated zero smoke at all operating conditions.

5.2 JIC COMBUSTOR

5.2.1 Combustor Modifications

The initial tests of the JIC combustor were conducted on the baseline config-uration described in Section 3.1.1. The emissions characteristics are shown in Figure 35 with the emissions indices of NO_x, CO and UHC plotted as a function of combustor temperature rise. The characteristics were typically those of a well stirred reactor; the NO_x level displayed an exponential dependency on reaction tem-perature and the CO and UHC values increased rapidly prior to the lean extinction limit which is shown as a bar on the NO_x characteristic.

The design point temperature rise NO_x of 5.3 gm NO_2/kg fuel was in excess of the results obtained with similar combustors during Solar's past experimentations and improvements were obviously a possibility.

To evaluate the effects of initial fuel distribution, the injection system was modified to that shown in Figure 36. The single point fuel injection system was replaced by a multi-point design where a 0.0032 m (0.125 in.) diameter fuel tube crossed the mixing tube entry at two perpendicular diameters. A total of 13 fuel injection holes 0.00038 m (0.015 in.) diameter were spaced on the fuel tube as shown in an upstream facing orientation, that is with the fuel injection against the incoming

SOLAR/NASA LRC. CONTRACT #NAS3-18028
LOW NOX COMBUSTORS
TEST DATE: 12- 5- 74   JIC COMB.
FUEL: JET-A!
    LEGEND: NOX-N, CO-C, UHC-H
P = 18.41 N/cm^2 (26.7 PSIA.)
T=   839 DEG.K (1051 DEG.F)
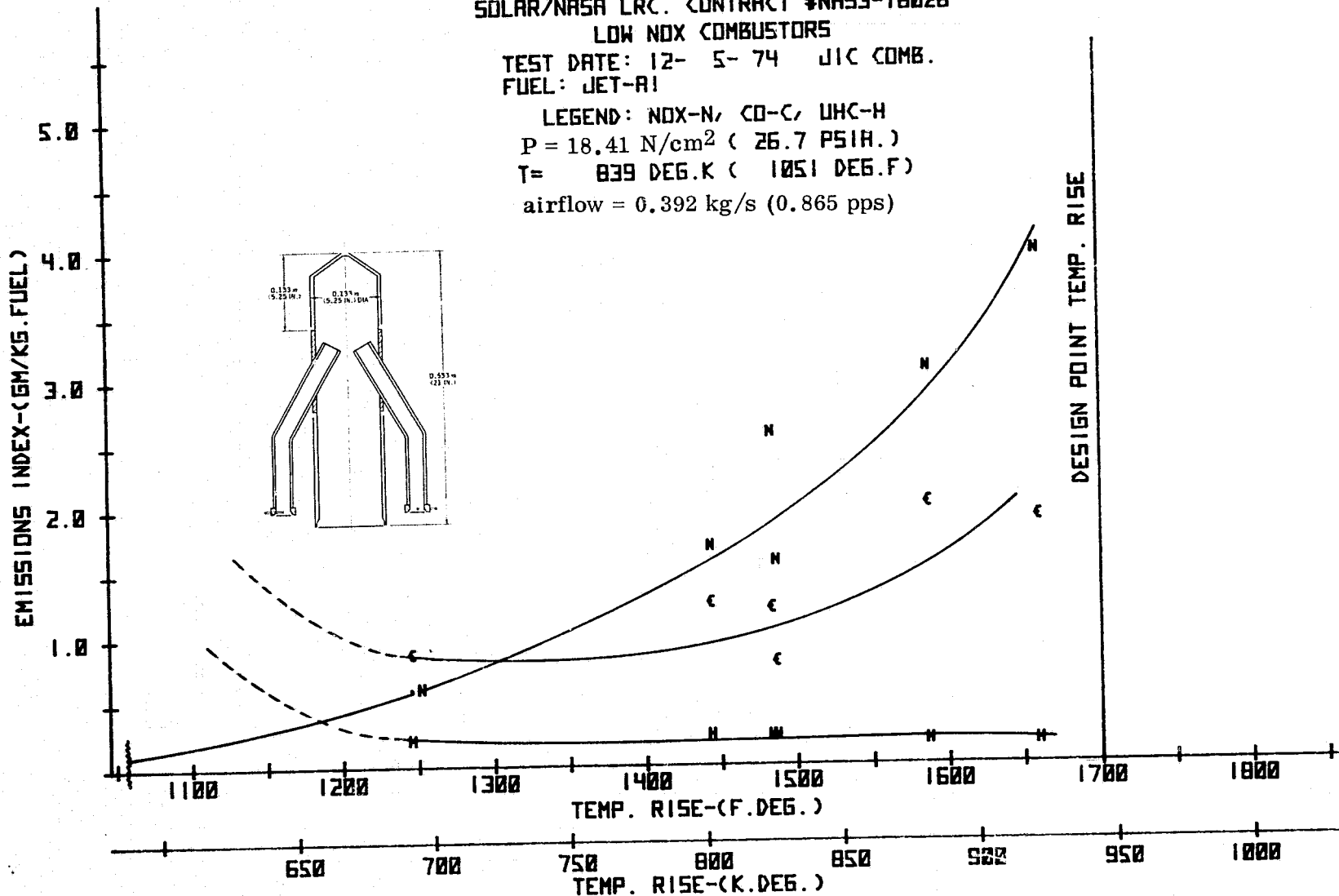airflow = 0.392 kg/s (0.865 pps)

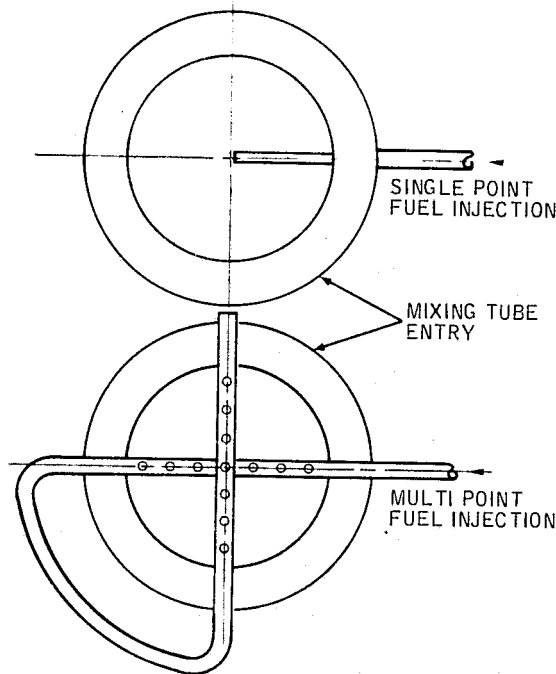FIGURE 35.   JIC COMBUSTOR TEST RESULTS - INITIAL CONFIGURATION

FIGURE 36. JIC COMBUSTOR - FUEL INJECTOR MODIFICATION

air flow. This provided an additional degree of spreading with the slight penetration of each fuel stream into the airflow before atomization occurred.

In Section 3.1.2 with reference to the diffusion equation (5), it was shown that single point fuel injection, even with complete evaporation of the fuel, could result in minimum and maximum fuel/air ratios at the mixing tube outlet of 34.7 and 138.1 percent, respectively, of the weighted average. Using a modification of the same diffusion equation it can be shown that for the same conditions and a 3-concentric ring manifold fuel injection system, the maximum and minimum fuel/air ratios at the tube outlet are improved to approximately ±6.0 percent above and below the weighted average.

A test of the modified combustor resulted in the characteristic shown in Figure 37. The design point temperature rise NO_x was reduced from the initial level of 5.3 gm NO_2/kg fuel to 3.3 gm NO_2/kg fuel with a slight change in CO emissions from 2.7 gm/kg fuel to 3.0 gm/kg fuel. Due to this slight increase in CO, a repeat of the test run was performed with the inter-port splash cooling strips removed in an effort to assess the possible effects of the cooling air injection on the unburnt species levels. The combustor configuration was otherwise identical to the previous run. The emissions results are shown in Figure 38 where at the design point temperature rise, the NO_x was found to be 3.0 gm NO_2/kg fuel with a CO level of 2.0 gm/kg fuel. This improvement in CO indicated the importance of careful control of the type and level of skin cooling as it is likely that the admission of the cooling airflow from the inter-port splash cooling strips
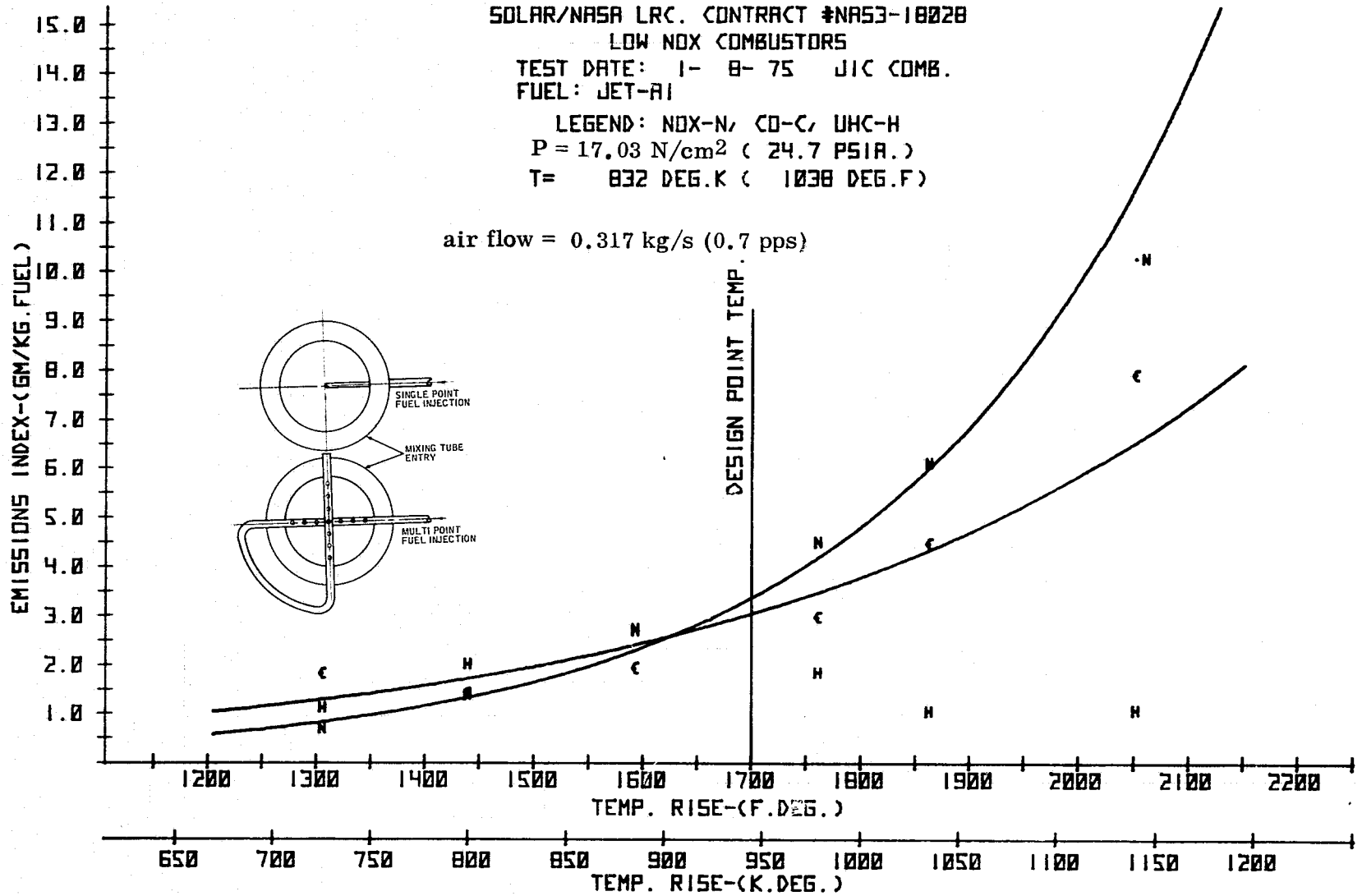
FIGURE 37. JIC COMBUSTOR TEST RESULTS - MODIFIED FUEL INJECTION
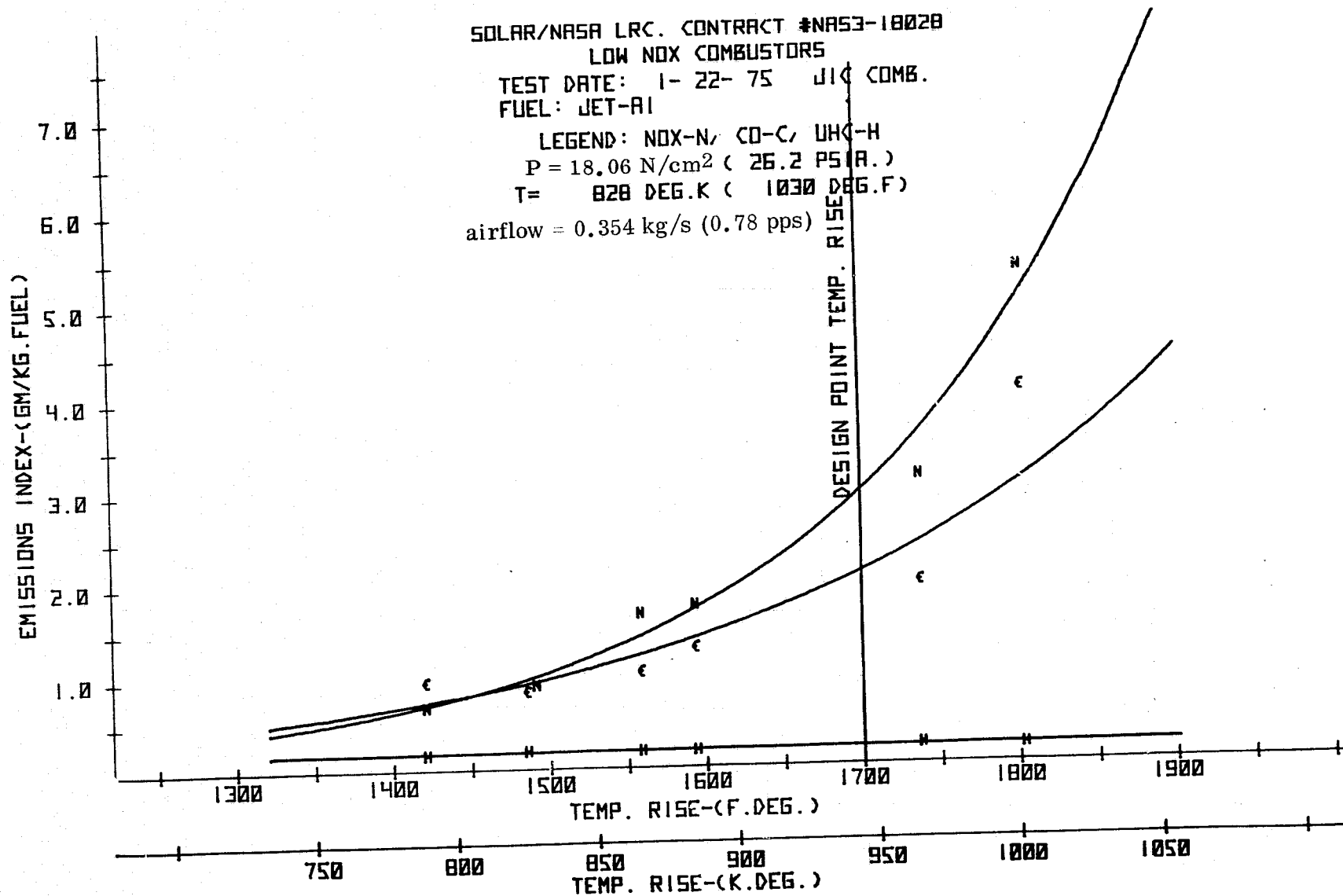
FIGURE 38. JIC COMBUSTOR TEST RESULTS – INTER-PORT COOLING REMOVED

into the product flow from the reaction zone was causing local reaction quenching manifested in the elevated CO levels.

Although the establishment of the maximum degree of pre-mixing in the four mixing tubes is vital for low NO_x operation of the JIC combustor, there exists at least the baseline maldistribution of fuel/air ratio in each port caused by the fuel flow variations delivered by the flow divider block. In order to minimize the effect of this fuel flow maldistribution, plus any existing degree of unmixedness in the mixing tubes, a high level of reaction zone mixing must be accomplished with maximum recirculation ratios. For a given number and size of the mixing tubes, an increase in the reaction zone recirculation ratio can be achieved by increasing the reaction zone diameter. This modification was made to the combustor and is shown in Figure 39. To preserve what was considered to be the optimum proportions of the reaction zone the length of the reaction zone was also increased. By increasing the reaction zone outside diameter from 0.122 m (5.24 in.) to 0.191 m (7.5 in.) the design point reference velocity was reduced from 30.48 m/sec (100 ft/sec) to 14.87 m (48.8 ft/sec). The combustor mixing tube section and the combustor secondary zones were retained without modification necessitating a step change in diameter to the enlarged reaction zone.

The emissions test results of this configuration are shown in Figure 40 where it can be seen that the NO_x level was further reduced to 2.0 gm NO_2/kg fuel at the design point temperature rise with an attendant drop on the CO level to 1.0 gm/kg fuel.
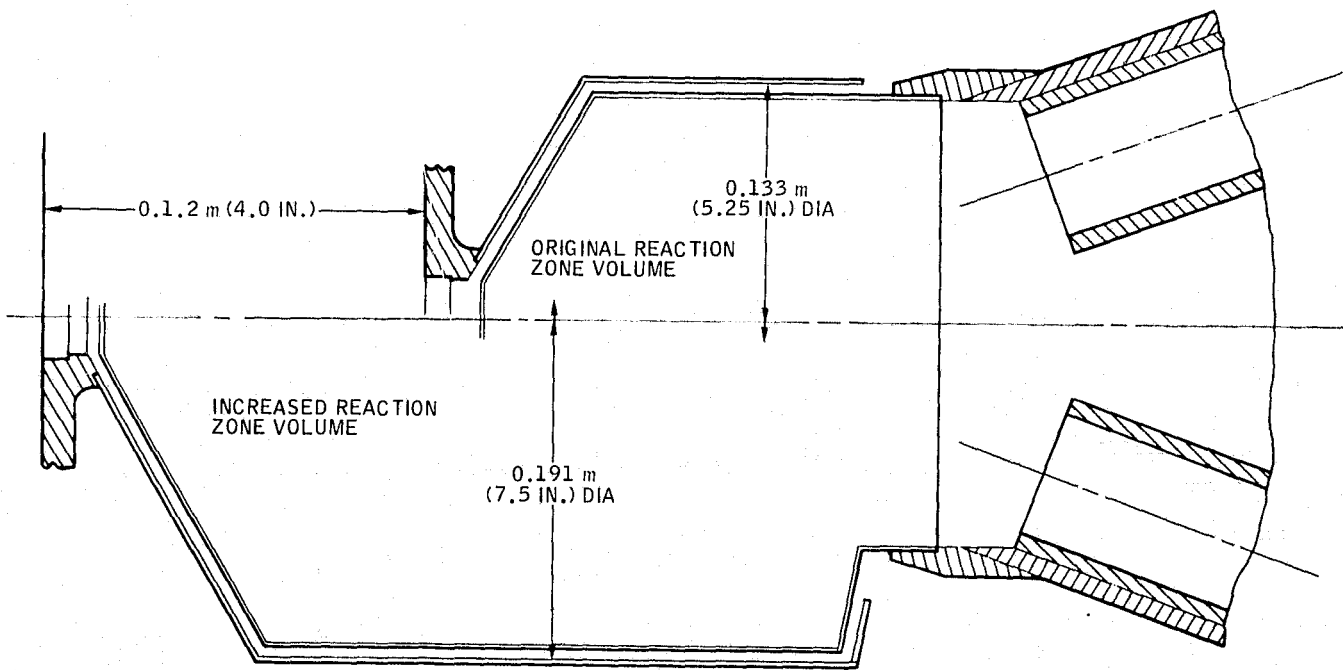

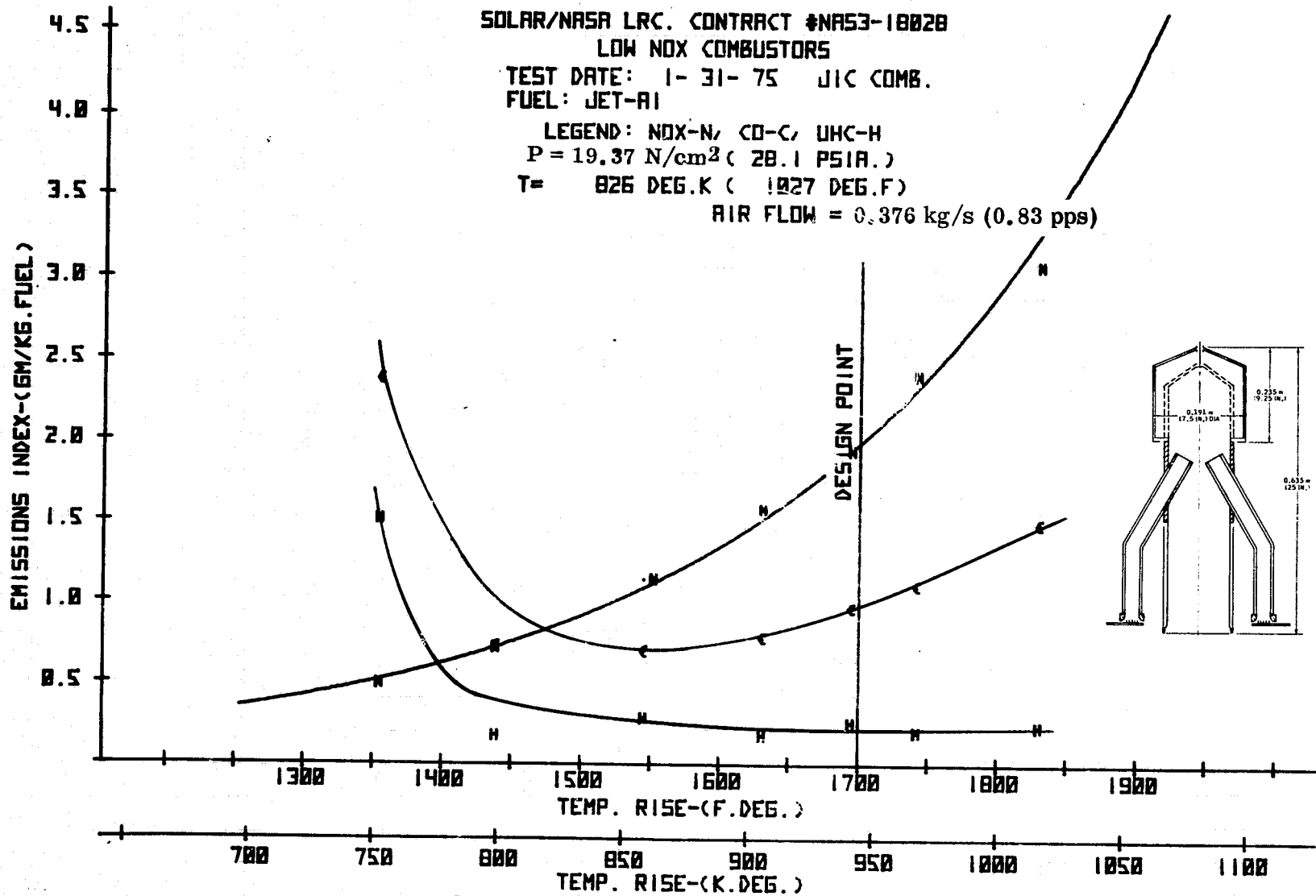FIGURE 39. JIC COMBUSTOR - REACTION ZONE VOLUME INCREASE

FIGURE 40. JIC COMBUSTOR TEST RESULTS - INCREASED VOLUME REACTION ZONE

The reduction in CO with the increased reaction zone volume was anticipated because of the higher reaction residence times. The NO_x improvement was considered due to the improved reaction zone recirculation ratios. The increase in reaction zone residence time is not a strong factor in NO_x formation within the equivalence ratio range in question. The role of the stepped diameter between the reaction zone and the mixing tube section in the promotion and anchoring of the reaction zone recirculation was not investigated.

As can be seen in Figure 1, the mixing tubes penetrate into the combustor. The design intent was to ensure adequate penetration and impingement of the mixing tube jets. The penetrating sections of the mixing tubes were uncooled and problems were encountered during the screening tests with burnout of the mixing tube ends thus an evaluation of a "flush" mixing tube configuration was made in an effort to remove a potential mechanical problem without compromising the emissions signature of the combustor.

The mixing tube modification is shown in Figure 41. The emissions test results are depicted in Figure 42, and show that the NO_x level was essentially unchanged at 2.1 gm NO_2/kg fuel at the design point temperature rise. The CO level however increased from 1.0 gm/kg fuel to 1.5 gm/kg fuel. This is believed to have been a result of some quenching at the edge of the mixing tube jets of the reaction products flowing rearwards between the jets rather than the high temperature mixing tubes walls as in previous configurations. A smokemeter survey made during this test run indicated zero smoke level across the complete characteristic.
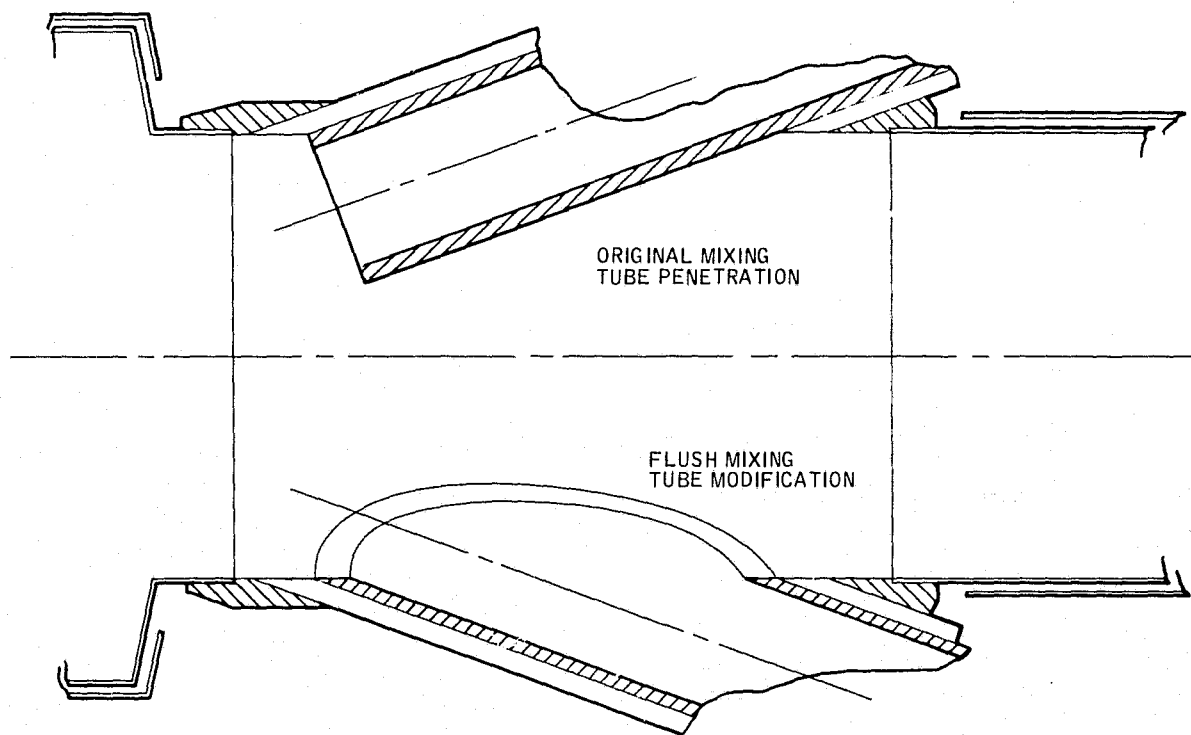

ORIGINAL MIXING
TUBE PENETRATION

FLUSH MIXING
TUBE MODIFICATION

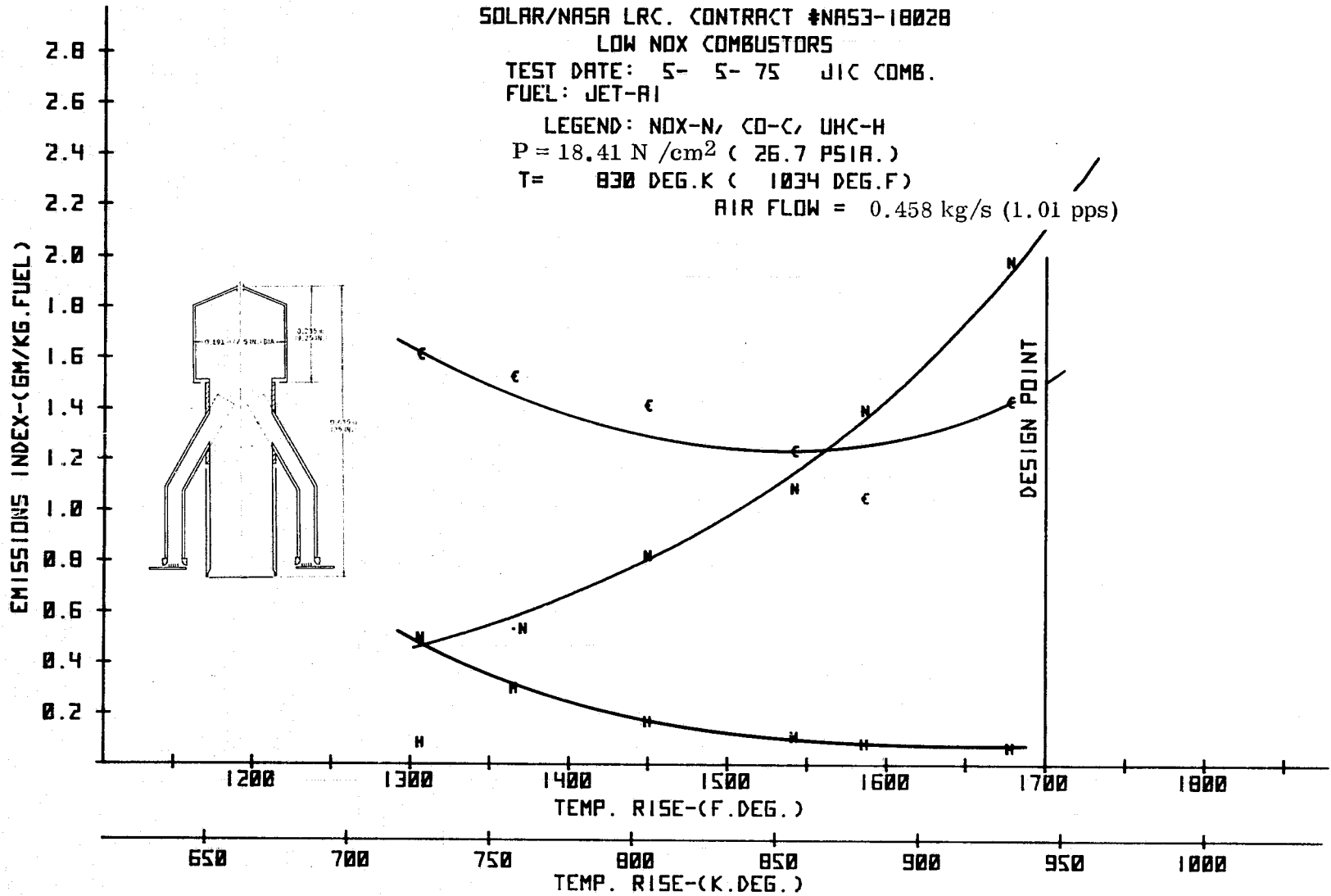FIGURE 41. JIC COMBUSTOR - MIXING TUBE MODIFICATION

FIGURE 42. JIC COMBUSTOR TEST RESULTS - "FLUSH" MIXING TUBES

A review of the effects on the NO_x emissions of the various modifications is given in Figure 43. The initial and final combustor configurations are outlined in Table II for comparison purposes. All subsequent tests were made with final combustor configuration as shown in Table II.

During the subsequent testing of the final JIC combustor configuration a tendency for occasional nonrepeatability of results, in particular NO_x, was observed with some accumulative damage to the lower sections of the mixing tubes. It was concluded that partial flashback into the mixing tubes was occurring at certain running conditions causing higher NO_x levels. No flashback had been observed during the previous tests with the penetrating mixing tubes as indicated by either internal tube damage or increases in mixing tube metal temperature during the test runs.

No investigation of this phenomenon with the final JIC configuration was possible due to schedule requirements. It was concluded that further improvements to the JIC NO_x characteristics were probable with further refinements to the mixing tube design, in particular the initial fuel distribution.

5.2.2 Effect of Fuel Type

As with the VAB combustor, a comparative test run was made on the final JIC combustor configuration using #2 Diesel fuel. The heavier fuel emissions characteristic is shown in Figure 44 and the composite results of #2 Diesel and Jet-A1 fuels are presented in Figure 45. Again, a significant NO_x increase for the #2 Diesel fuel was seen at the design point temperature rise which can only in part be explained by the conversion of the bound nitrogen. The balance of the NO_x increase was considered due to the reduced level of mixing tube pre-mixing caused by the likely reduction in atomization quality and the reduced vaporization rates of the heavier fuel.

5.2.3 Effect of Combustor Inlet Pressure

As previously noted with the VAB combustor, the screening test data were obtained at combustor inlet pressures considerably lower than the design point cruise pressure of 50.68 N/cm^2 (5 atm).

The effects of pressure were evaluated on the final JIC combustor configuration and are shown in Figure 46 at a reduced inlet temperature of 756°K (900°F). Unlike the case of the VAB combustor, a distinct NO_x dependency on pressure was observed. Although the pressure exponent varied over the range of reaction temperature, at the design point outlet temperature of 1778°K (2740°F) a square root pressure dependency was observed. Applying a square root NO_x pressure dependency to the final JIC configuration at the design inlet temperature predicts a cruise condition NO_x level of 3.5 gm NO_2/kg fuel. The CO levels decreased with the higher inlet pressure as the combustor loading was reduced.

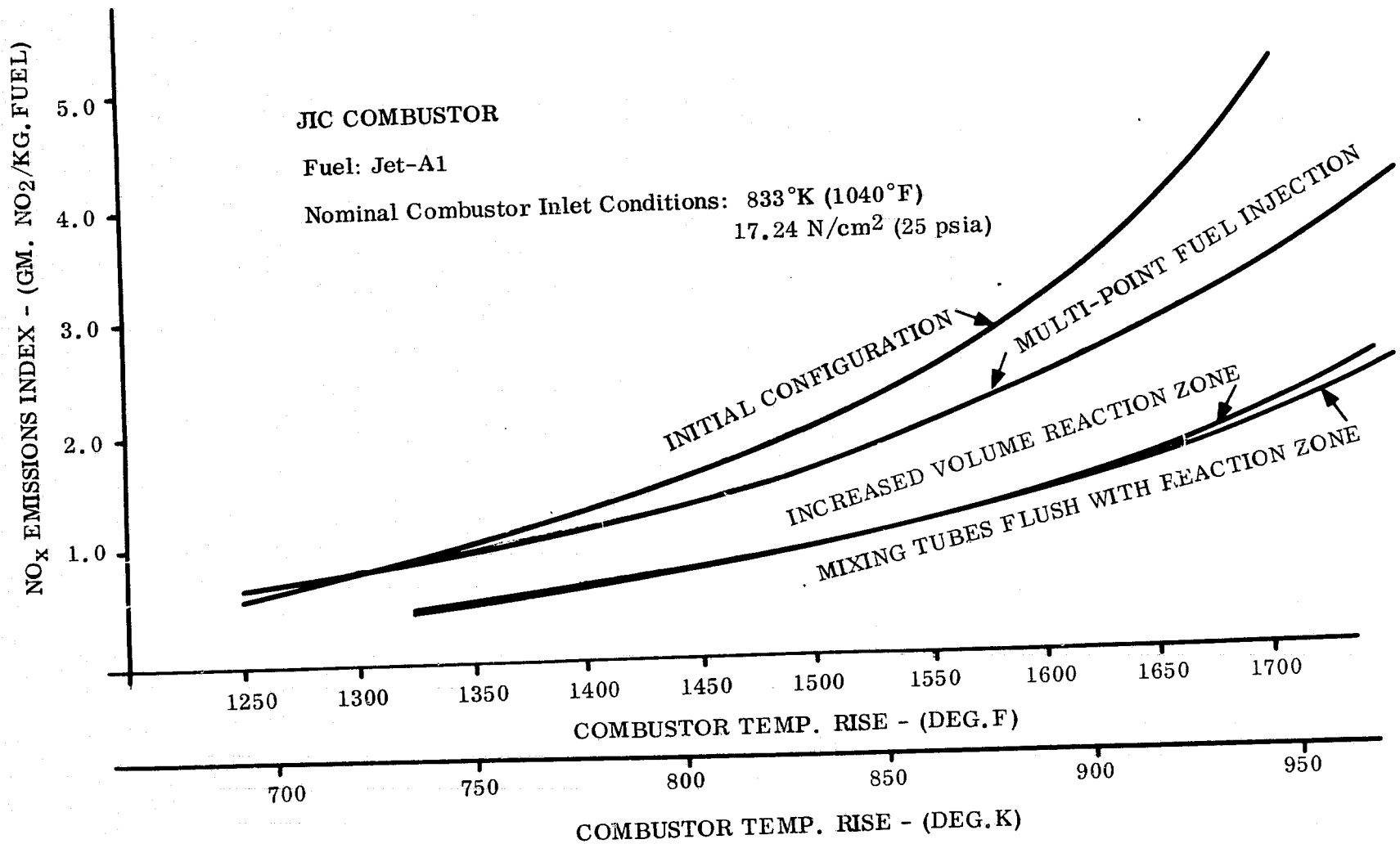FIGURE 43. JIC COMBUSTOR NO_x TEST RESULTS

TABLE II

JIC COMBUSTOR CONFIGURATIONS

Item	Initial	Final
Fuel Injection	• Air Blast • Mixing tube entry center point • Injection with airflow direction	• Air Blast • 13 points on two diameters at each mixing tube entry • Injection against airflow direction
Reaction Zone	Outside diameter = 0.133 m Overall length = 0.133 m	Outside diameter = 0.191 m Overall length = 0.235 m
Liner Cooling	Inter-port cooling strips	Inter-port cooling strips deleted
Mixing Tube	Penetrating into reaction zone	End of mixing tube flush with inside of reaction zone

The explanations for the difference in NO_x pressure dependency between the VAB and JIC combustors are not available due to insufficient test data.

It may be significant, however, that the VAB combustor design that exhibits the better NO_x signature also demonstrates a lack of NO_x pressure dependency. If a high level of pre-mixing in a combustor reduces the NO_x sensitivity to pressure, then improvements to the fuel/air preparation system in the JIC combustor could also reduce the pressure effect as well as diminish the basic NO_x signature.

The difference in physical configuration between the JIC and VAB combustors might also be a factor in their relative performance limitations at high pressures. Whereas in the JIC combustor the fuel/air preparation is performed in the mixing tubes that are essentially uncoupled from the reaction zone, the VAB combustor swirler is more sensitive to possible wall temperature effects that could enhance the fuel vaporization process. Relative reaction zone mixing levels and the different flame propogation modes might also play a role.

66

SOLAR/NASA LRC. CONTRACT #NAS3-18028
LOW NOX COMBUSTORS
TEST DATE: 5- 5- 75   JIC COMB.
FUEL: #2D.
LEGEND: NOX-N, CO-C, UHC-H
$P = 18.41 \ N/cm^2$ (26.7 PSIA.)
T=   830 DEG.K (1034 DEG.F)
AIR FLOW = 0.458 kg/s
(1.01 pps)
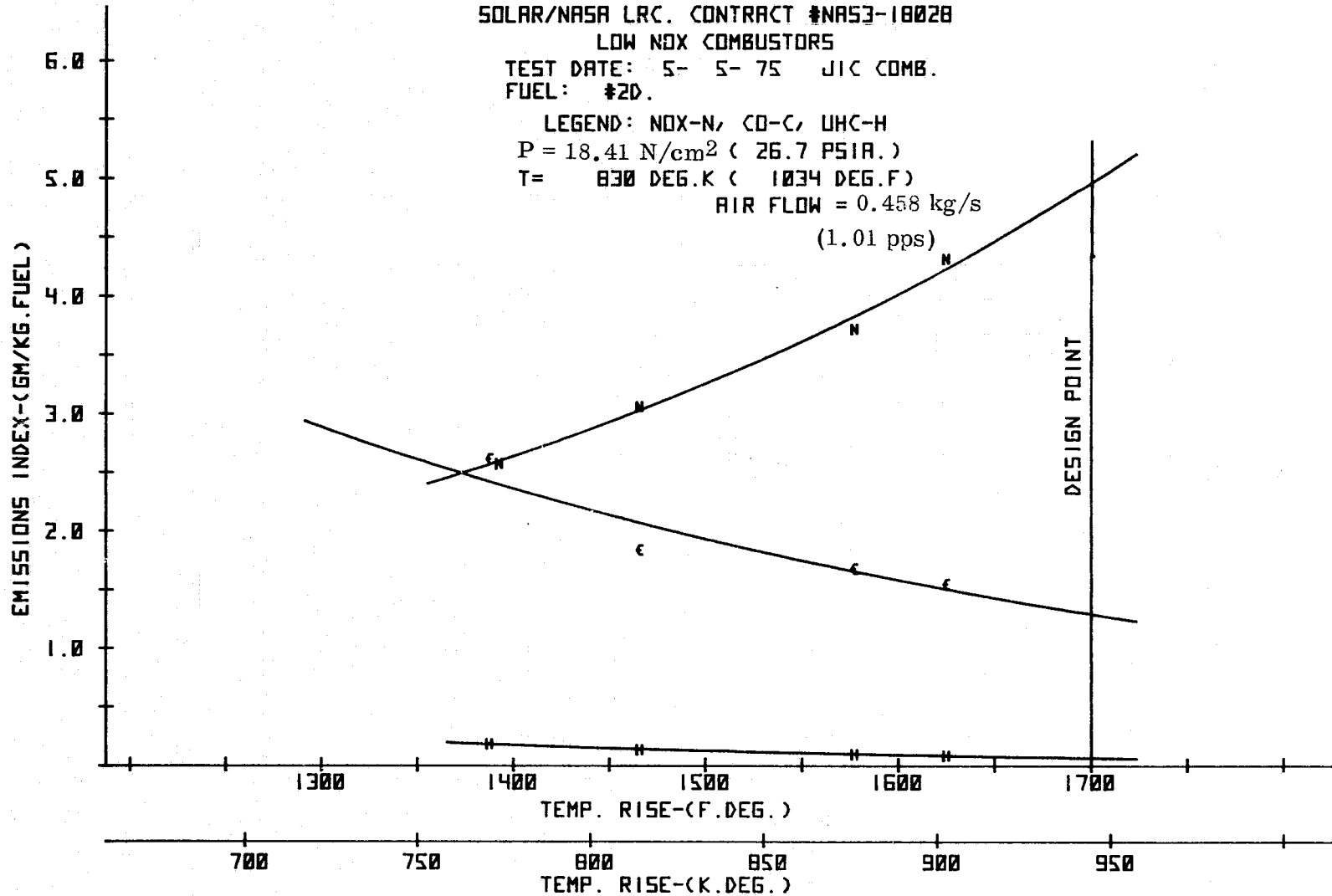
FIGURE 44.   JIC COMBUSTOR TEST RESULTS - #2 DIESEL FUEL

67

SOLAR/NASA LRC. CONTRACT #NAS3-18028
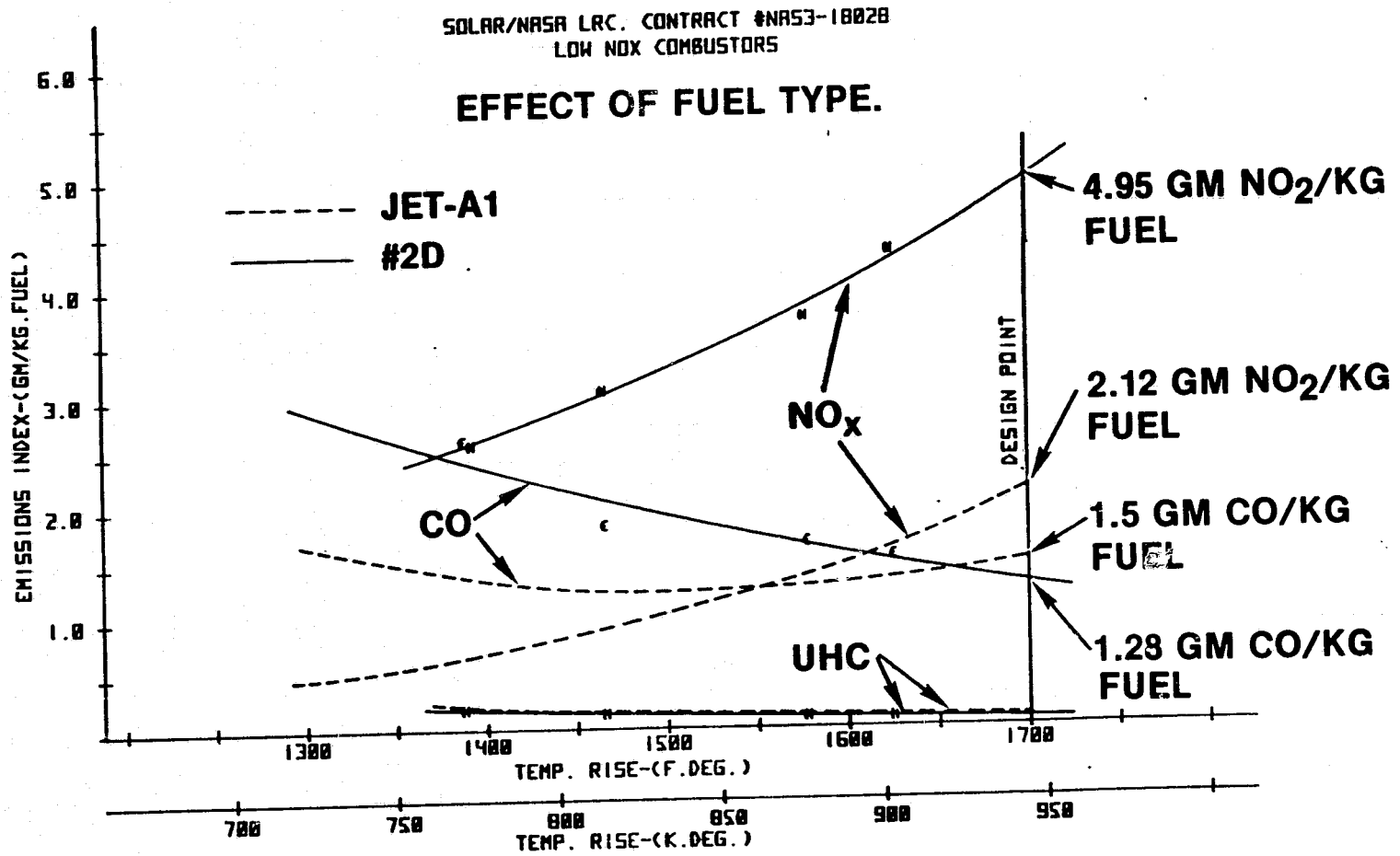LOW NOX COMBUSTORS

EFFECT OF FUEL TYPE.

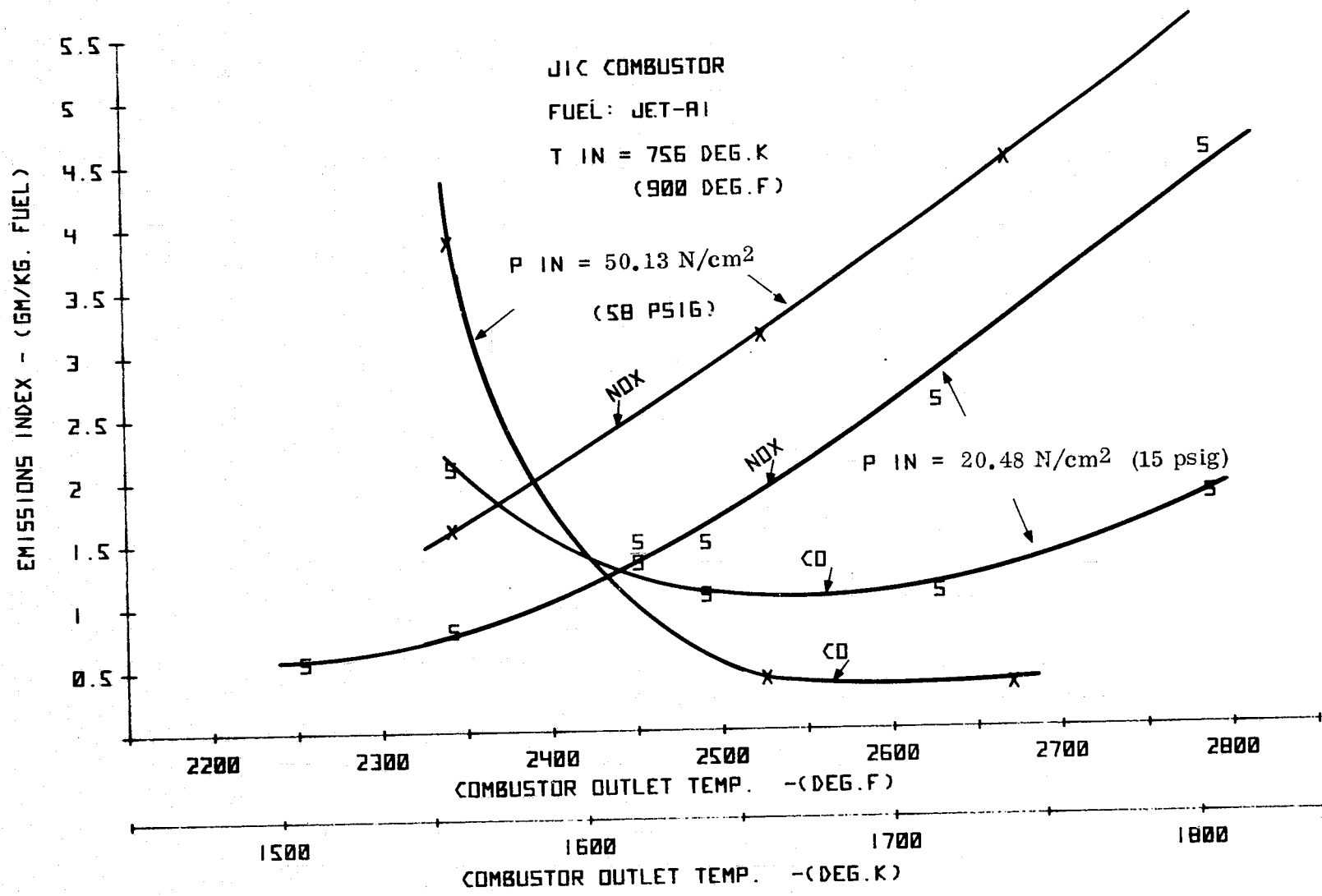FIGURE 45. JIC COMBUSTOR TEST RESULTS - EFFECT OF FUEL TYPE

FIGURE 46. JIC COMBUSTOR TEST RESULTS – EFFECT OF COMBUSTOR INLET PRESSURE.

5.2.4 Effect of Combustor Inlet Temperature

The final JIC combustor configuration was tested over a range of inlet temperatures, as was the case with the VAB combustor, in an initial attempt at evaluating the potential emissions of such a system at an engine off-design condition, such as idle.

The emissions results are shown in Figure 47 and Figure 48 that represent the NO_x and CO emissions signatures, respectively, over a range of combustor inlet temperatures from 831°K (1035°F) to 431°K (315°F).

Generally the results demonstrate the same trends as were observed for the VAB combustor in terms of increasing NO_x with decreasing inlet temperature or "unmixedness" level. A major difference between the VAB and the JIC characteristics can be seen from Figure 47 where there was considerable separation between the 756°K (900°F) and 831°K (1035°F) inlet temperature NO_x characteristics. In the VAB combustor these two characteristics were close in magnitude indicating that even at 756°K (900°F), mixing and not fuel vaporization was controlling the final NO_x level. The difference in the two characteristics suggests that this was not the case with the JIC combustor and that further improvements in fuel distribution and vaporization could produce lower NO_x levels. As with the VAB combustor, decreasing inlet temperatures down to 644°K (700°F) had little effect on CO emissions; below this value CO increased rapidly due to reduced evaporation and mixing.

Particulate emissions surveys taken during the high inlet pressure and low inlet temperature test runs indicated zero smoke at all operating conditions.

5.3 CATALYTIC COMBUSTOR

A decision was made to use natural gas rather than Jet-A1 as the test fuel for the initial tests of the catalytic combustor because at that relatively late point in the overall test program schedule there appeared to be insufficient definition of the VAB combustor fuel preparation system, in terms of atomization configuration and swirler design, to be able to formulate an optimum scheme for the catalytic combustor.

The use of natural gas obviates the requirements for an atomization system and allows operation of the fuel preparation section of the combustor at pressure drops that would be too low for adequate liquid fuel air-blast atomization. This means that the catalytic bed can be run at reference velocities lower than the design level at the design inlet temperature.

The natural gas was introduced near the inlet to each swirler vane-passage through a series of 24 tubes, each 0.0064 m (0.25 in.) diameter as depicted in Figure 49. The fuel tubes were externally manifolded to a common natural gas supply.
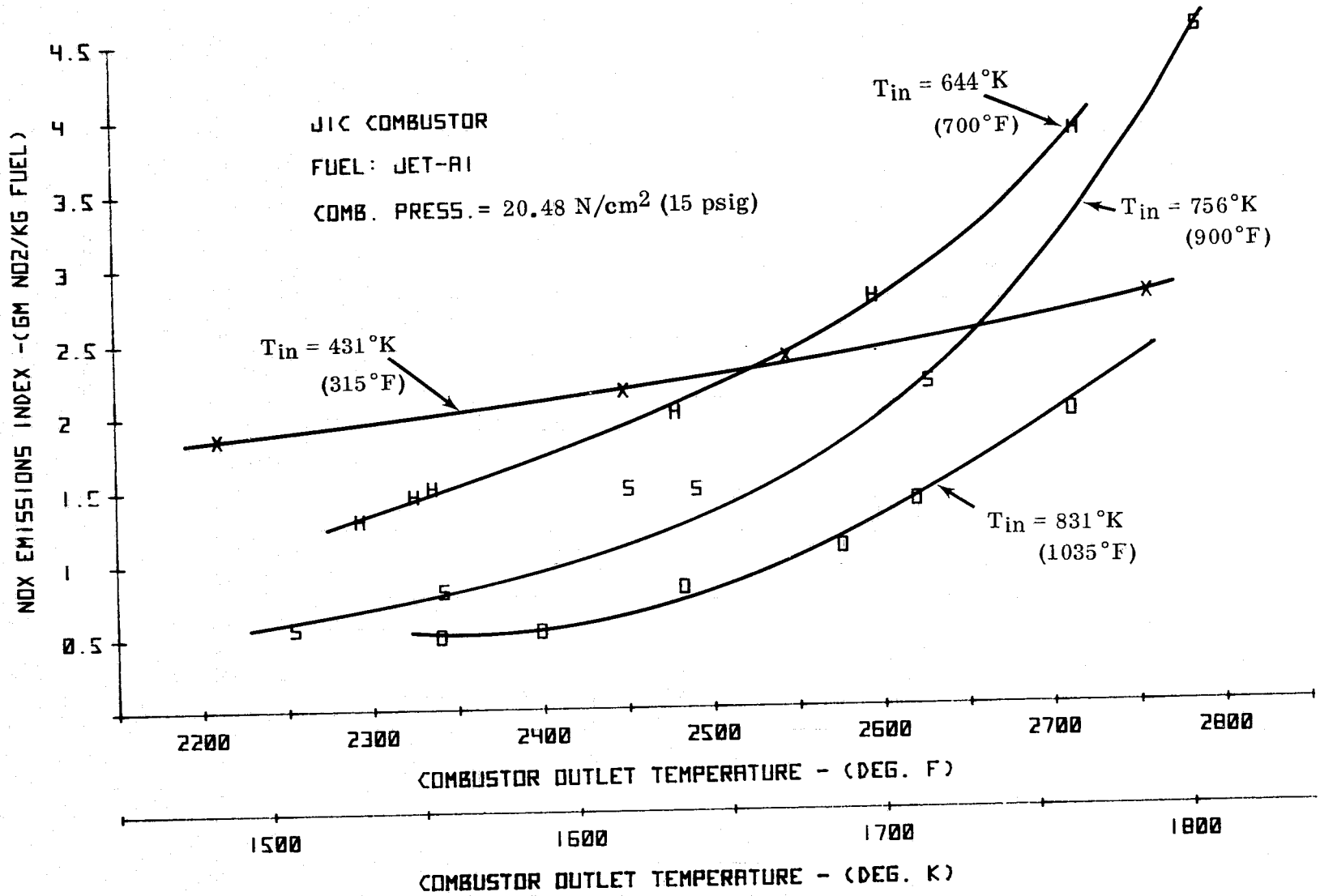
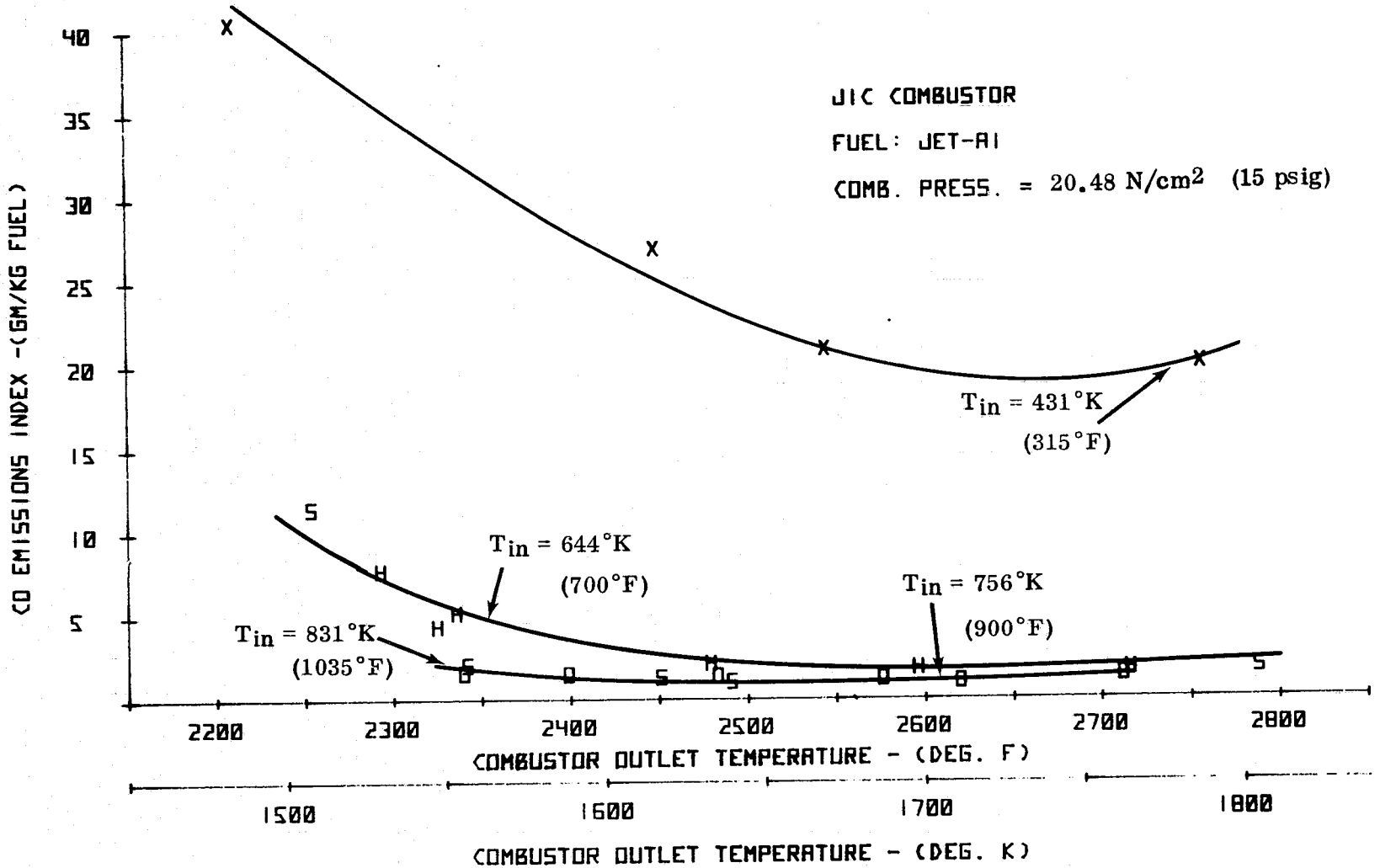FIGURE 47. JIC COMBUSTOR NO$_X$ TEST RESULTS - EFFECT OF COMBUSTOR INLET TEMPERATURE.

FIGURE 48. JIC COMBUSTOR CO TEST RESULTS - EFFECT OF COMBUSTOR INLET TEMPERATURE.
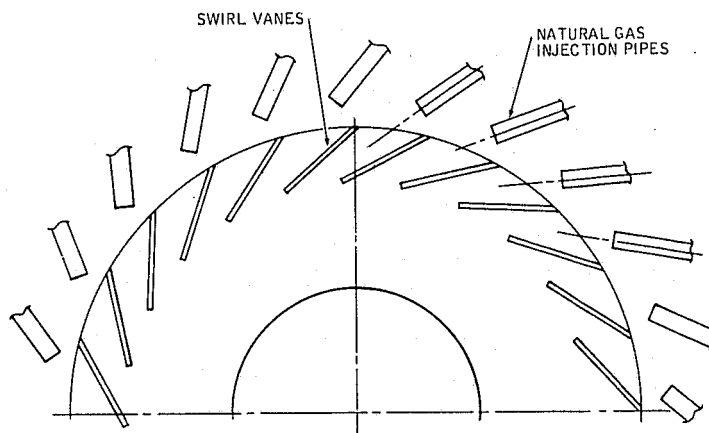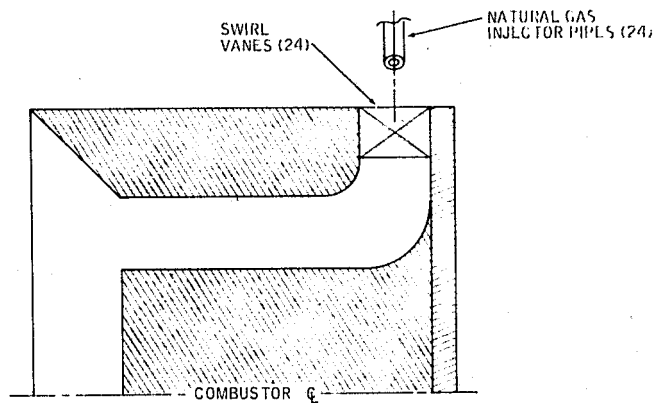
FIGURE 49. CATALYTIC COMBUSTOR NATURAL GAS INJECTION SYSTEM

The initial test attempts were conducted at low pressures within the range 13.79 to 20.68 N/cm^2 (20 to 30 psia) at the design point inlet temperature of 833°K (1500°R) on the configuration described in Section 3.3.1. A wide range of reference velocities and fuel/air ratios were applied to the combustor but only very slight activity of the bed was apparent, represented by small increases of the bed outlet temperature and simultaneous low level carbon dioxide readings.

A bed pre-heat system was next installed so that the bed inlet temperature could be transiently augmented prior to the introduction of the fuel/air mixture. This was accomplished by installing an igniter plug in the pre-bed space between the swirler outlet plane and the bed inlet. By stabilizing combustion on the back face on the flow straightening screen the bed was pre-heated to a level higher than the design point combustor inlet temperature. Upon achievement of a given level of bed pre-heat the pre-bed combustion was extinguished by cutting-off the fuel flow. The fuel flow was then re-established before the bed cooled. In this manner reaction could be achieved

with a minimum bed inlet preheat temperature of approximately 922°K (1660°R). No emissions characteristics were obtained due to a failure of the cordierite bed module caused by an inadvertant overtemperature during the pre-heat phase of the operation.

The bed pre-heat system was not pursued further at this point as the inability of the combustor to start at an inlet temperature of 833°K (1500°R) was obviously a performance limitation. Similar studies by Anderson, Tacina and Mroz (Ref. 10) using a proprietary catalyst material and propane fuel showed that a starting temperature of 700°K (1260°R) was sufficient for catalyst bed operation at reference velocities up to 30 m/sec (98.7 fps) corresponding to a space velocity of 780,000 hr^{-1} for the reactor used. This value of space velocity is considerably greater than the design point value for the combustor under test indicating that bed residence time was not limiting the performance.

Examination of a sample of the kanthal catalytic core by a scanning electron beam microscope indicated that the deposited platinum was segregated in clumps rather than being finely dispersed throughout the alumina coating. Acting on the assumption that the clumping of the platinum on the kanthal cores was a characteristic of the deposition process and unlikely to improve with increased platinum concentrations, a final test of the catalytic combustor was made with a bed consisting of an initial two cordierite modules followed by three kanthal cores.

The two cordierite cores were resensitized with platnium to a level of approximately 5 x 10^{-3} Kg Pt/m^2 (7.11 x 10^{-6} lb Pt/$in.^2$) while the kanthal units were as previously used.

The results of this final test were again unsuccessful with little noticeable catalyst activity at an inlet temperature of 833°K (1500°R). No further investigations of the catalytic combustor were undertaken so as to apply the remaining program resources to the JIC and VAB combustors that had both already demonstrated promising results.

As noted previously, the initial design space velocity of the catalytic bed at 280,000 hr^{-1} is unlikely to represent the performance limitation of the combustor. Comparable work on similar pre-mixed combustors by Anderson, Tacina and Mroz (Ref. 10) on propane and also Blazowski and Bresowar (Ref. 11) on JP-4 fuel demonstrated successful operation of catalytic reactors at space velocities in excess of 280,000 hr^{-1} at inlet temperatures lower than 833°K (1500°R). It should be noted however that the effective space velocity of the final configurations tested would be 700,000 hr^{-1} assuming negligible reactivity of the final three kanthal modules.

The twin keys to the operation of a catalytic reactor are the selection of the optimum catalyst and the deposition of the catalyst in sufficient concentration on the

substrate in a manner that presents the maximum available effective area. The selection of platinum as the combustor catalyst might not be the optimum choice for use with either Jet-A1 or natural gas fuel but there has been adequate demonstration in the past by Solar and others that platinum is an effective oxidation catalyst of natural gas and it is felt that the selection did not represent the combustor performance limitation.

The deposition process as applied to the kanthal cores was apparently unsuccessful in producing finely dispersed platinum within a matrix of alumina; hence the effectivity of these cores would be expected to be low. The cordierite cores, in contrast, appeared uniformly black after sensitization with platinum and a chemical analysis of samples confirmed the calculated platinum concentrations of the cores used in the final tests as comparable to current industrial catalyst practice.

It is possible that the substrate microporosity represented the major limitation of the cordierite cores. Although cordierite has been used previously in such applications as automotive catalyst substrates, a wash coating of γ-alumina is normally applied to augment the natural porosity of the cordierite. Such a wash coat can increase the effective area by an order of magnitude and if the catalyst can be correctly applied, a corresponding increase in "active sites" can be achieved.

6

CONCLUSIONS

- Lean reaction, pre-mixed systems are capable of demonstrating NO_x levels considerable lower than those of current technology combustor designs or near term projected improvements to the "state-of-the-art". NO_x levels as low as 1.0 gm NO_2/kg fuel at the cruise condition were demonstrated with very low unburned hydrocarbon levels and essentially equilibrium carbon monoxide levels at near 100 percent (>99.8) combustion efficiency.

- A simple, constant geometry, pre-mixed combustor is not capable of stable operation across the full range of inlet and loading conditions normally encountered in an aircraft gas turbine. The available, low-emissions equivalence ratio operating bandwidth between a limiting NO_x level of, for example, 1.0 gm NO_2/kg fuel and a CO level that provides an acceptable margin on lean extinction, is very narrow. Further development of the concept is required to extend the operational range by such means as fuel staging or variable geometry, for example.

- Of the three combustor concepts evaluated, the Vortex Air Blast (VAB) demonstrated the superior emissions signature, essentially meeting the cruise NO_x goal of 1.0 gm NO_2/kg fuel. In addition there exists the potential of further improvements in NO_x levels by extensions of modifications tested but not completely evaluated such as longer swirler outlet throats and an increased number of fuel injection points. Although the Jet Induced Circulation Combustor (JIC) produced higher NO_x levels it is felt that further improvements to the fuel preparation and mixing tube system could be made, without departing from a practical physical envelope, that would reduce the emissions to the same level as that of the VAB combustor. In addition, the JIC combustor demonstrated the ability to operate successfully at the higher reference velocity level of 30.48 m/sec (100 fps) although with an attendant penalty in NO_x emissions, making the JIC system superior if reference velocity or size were a major constraint.

- Over the range of combustor pressures tested, the VAB combustor NO_x production appeared to be independent of pressure while the JIC system exhibited a significant pressure effect. The test results were insufficient to enable a definitive explanation for this difference in behavior to be formulated.

- Both the JIC and VAB combustors demonstrated the same trend of emission characteristics with reduced inlet temperatures. Increasing NO_x and CO emissions and reduced flame stability marked the operation at low inlet temperatures. The general level of emissions at combustor inlet and outlet temperatures corresponding to an engine idle condition suggests that operating such a system need not be a NO_x or CO emissions problem if reaction zone equivalence ratio control can be maintained.

- In addition to the monitored NO_x, CO and UHC levels, no smoke was detected at any operating condition on either the JIC or VAB combustor down to an inlet temperature of 422°K (300°F).

- Although not evaluated in any depth, the indications are that the liner cooling requirements and reaction zone outlet temperature exhaust pattern factor of the lean reaction, pre-mixed JIC and VAB combustion systems can both be significantly less than that of conventional combustors.

- The catalytic combustor demonstrated negligible activity at the design point combustor inlet temperature of 833°K (1500°R). Although the combustor testing was not pursued in sufficient depth for a clear understanding of the problems, it is likely that the effective catalyst area and/or method of substrate impregnation was deficient.

REFERENCES

1. Nukiyama, S., and Tanasawa, Y., Trans. Soc. Mech. Engrs. Japan 4, 86, 138, (1938); 5, 63, 68 (1939); 6, II-7, II-8 (1940).

2. Mellor, A. M., "Current Kinetic Modelling Techniques for Continuous Flow Combustors", Proceedings of the Symposium on Emissions from Continuous Combustion Systems, Plenum Press (1972).

3. Baron, T., and Bollinger, E. H., "Mixing of High-Velocity Air Jets", M.S. Thesis, University of Illinois (1952).

4. SAE Aerospace Recommended Practice, "Procedure for the Continuous Sampling and Measurement of Gaseous Emissions from Aircraft Turbine Engines", ARP 1256 (1971).

5. Marchionna, N. R., "Effect of Inlet-Air Humidity on the Formation of Oxides of Nitrogen in a Gas-Turbine Combustor", NASA TMX-68209, Lewis Research Center (1973).

6. Maybach, G. W., "The Film Vaporization Principle for Gas Turbine Combustors", The Pennsylvania State University (1959).

7. Appleton, J. P. and Heywood, J. B., "The Effects of Imperfect Fuel-Air Mixing in a Burner on NO Formation From Nitrogen in the Air and the Fuel," Fourtheenth Symposium (International) on Combustion, pp. 777-786 (1973).

8. Dilmore, J. A., and Rohrer, W., "Nitric Oxide Formation in the Combustion of Fuels Containing Nitrogen in a Gas Turbine Combustor," ASME Paper No. 74-GT-37 (1974).

9. Pompei, F., and Heywood, J. B., "The Role of Mixing in Burner-Generated Carbon Monoxide and Nitric Oxide", Combustion and Flame, 19, 407-418 (1972).

10. Anderson, D. N., Tacina, R. R., and Mroz, T. S., "Performance of a Catalytic Reactor at Simulated Gas Turbine Combustor Operating Conditions", NASA TMX-71747, Lewis Research Center (1975).

11.   Blazowski, W. A., and Bresowar, G. E., "Preliminary Study of the Catalytic Combustor Concept as Applied to Air Craft Gas Turbines," AFAPL-TR-74-32, Air Force Aero Propulsion Lab (1974).